

DETECTION OF COLD FLOW PROPERTIES OF DIESEL AND BIODIESEL FUEL
USING OPTICAL SENSOR

A Thesis
presented to
the Faculty of the Graduate School
University of Missouri- Columbia

In Partial Fulfillment
Of the Requirements for the Degree
Master of Science

by
SUMIT TAYAL

Dr. Brain Adams, Thesis Supervisor

MAY 2006


The undersigned, appointed by the Dean of the Graduate School, have examined the thesis entitled

DETECTION OF COLD FLOW PROPERTIES OF DIESEL AND BIODIESEL
FUEL USING OPTICAL SENSOR

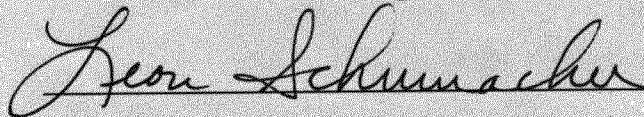
Presented by Sumit Tayal

A candidate for the degree of Master of Science

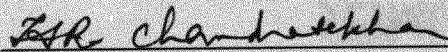
And hereby certify that in their opinion it is worthy of acceptance.



Dr. Brian T. Adams - Biological Engineering



Dr. Leon Schumacher - Biological Engineering



Dr. H. R. Chandrasekhar - Department of Physics and Astronomy

ACKNOWLEDGEMENTS

I learned many things in the Biological Engineering Department at University of Missouri-Columbia. This research offered me a lot of knowledge and experience on biodiesel fuel and optical sensors. I deeply appreciate the school for giving me a chance. Many people supported me when I worked to finish the project.

I would like to express gratitude to my advisor, Dr. Brian Adams for picking me for this project and guiding me in the right direction.

I wish to thank Dr. Leon Schumacher for guiding my research and providing with the material for testing the sensor.

I would like to thank Dr. H. R. Chandrasekhar for allowing me to work in the Optics Laboratory that helped me in my research.

I wish to thank Dr. Kenneth A. Sudduth for allowing me to use his spectrometer.

Finally, I would like to thank my wife, Deepa, my parents - Jitendra and Laxmi, my elder sister, Ila. I would not have been able to achieve much without their immense encouragement.

TABLE OF CONTENTS

ACKNOWLEDGEMENTS	ii
LIST OF TABLES	vii
LIST OF FIGURES	viii
ABSTRACT	xi

Chapter

1. INTRODUCTION.....	1
1.1 INTRODUCTION TO BIODIESEL	1
1.2 NEED FOR BIODIESEL	1
1.3 MANUFACTURING OF BIODIESEL.....	2
1.4 CHEMICAL REACTION	3
1.5 CHEMICAL AND PHYSICAL PROPERTIES OF BIODIESEL AND DIESEL PRODUCTS.....	4
1.5.1 ENERGY CONTENT.....	4
1.5.2 CETANE NUMBER.....	5
1.5.3 EMISSIONS	6
1.5.4 FLASHPOINT	7
1.6 PROTECTIVE MEASURES WITH BIODIESEL FUEL.....	8
1.6.1 EFFECT OF BIODIESEL ON PAINTED SURFACE	8
1.6.2 BIODIESEL SOAKED RAGS	9
1.7 USING BIODIESEL IN COLD WEATHER.....	9
1.8 LIMITATIONS WITH BIODIESEL FUEL.....	9
1.8.1 COST	9
2. LITERATURE REVIEW	11
2.1 INTRODUCTION	11
2.2 COLD FLOW PROPERTIES OF DIESEL AND BIODIESEL.....	11
2.2.1 CLOUD POINT	11
2.2.2 POUR POINT	13
2.2.3 LOW TEMPERATURE FLOW TEST (LTFT)	14

2.2.4 COLD FILTER PLUGGING POINT (CFPP)	15
2.3 WHY DETECT CLOUD POINT?	17
2.4 DETECTION OF CLOUD POINT USING SENSOR	
TECHNOLOGIES	19
2.4.1 CAPACITIVE SENSOR	19
2.4.2 OPTICAL SENSOR	20
2.5 ASTM STANDARDS	21
2.5.1 ASTM D5771.....	21
2.5.2 ASTM D5772.....	22
2.5.3 ASTM D5773.....	24
2.6 COMMERCIALY AVAILABLE CLOUD POINT DETECTORS.....	25
2.6.1 KLA-3 AUTOMATIC CLOUD POINT SYSTEM.....	25
2.6.2 KITTIWAKE CLOUD POINT DETECTOR.....	25
2.6.3 CRYSTAL CLOUD POINT DETECTOR.....	26
2.7 OBJECTIVES	27
3. MATERIAL AND METHODS	28
3.1 APPARATUS	28
3.1.1 TEST STAND.....	28
3.1.2 BIODIESEL COOLING CYLINDER.....	30
3.1.3 COOLING SYSTEM EXCHANGER	31
3.2 SENSOR	32
3.2.1 BASIC PRINCIPLE.....	32
3.2.2 SENSOR CONSTRUCTION	33
3.2.3 SNELL’S LAW	35
3.3 MATERIALS REQUIRED	37
3.3.1 LIGHT SOURCE.....	37
3.3.2 MOTORS.....	38
3.3.3 PUMP.....	38
3.3.4 SPECTROMETER	38
3.3.5 MULTIMETER	39

3.4 FUELS SAMPLE PREPARATION	39
3.4.1 FUEL.....	39
3.4.2 BLENDING OF BIODIESEL FUEL WITH DIESEL FUEL	39
3.5 EXPERIMENTAL DESIGN	42
3.6 EXPERIMENTAL PROCEDURE	43
3.6.1 SETTING BASELINE.....	43
3.6.2 PRE-EXPERIMENTAL MEASURES.....	43
3.6.2.1 SYSTEM CLEANING	43
3.6.2.2 SAMPLE QUANTITY	43
3.6.2.3 STARTING THE TEST STAND	44
3.6.2.4 COLLECTING READINGS	44
4. RESULTS AND DISCUSSION	45
4.1 FUEL ANALYSIS.....	45
4.2 FUEL PROPERTIES	49
4.3 DATA COLLECTION	50
4.4 BLENDS OF BIODIESEL	54
4.4.1 B100 (100% BIODIESEL)	55
4.4.2 D2B0 (100% NO. 2 DIESEL)	57
4.4.3 D2B2 (98% NO. 2 DIESEL AND 2% BIODIESEL).....	59
4.4.4 D2B5 (95% NO. 2 DIESEL AND 5% BIODIESEL).....	61
4.4.5 D2B20 (80% NO. 2 DIESEL AND 20% BIODIESEL).....	63
4.4.6 D1B0 (100% NO. 1 DIESEL)	65
4.4.7 D1B2 (98% NO. 1 DIESEL AND 2% BIODIESEL).....	67
4.4.8 D1B5 (95% NO. 1 DIESEL AND 5% BIODIESEL).....	69
4.4.9 D1B20 (80% NO. 1 DIESEL AND 20% BIODIESEL).....	71
4.5 TRANSMITTANCE VS WAVELENGTH- CLOUD POINT	73
4.6 TRANSMITTANCE VS TEMPERATURE.....	75

5. CONCLUSIONS	80
6. RECOMMENDATIONS.....	81
APPENDICES	82
APPENDIX A- SENSOR DRAWINGS.....	82
APPENDIX B- STATISTICAL ANALYSIS SOFTWARE PROGRAM TO CONVERT RAW DATA INTO TRANSMITTANCE.....	85
APPENDIX C- REPLICATE 2 AND REPLICATE 3 FOR ALL BLENDS OF BIODIESEL FUEL	86
APPENDIX D- STATISTICAL ANALYSIS SOFTWARE PROGRAM- TRANSMITTANCE VS WAVELENGTH.....	95
APPENDIX E- STATISTICAL ANALYSIS SOFTWARE PROGRAM- TRANSMITTANCE VS TEMPERATURE.....	98
REFERENCES.....	105

LIST OF TABLES

Table	Page
2.1: Tenth Percentile Minimum Ambient Air Temperature for the United States	18
3.1: Biodiesel Blends Prepared with No. 1 Diesel.....	41
3.2: Biodiesel Blends Prepared with No. 2 Diesel.....	41
3.3: Order of Experiment Performance.....	42
4.1: Fuel Analysis for No. 1 Diesel Fuel	46
4.2: Fuel Analysis for No. 2 Diesel Fuel	47
4.3: Fuel Analysis for Biodiesel Fuel	48
4.4: Cloud Point Temperature of Different Blends of Biodiesel Fuel	49

LIST OF FIGURES

Figure	Page
1.1: Transesterification of Vegetable oil to Biodiesel	3
1.2: Formation of Methyl Ester from Triglycerides.....	3
1.3: Energy Content of Biodiesel and Petroleum Diesel	5
1.4: Cetane Numbers for Common Diesel and Biodiesel fuel.....	6
1.5: Average Biodiesel Emissions Compared to Conventional Diesel Using Different Models of Heavy Duty Engine.....	7
1.6: Fuel Flashpoint Comparisons Between Gasoline, Jet Fuel, Diesel, Bunker Fuel (No. 6 Fuel Oil) and Biodiesel.....	8
2.1: Apparatus for Cloud Point Test	12
2.2: Detection of Test Fuel Movement in Test Chamber.....	13
2.3: LTFT Sample Filtration Assembly	14
2.4: CFPP Apparatus Assembly.....	16
2.5: Schematic of Optical Fuel Sensor.....	20
2.6: Detection of Cloud Point Using Light Emitter	21
2.7: Test Jar Cooling Chamber and Circulating Bath	22
2.8: Test Assembly for Measuring Cloud Point Using Linear Cooling Rate Method	23
3.1: Test Stand Diagram for Testing Sensor Operation.....	29
3.2: Biodiesel Cooling Cylinder	30
3.3: Temperature Control for the Test Stand	31

Figure	Page
3.4: Transmittance of Light Through the Test Cell	32
3.5: Overview of Detection of Signal Using Optical Sensor	33
3.6: Outerview of the Sensor Housing.....	34
3.7: Parts Assembly Inside the Sensor.....	34
3.8: Illustration of Law of Refraction	35
3.9: Light Source at Focal Point and Light Source at Infinity	36
3.10: Output Power of Tungsten Halogen Light Source for Wavelength From 340nm – 940nm	37
4.1: Raw Data Vs Wavelength with Change in Speed.....	51
4.2: Raw Data Vs Wavelength (nm) for B100 (100% Biodiesel) at Different Temperatures (°C)	52
4.3: Baseline (No.1 Diesel) Vs Wavelength (nm) for D1B5 (95% Diesel and 5% Biodiesel).....	53
4.4: Transmittance Vs Wavelength (nm) for B100 (100% Biodiesel) at Different temperatures (°C) The dark black line indicates the spectrum at the cloud point of the fuel	56
4.5: Transmittance Vs Wavelength (nm) for D2B0 (100%No. 2 Diesel and 0% Biodiesel) at Different temperatures (°C) The dark black line indicates the spectrum at the cloud point of the fuel	58
4.6: Transmittance Vs Wavelength (nm) for D2B2 (98%No. 2 Diesel and 2% Biodiesel) at Different temperatures (°C) The dark black line indicates the spectrum at the cloud point of the fuel	60
4.7: Transmittance Vs Wavelength (nm) for D2B5 (95% No. 2 Diesel and 5% Biodiesel) at Different temperatures (°C) The dark black line indicates the spectrum at the cloud point of the fuel	62
4.8: Transmittance Vs Wavelength (nm) for D2B20 (80%No. 2 Diesel and 20% Biodiesel) at Different temperatures (°C) The dark black line indicates the spectrum at the cloud point of the fuel	64

Figure	Page
4.9: Transmittance Vs Wavelength (nm) for D1B0 (100%No. 1 Diesel and 0% Biodiesel) at Different temperatures (°C) No cloud point obtained for D1B2 (98%No. 1 Diesel and 2% Biodiesel) because experimental setup does not go beyond -40° C	66
4.10: Transmittance Vs Wavelength (nm) for D1B2 (98%No. 1 Diesel and 2% Biodiesel) at Different temperatures (°C) No cloud point obtained for D1B2 (98%No. 1 Diesel and 2% Biodiesel) because experimental setup does not go beyond -40° C	68
4.11: Transmittance Vs Wavelength (nm) for D1B5 (95%No. 1 Diesel and 5% Biodiesel) at Different temperatures (°C) The dark black line indicates the spectrum at the cloud point of the fuel	70
4.12: Transmittance Vs Wavelength (nm) for D1B20 (80%No. 1 Diesel and 20% Biodiesel) at Different temperatures (°C) The dark black line indicates the spectrum at the cloud point of the fuel	72
4.13: Transmittance Vs Wavelength for Different Blends of Diesel and Biodiesel Fuel at Their Respective Cloud Point Temperatures	74
4.14: Transmittance Vs Temperature for Different Blends of Diesel and Biodiesel Fuel at 660nm	77
4.15: Transmittance Vs Temperature for Different Blends of Diesel and Biodiesel Fuel at 750nm	78
4.16: Transmittance Vs Temperature for Different Blends of Diesel and Biodiesel Fuel at 1600nm	79

DETECTION OF COLD FLOW PROPERTIES OF DIESEL AND BIODIESEL FUEL USING OPTICAL SENSOR

Sumit Tayal

Dr. Brian T. Adams, Thesis Supervisor

ABSTRACT

Identification of cloud point for biodiesel fuel can be used to optimize the performance of biodiesel fueled vehicles in cold weather. Cloud point is the temperature at which the smallest cluster of wax crystal is observed upon cooling under prescribed conditions. Cloud point is determined by inspecting for a haze in the normally clear liquid fuel. This research assesses the optical properties of biodiesel at cold temperatures to develop a reliable, robust and compact sensor that can detect the transmittance of light through biodiesel fuel. Results showed that the experimental optical sensor cannot detect the cloud point of the biodiesel fuel but can be useful in finding the cold flow properties of biodiesel fuel. It showed that lowest value of transmittance for all blends of biodiesel is 0.3 or lower.

CHAPTER 1

INTRODUCTION

1.1 INTRODUCTION TO BIODIESEL

Biodiesel is a clean burning alternative fuel, produced from renewable and biodegradable resources. Biodiesel is nontoxic, and essentially free of sulfur and aromatics. Biodiesel can be made from a variety of products, including animal tallow or vegetable oils derived from soybeans, rapeseed, canola, corn and sunflowers. Biodiesel is an ester that can be blended with diesel to form into a biodiesel blend (Cheng, et al., 1991). Biodiesel blends can be used in compression-ignition (diesel) engines with little or no modifications.

1.2 NEED FOR BIODIESEL

Increased dependence on imported fuel and regulations on the exhaust emissions of vehicles established by the Environmental Protection Agency (EPA) has increased the need for alternative fuels. Alternative fuels from agricultural crops are the desirable substitute for diesel because they are sustainable and have fewer emissions than petroleum products.

In January 2001, the EPA finalized a rule that will require sulfur levels in diesel fuel to be reduced from 500 parts per million (ppm) to 15 ppm, in the year 2006. The petroleum industry and equipment manufacturers all acknowledged during the rulemaking process that the refinery changes necessary to meet this requirement would also dramatically reduce the lubricity of the fuel (ISA, 2004). Lubricity is the

characteristic in diesel fuel necessary to keep fuel injection pumps properly lubricated. Fuel that lacks lubricity can cause premature wear or malfunction (ISA, 2004). Biodiesel fuel has higher lubricity than a diesel fuel and can be used as an additive to improve the lubricity of the diesel fuel (Howell, 1995; Knothe and Steidley, 2004).

1.3 MANUFACTURING OF BIODIESEL

Biodiesel fuel is a fuel extracted from a fat or vegetable oil, such as soybean and rapeseed, and is processed by using a base or acid to catalyze or accelerate the transesterification (Ma and Hanna, 1999; Holmberg and Osterberg, 1989). A base catalyst is preferred, because the reaction is fast and thorough, and occurs at lower temperature and pressure (150° F and 20 psi). The catalyst used for a base reaction is typically sodium or potassium hydroxide. Methanol and the catalyst are mixed to produce methoxide. The methoxide is then mixed with the vegetable oil to produce methyl ester (biodiesel) and glycerin (Figure 1.1). Methanol is recovered and can be used again for the reaction (NBB, 2004; Schuchardta, et al., 1998; Vicente, et al., 2004).

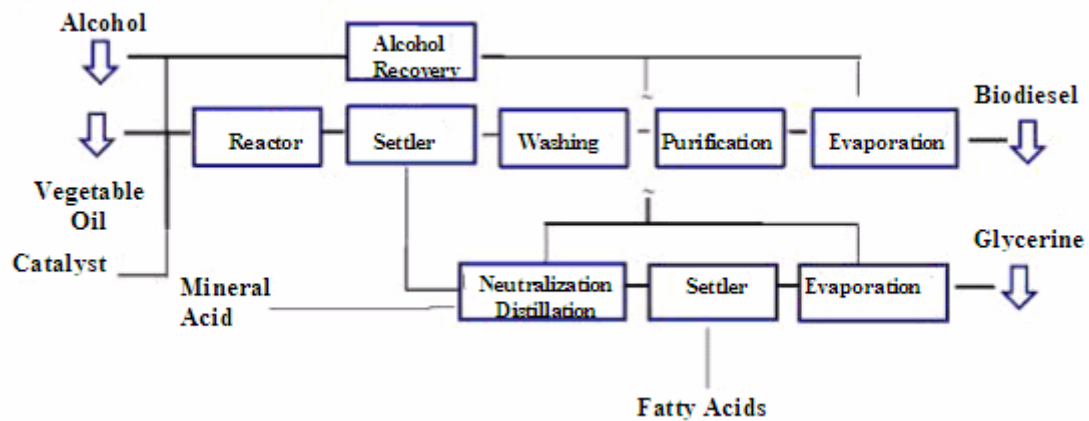


Figure 1.1: Transesterification of Vegetable Oil to Biodiesel (NBB, 2004)

1.4 CHEMICAL REACTION

The chemical reaction for making methyl esters of fatty acids from triglycerides is shown in Figure 1.2. The fat or oil used is reacted with methoxide to produce the biodiesel and glycerol.

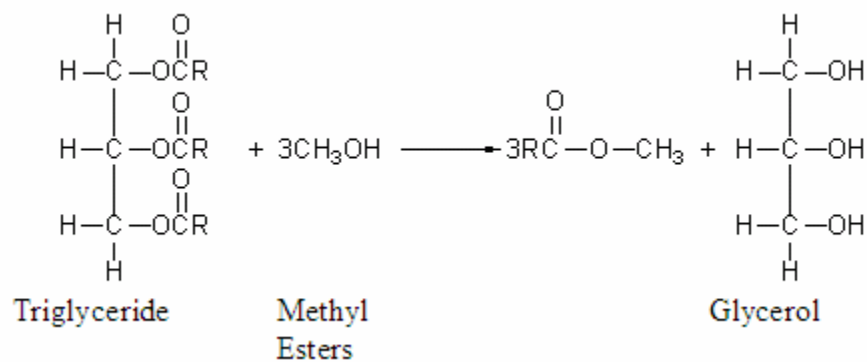


Figure 1.2: Formation of Methyl Ester from Triglycerides (NI, 2005)

1.5 CHEMICAL AND PHYSICAL PROPERTIES OF BIODIESEL AND DIESEL PRODUCTS

Biodiesel is a renewable, non-toxic and biodegradable source of energy; however due to the current price of soybean oil, biodiesel is more expensive to produce than petroleum derived diesel fuel. Most commonly used is 20% blend of biodiesel with petroleum diesel is commonly used. Biodiesel is 11% oxygen by weight and contains no sulfur. The use of biodiesel can extend the life of diesel engines because it is a better lubricant than petroleum diesel fuel, while fuel consumption, auto ignition, power output, and engine torque are relatively unaffected by biodiesel (NBB, 2005a). Therefore mixing biodiesel with diesel ensures adequate fuel lubricity while eliminating overdosing concerns present with other additives. This gives a clear advantage to use biodiesel blends (Wang, 2003).

1.5.1 ENERGY CONTENT

Biodiesel has lower energy content than petroleum diesel - both on a weight basis and a volume basis. The Figure 1.3 showed the comparison of energy contents of biodiesel with No. 2 diesel (NI, 2005).

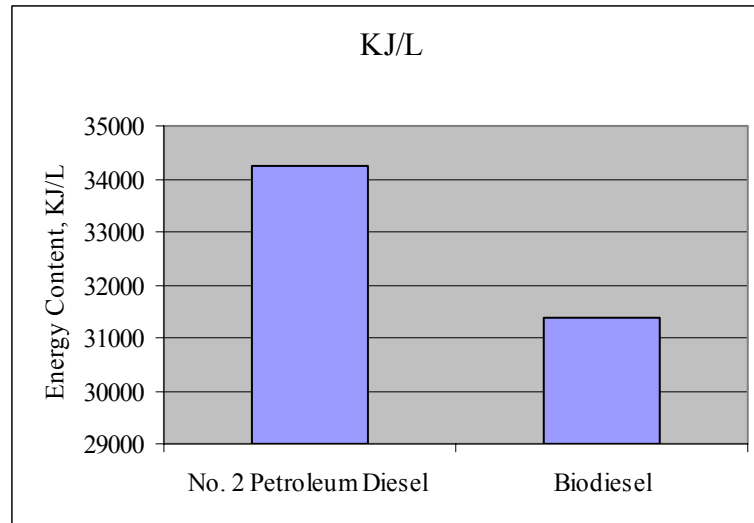


Figure 1.3: Energy Content of Biodiesel and Petroleum Diesel (NI, 2005)

1.5.2 CETANE NUMBER

The Cetane number measures the ignition delay and smoothness of combustion. High Cetane helps improve ignition and starting, even at low temperature and low ignition pressure (Akasaka and Sakurai, 1994; Knothe, et al., 2003; Krisnangkura, 1986; Ladommatos and Goacher, 1995). Figure 1.4 shows the Cetane number for different biodiesel with normal diesel fuel.

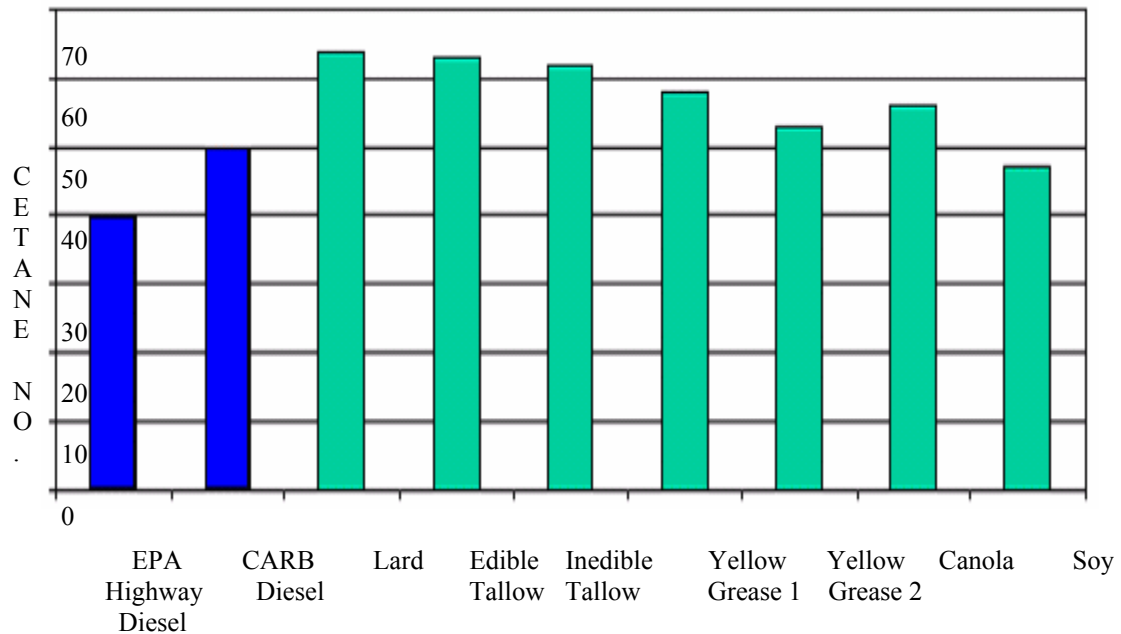


Figure 1.4: Cetane Numbers for Common Diesel and Biodiesel Fuel (NBB, 2005a)

1.5.3 EMISSIONS

In addition to some improved chemical properties, biodiesel also has low emissions of particulate matter, unburned hydrocarbon particles and carbon monoxide, except oxides of nitrogen which is minimally higher than diesel fuel (PF, 2005).

Biodiesel fuel reduces most of the exhaust emissions from the engine; however, an increase in NO_x has been noted (Tat and Van Gerpen, 2001; Choi and Reitz, 1999; Song, et al., 2002). But there are antioxidants additions that can reduce the NO_x effect (Hess, et al., 2005). Figure 1.5 compares the emissions of major air pollutants from diesel and biodiesel.

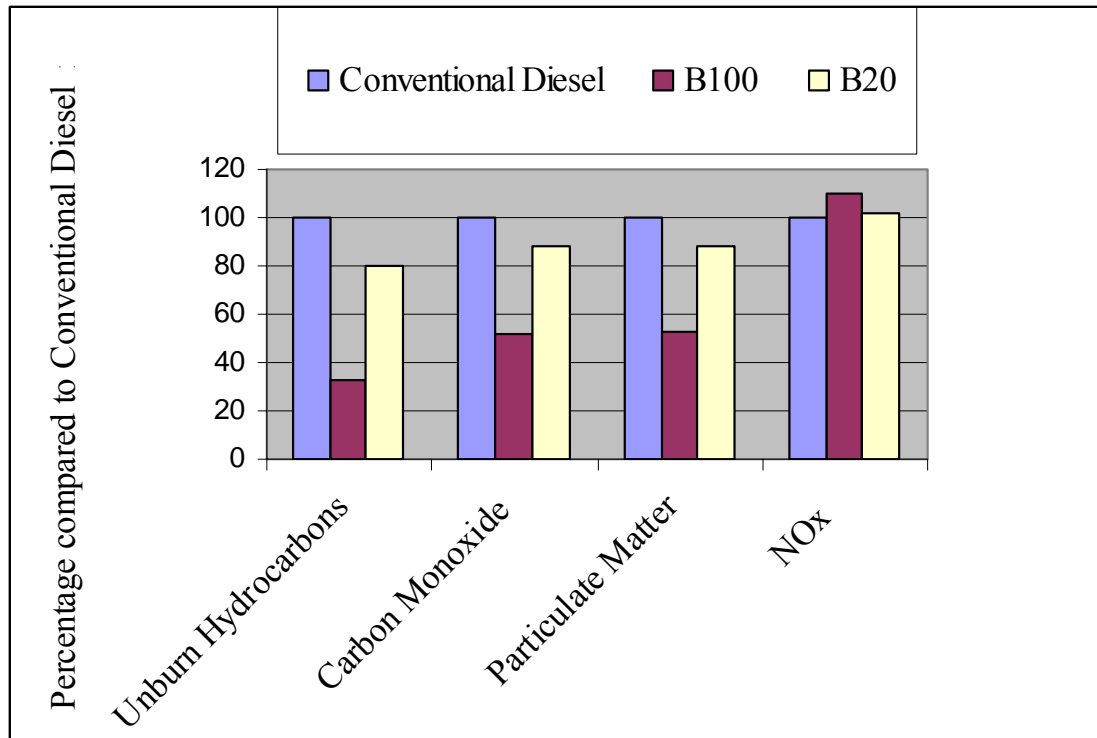


Figure 1.5: Average Biodiesel Emissions Compared to Conventional Diesel (NBB, 2005b)

1.5.4 FLASHPOINT

The flashpoint temperature is the temperature at which a fuel ignites when a spark is provided to the fuel. Biodiesel has a higher flashpoint when compared to diesel fuel which means biodiesel is safer than standard diesel fuel. Figure 1.6 shows the fuel flashpoint comparison (NBB, 2005c). Here Bunker fuel is the No. 6 fuel oil.

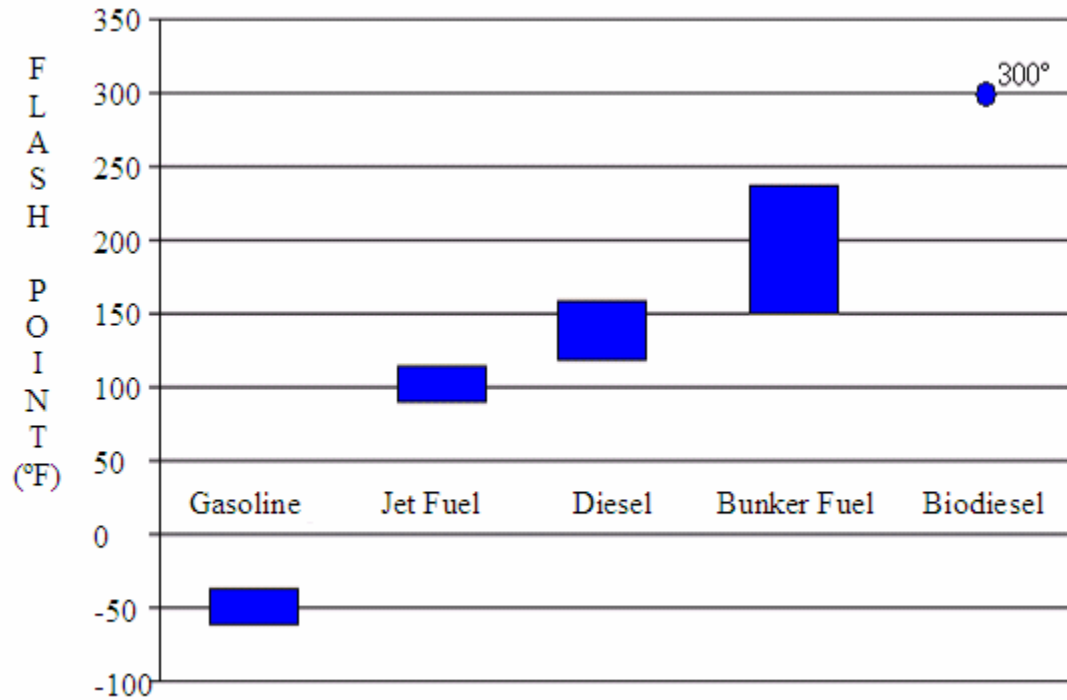


Figure 1.6: Fuel Flashpoint Comparisons between Gasoline, Jet Fuel, Diesel, Bunker Fuel (No. 6 Fuel Oil) and Biodiesel (NBB, 2005c)

1.6 PROTECTIVE MEASURES WITH BIODIESEL FUEL

1.6.1 EFFECT OF BIODIESEL ON PAINTED SURFACE

Biodiesel is a good solvent and if left on a painted surface will dissolve certain types of paints. Therefore, it is recommended to wipe any biodiesel or biodiesel blend spills from painted surfaces immediately and wash with warm soapy water.

1.6.2 BIODIESEL SOAKED RAGS

Biodiesel soaked rags should be stored in a safety can or dried individually to avoid the potential for spontaneous combustion. Biodiesel can oxidize and degrade over time, which can produce heat. In certain environments, for example, a pile of oil soaked rags can become concentrated enough to result in a spontaneous fire (as can petroleum soaked rags).

1.7 USING BIODIESEL IN COLD WEATHER

A major drawback with the use of biodiesel is that it has poor cold flow properties as compared to diesel fuel. Cloud point is the temperature at which the fuel starts to appear cloudy due to the wax crystals that can block the fuel lines and filters. Since the cloud and pour points of biodiesel are higher than diesel fuel, vehicles running on biodiesel may experience more fuel system plugging problems than petroleum diesel fuel products (Chiu, et al., 2004; Copeland, et al., 2006).

1.8 LIMITATIONS WITH BIODIESEL FUEL

1.8.1 COST

The cost of biodiesel fuels varies depending on the feedstock, geographic area, and variability of crop production from season to season, production facilities and many other factors. This cost may be reduced if a relatively inexpensive feedstocks, such as waste oils or rendered animal fat are used instead of soybean, corn or other virgin plant oil. However, even if waste oils are used, the average cost of biodiesel fuel often exceeds that of petroleum-based diesel fuel.

One advantage is the cost of converting to biodiesel blends, to the cost to begin fueling with biodiesel blend is much lower than the cost of converting to any other alternative fuel because no major engine, vehicle, or dispensing system changes are required (Holfman, 2003).

CHAPTER 2

LITERATURE REVIEW

2.1 INTRODUCTION

Although biodiesel can be used in engine with very little or no modification, improvements that prevent the fuel from plugging the engine in cold weather would be beneficial (Bessee and Fey, 1997).

To overcome this problem biodiesel fuel should not reach the cloud point in the vehicle. To keep fuel liquid, vehicles used fuel line heaters and fuel tank heaters (CDCI, 2005). Turning on fuel line or fuel tank heaters causes the vehicle to consume more energy, which is not efficient and essentially increases the cost of biodiesel.

2.2 COLD FLOW PROPERTIES OF DIESEL AND BIODIESEL

Several cold flow properties of the diesel and biodiesel fuel are generally used to classify cold weather performance: cloud point (CP), pour point (PP), low temperature filterability test (LTFT) and cold filter plugging point (CFPP).

2.2.1 CLOUD POINT

Cloud point is the temperature of a liquid specimen when the smallest observable cluster of wax crystals first appears upon cooling under prescribed conditions (ASTM, 2002a). ASTM D2500-02 is the standard manual test method for cloud point of petroleum products.

The cooling bath temperature is maintained at 0 ± 1.5 degree Celsius. Each test is taken at the multiples of 1 degree Celsius, until the fuel candidate shows a cloud of wax crystals in the test jar. The standard also states that a wax cloud always forms first at the bottom of a test jar where the temperature of the fluid is lowest.



2.2.2 POUR POINT

The pour point is the lowest temperature at which movement of the test specimen is observed under the prescribed conditions (ASTM, 2002b).

ASTM D5949-02 is the standard method for detecting the pour point of petroleum products using an automatic pressure pulsing method. An automatic apparatus consisting of a microprocessor controlled test chamber for controlled heating and cooling of the test fuel, as well as sensors for recording temperature and optically detecting the test fuel movement as shown in the Figure 2.2. The fuel is first heated and then cooled using the Peltier device at the rate of $1.5 \pm 0.1^\circ\text{C}/\text{min}$. A pulse of pressurized nitrogen gas is applied to the surface of the fuel. The specimen is illuminated by the light source and the movement of fuel is monitored using an array of optical sensors. The temperature is decreased at $0.1^\circ\text{C}/\text{min}$ until no movement of specimen is observed. The lowest temperature at which the movement of fuel was observed is established as the pour point.

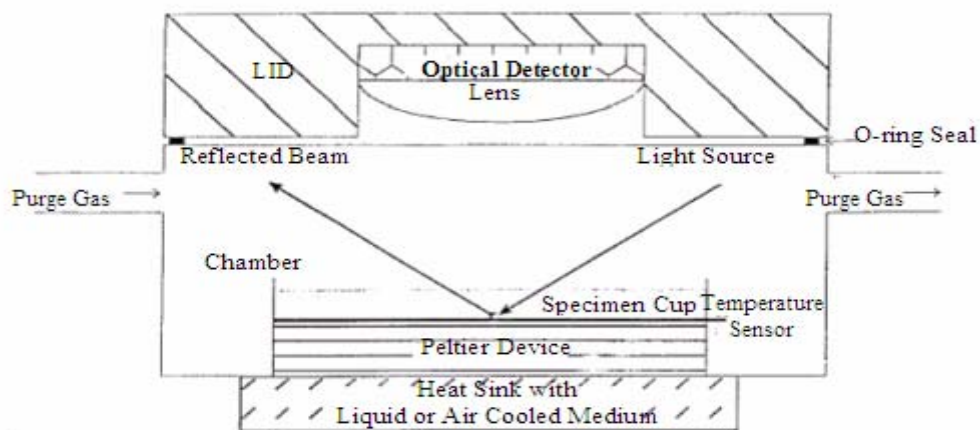


Figure 2.2: Detection of Test Fuel Movement in Test Chamber (ASTM, 2002b)

2.2.3 LOW-TEMPERATURE FLOW TEST (LTFT)

The Low Temperature Flow Test (LTFT) is a minimum pass temperature, expressed as a multiple of 1°C, at which a test fuel can be filtered in 60 seconds or less (ASTM, 2003).

ASTM D4539-03 consists of an apparatus having a filter assembly as shown in Figure 2.3, with a programmable cooling system, capable of cooling multiple samples, to the desired temperature at the mean rate of 1°C per hour between +10°C and -30°C.

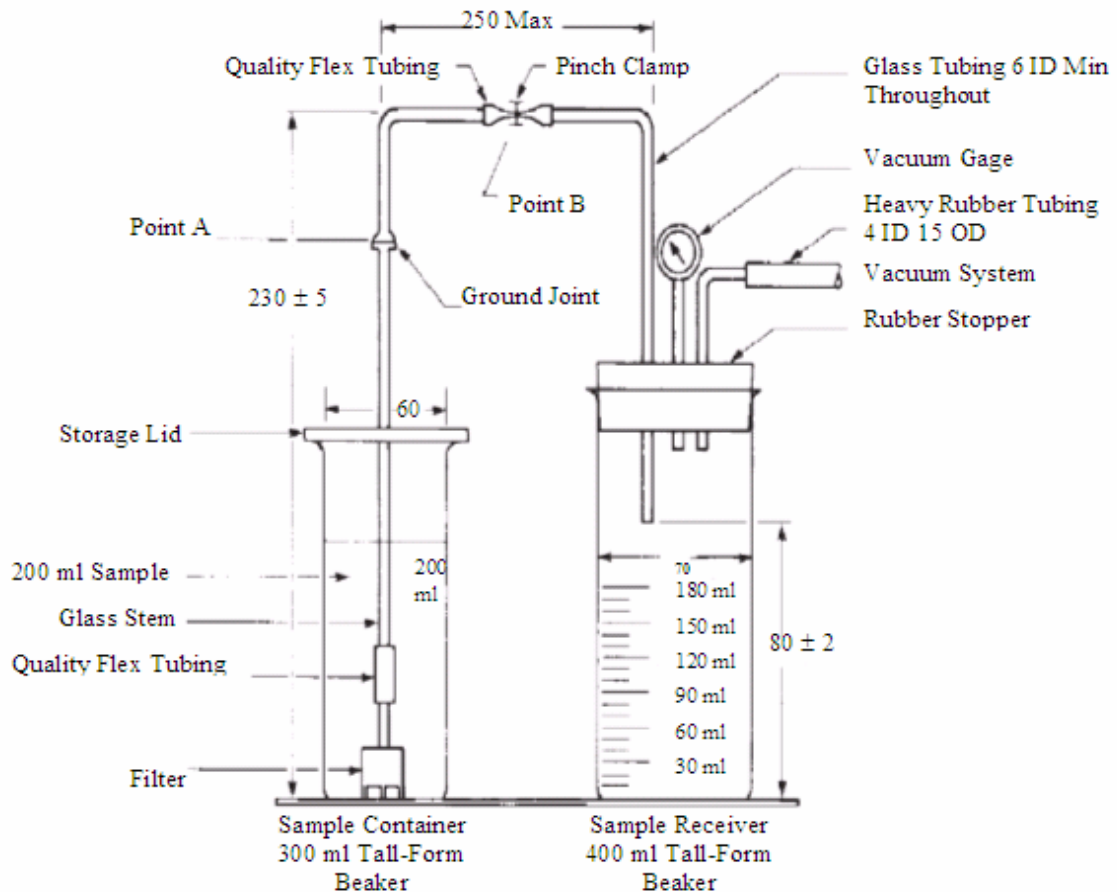


Figure 2.3: LTFT Sample Filtration Assembly (ASTM, 2003)

2.2.4 COLD FILTER PLUGGING POINT (CFPP)

The Cold Filter Plugging Point is the highest temperature, expressed in the multiples of 1° C, at which a given volume of fuel fails to pass through a standardized filtration device in a specified time when cooled under the conditions prescribed in test method (ASTM, 1999).

The sample to be tested is cooled at an interval of 1° C. The fuel is drawn into the pipette under controlled vacuum. The testing is continued until the wax crystals that have been separated from out of solution is sufficient to stop or slow down the flow, so that the time of flow through the pipette is more than 60 seconds (Figure 2.4).

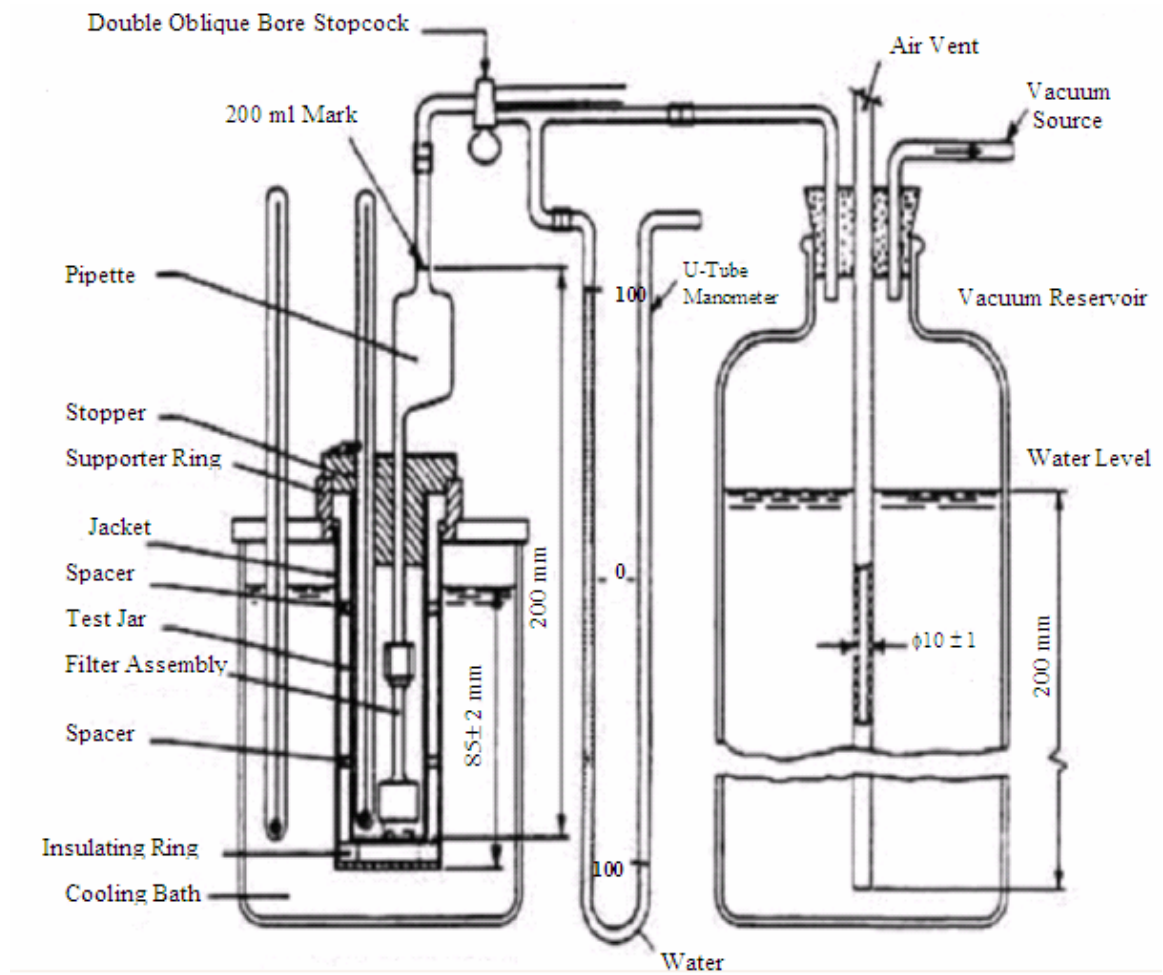


Figure 2.4: CFPP Apparatus Assembly (ASTM, 1999)

2.3 Why Detect Cloud Point?

In the winter season, the temperature of the environment can drop below the freezing point and the cloud point of biodiesel fuel (Table 2.1).

Table 2.1 shows the tenth percentile minimum ambient air temperatures taken from a study conducted by the U.S. Army Mobility Equipment Research and Development Center, Coating and Chemical Laboratory, Aberdeen Proving Ground, MD 21005 (ASTM, 2004). The readings are recorded over a period of 15 to 21 years from 345 weather stations in the United States (ASTM, 2004).

In most of the United States, especially in the months of December through March, the environmental temperature can drop low enough to freeze biodiesel fuel. Therefore, it is important to know the anticipated environmental temperature so that protective measures are taken to prevent freezing of biodiesel fuel in an automobile.

Table 2.1: Tenth Percentile Minimum Ambient Air Temperature for the United States (ASTM, 2004)

State		10th Percentile Temperature°C, min					
		Oct.	Nov.	Dec.	Jan.	Feb.	March
Alabama		4	-3	-6	-7	-3	-2
Alaska	Northern	-25	-37	-45	-49	-47	-43
	Southern	-11	-13	-18	-32	-32	-29
	South East	-4	-11	-16	-19	-13	-12
Arizona	North 34° latitude	-4	-12	-14	-17	-16	-12
	South 34° latitude	7	0	-2	-4	-3	-1
Arkansas		2	-4	-7	-11	-7	-3
California	North Coast	3	0	-2	-2	-1	-1
	Interior	2	-3	-4	-7	-6	-6
	South Coast	6	2	0	-1	0	2
	Southeast	1	-6	-8	-11	-7	-5
Colorado	East 105° long	-2	-12	-14	-19	-15	-12
	West 105° long	-8	-18	-25	-30	-24	-16
Connecticut		-1	-7	-16	-17	-16	-9
Delaware		2	-3	-10	-11	-10	-6
Florida	North 29° latitude	7	1	-2	-3	-1	2
	South 29° latitude	14	7	3	3	5	7
Georgia		3	-2	-6	-7	-6	-2
Idaho		-4	-13	-18	-21	-18	-13
Illinois	North 40° latitude	-1	-9	-19	-21	-18	-11
	South 40° latitude	1	-7	-16	-17	-15	-8
Indiana		-1	-7	-16	-18	-16	-9
Iowa		-2	-13	-23	-26	-22	-16
Kansas		-2	-11	-15	-19	-14	-13
Kentucky		1	-6	-13	-14	-11	-6
Louisiana		5	-1	-3	-4	-2	1
Maine		-3	-10	-23	-26	-26	-18
Maryland		2	-3	-10	-12	-10	-4
Massachusetts		-2	-7	-16	-18	-17	-10
Michigan		-2	-11	-20	-23	-23	-18
Minnesota		-4	-18	-30	-34	-31	-24
Mississippi		3	-3	-6	-6	-4	-1
Missouri		1	-7	-14	-16	-13	-8
Montana		-7	-18	-24	-30	-24	-21
Nebraska		-3	-13	-18	-22	-19	-13
Nevada	North 38° latitude	-7	-14	-18	-22	-18	-13
	South 38° latitude	8	0	-3	-4	-2	1
New Hampshire		-3	-8	-18	-21	-21	-12
New Jersey		2	-3	-11	-12	-11	-6
New Mexico	North 34° latitude	-2	-11	-14	-17	-14	-11
	South 34° latitude	4	-4	-8	-11	-7	-3
New York	North 42° latitude	-3	-8	-21	-24	-24	-16
	South 42° latitude	-1	-5	-14	-16	-15	-9
North Carolina		-1	-7	-10	-11	-9	-5
North Dakota		-4	-20	-27	-31	-29	-22
Ohio		-1	-7	-16	-17	-15	-9
Oklahoma		1	-8	-12	-13	-8	-7
Oregon	East 122° long	-6	-11	-14	-19	-14	-9
	West 122° long	0	-4	-5	-7	-4	-3
Pennsylvania	North 41° latitude	-3	-8	-19	-20	-21	-15
	South 41° latitude	0	-6	-13	-14	-14	-8
Rhode Island		1	-3	-12	-13	-13	-7
South Carolina		5	-1	-5	-5	-3	-2
South Dakota		-4	-14	-24	-27	-24	-18
Tennessee		1	-5	-9	-11	-9	-4
Texas	North 31° latitude	3	-6	-9	-13	-9	-7
	South 31° latitude	9	2	-2	-3	-1	2
Utah		-2	-11	-14	-18	-14	-8
Vermont		-3	-8	-20	-23	-24	-15
Virginia		2	-3	-9	-11	-9	-4
Washington	East 122° long	-2	-8	-11	-18	-11	-8
	West 122° long	0	-3	-3	-7	-4	-3
West Virginia		-3	-8	-15	-16	-14	-9
Wisconsin		-3	-14	-24	-28	-24	-18
Wyoming		-4	-15	-18	-26	-19	-16

2.4 DETECTION OF CLOUD POINT USING SENSOR TECHNOLOGIES

In recent years, vehicles with advanced technology have been developed that are more flexible so that they can run on fuels such as ethanol and gasoline. Sensors were developed to maintain the compatibility between the engine and the fuel, so that the performance can be improved or maintained with reduced emissions (Kopera, 1992; Meitzer and Saloka, 1992; Niehaus, et al., 1985 and Schmitz, et al., 1990). But this has not yet happened for biodiesel operated vehicles in United States.

There are number of technologies that exist to measure the cloud point of a biodiesel fuel; the most common sensor technologies being capacitive and optical.

2.4.1 CAPACITIVE SENSOR

Capacitive sensors developed are cylindrical capacitor sensors used to detect the changes in dielectric constant as the fuel composition changes (Wigg and Lunt, 1974; Schmitz and Kutz, 1990). The capacitor is housed in a cell incorporated into the fuel line of a vehicle and placed close to the engine (Meitzer and Saloka, 1992).

A dielectric sensor was used to measure the blend ratio of the biodiesel fuel (Javvadi, 2005). It worked on the principle of capaciflector. When the object was placed in the electric field, the dielectric constant of the sample changed, due to the blend ratio of the biodiesel / petroleum diesel.

2.4.2 OPTICAL SENSOR

Optical sensors have been developed for measuring blend concentration in blended fuel and to measure gasoline quality (Schmitz, et al., 1990). They used a fuel composition sensor. A parallel beam of light is emitted from a near infrared LED through the rod prism at one end of prism where the fuel is to be measured. After the light beam is refracted through the boundary surface, the light beam is reflected by the reflex mirror (Suzuki and Ogawa, 1991).

Figure 2.5 shows the cross sectional view of the structure of the sensor. An optical sensor was also used for assessing biodiesel fuel quality by near-infrared spectroscopy using a fiber-optic probe (Knothe, 1998; Knothe 1999).

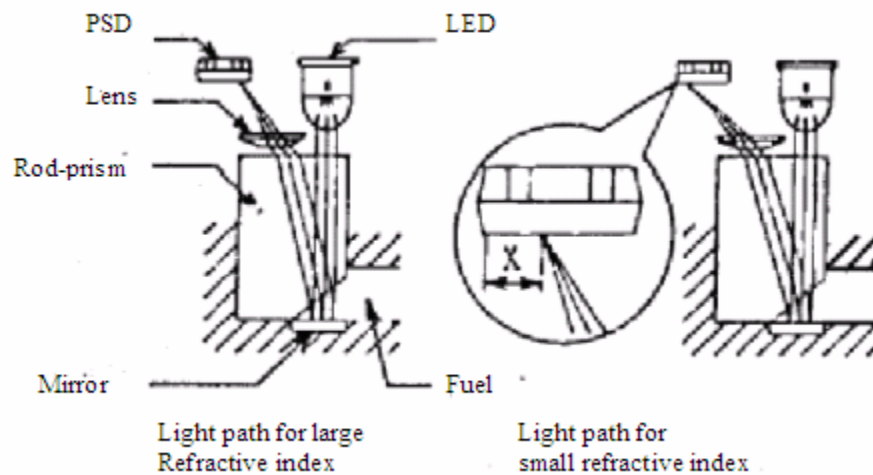


Figure 2.5: Schematic of Optical Fuel Sensor (Suzuki and Ogawa, 1991)

2.5 ASTM STANDARDS

Several ASTM standards exist to determine the cloud point of a fuel like ASTM D5771-02, ASTM D5772-02 and ASTM D5773-02. These ASTM Standards that are used to determine cloud point for diesel and biodiesel blends are described below.

2.5.1 ASTM D5771

ASTM D5771 (2002) is a standard test method to determine the cloud point of petroleum products. This test method uses an optical detection stepped cooling method. It covers the range of temperatures from -40°C to 49°C with a temperature resolution of 0.1°C . A microprocessor controlled cloud point apparatus can continuously controls the temperature of one or more independent test cells and detects the appearance of the cloud point at the bottom of the beaker. The detection of cloud point is done using a light emitter on one side and light receiver at the other side of the beaker (Figure 2.6).

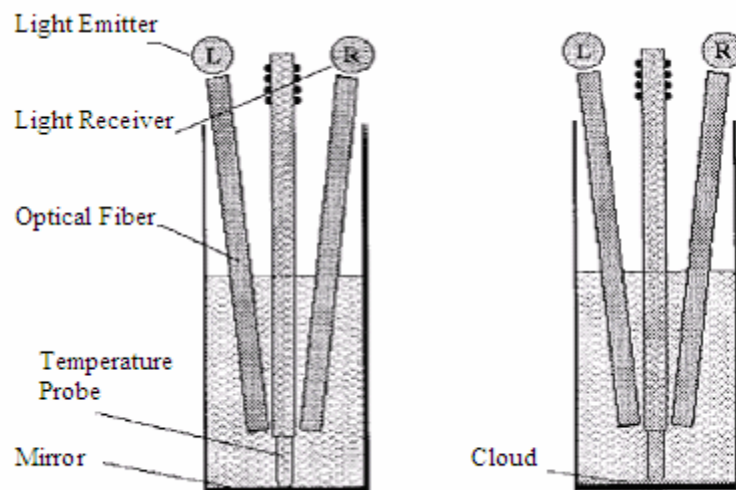


Figure 2.6: Detection of Cloud Point Using Light Emitter (ASTM, 2002c)

The control of temperature is governed by the cooling circulation bath as shown in the figure 2.7. To avoid the moisture in the sample, the sample is filtered through dry lint- free filter paper, until the fuel is clear.

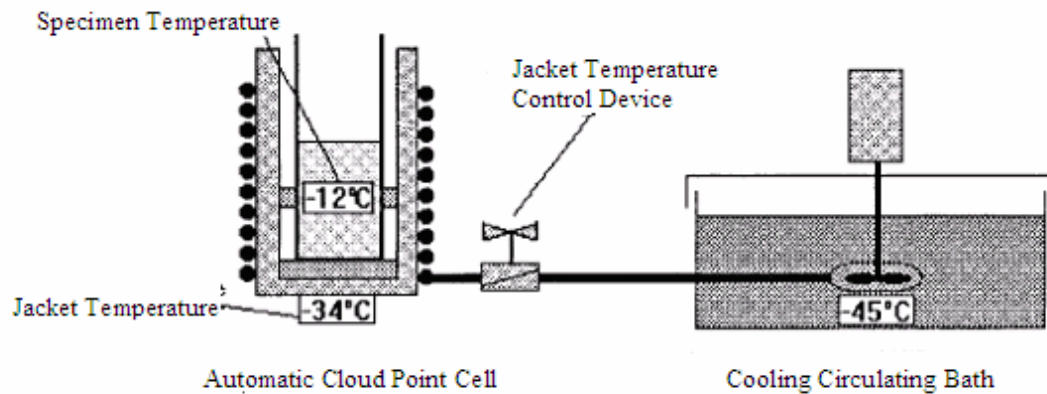


Figure 2.7: Test Jar Cooling Chamber and Circulating Bath (ASTM, 2002c)

2.5.2 ASTM D5772

ASTM D 5772 (2002) uses the linear cooling rate method for detection of the cloud point of biodiesel and diesel fuel. It consists of an automatic cloud point apparatus that has a microprocessor- controlled measuring unit. The unit is capable of cooling the sample, optically observing the cloud point and recording the temperature with a resolution of 0.1° C. This method uses an optical barrier assembly and test cell that consists of a light transmitter and the light receiver, with the temperature measuring device mounted on the top of the assembly (Figure 2.8). For the circulating bath, a refrigerator equipped circulation pump is used with a temperature at least 20° C lower than expected cloud point of the fuel.

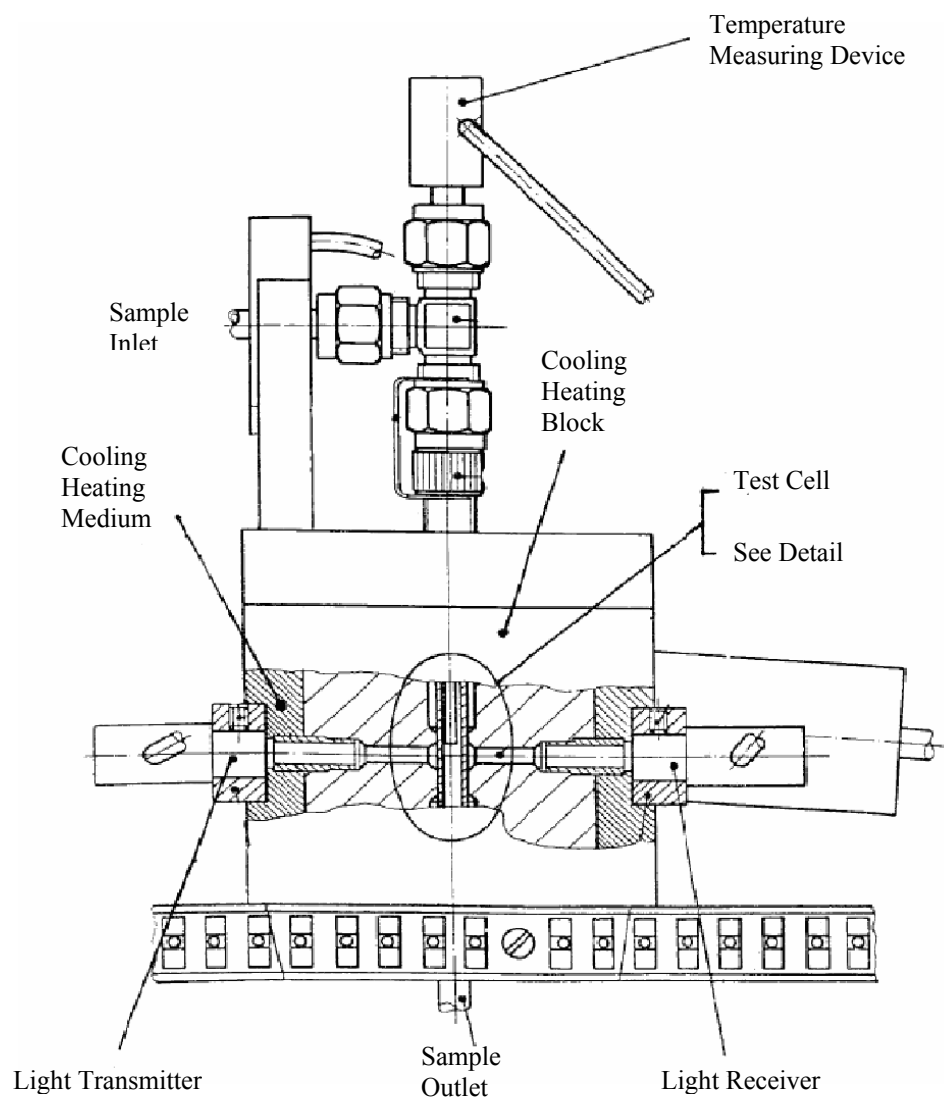


Figure 2.8: Test Assembly for Measuring Cloud Point Using Linear Cooling Rate Method (ASTM, 2002d)

2.5.3 ASTM D5773

ASTM D5773 (2002) uses a constant cooling rate to determine cloud point by an automatic instrument using an optical device to detect crystal formation. It consists of a solid-state thermoelectric device that has semiconductor material called a Peltier device to cool the fuel sample. It uses the same peltier device shown in Figure 2.2. It uses a light source with wavelength 660 ± 10 nm positioned at an acute angle with the light reflected off the polished bottom of the specimen cup. A microprocessor uses a temperature sensor with resolution of 0.1°C to control the cooling of the fuel test. When wax crystals appear in the fuel, there will be change in the phase boundaries of the reflected beam. This change indicates the cloud point (ASTM, 2002e).

2.6 COMMERCIAL AVAILABLE CLOUD POINT DETECTORS

2.6.1 KLA-3 AUTOMATIC CLOUD POINT SYSTEM

KLA-3 Automatic Cloud Point System (Koehler Instrument Company, Bohemia, N.Y., 2004) is an instrument that detects cloud point by emitting a light pulse every 1 degree Celsius, the light pulse reflects off the silver coating on the bottom test jar surface to an optical sensor. The software analyzes the light response until an initial haze is detected by the light scattering (KIC, 2004). KLA-3 automatic cloud point system, meets ASTM D2500 requirements.

2.6.2 KITTIWAKE CLOUD POINT DETECTOR

The Cloud Point Detector is an automatic device, used for detecting the temperature at which wax crystals form in a translucent oil sample, causing it to become cloudy in appearance. This device operates by cooling an oil sample and monitoring the intensity of light transmitted through the sample (Figure 2.11). It meets IP 219 and ASTM D2500 requirements. The unit allows cloud point tests to be carried out before accepting the fuel and a normal test takes less than 10 minutes (Kittiwake, 2006).

2.6.3 CRYSTAL - CLOUD POINT DETECTOR

The crystal cloud point detector is intended for crystallization temperature measurement of the jet-plane fuel, diesel fuel cloud-point and freezing temperature measurement, motor oil freezing temperature and dynamic viscosity measurement in laboratory and field conditions. The instrument can detect up to -60°C and has an LCD display which shows the examination process in real time mode. It meets ISO 9000 requirements (EAL, 2006).

2.7 OBJECTIVES

The goal of this research is to determine the optical properties of biodiesel fuel and blends of biodiesel fuel as they start to cloud from the liquid to solid phase. Specific goals were to:

- Develop a test stand and sensor configuration for the system.
- Measure the spectral properties of blends of biodiesel fuel using the test stand.
- Detect the phase change in blends of biodiesel fuel due to the change in optical properties.
- Determine the best optical wavelength for detecting cloud point in blends of biodiesel.

CHAPTER 3

MATERIAL AND METHODS

This chapter discusses the apparatus used to detect optical properties of different blends of biodiesel fuel. It shows the test stand, the optical sensor that we developed, and the materials required for the experimentation process.

3.1 APPARATUS

3.1.1 TEST STAND

The test stand consists of two pumps, one to control the flow of alcohol through the dry ice bath and second to control the flow of biodiesel fuel. Dry ice was purchased from Columbia Ice (Columbia, MO). Hot water was connected directly from hot water tap to warm the fuel. Thermocouples were connected to measure the temperature of the fuel before and after the heat exchangers. The fuel was circulated through the system as shown in Figure 3.1.

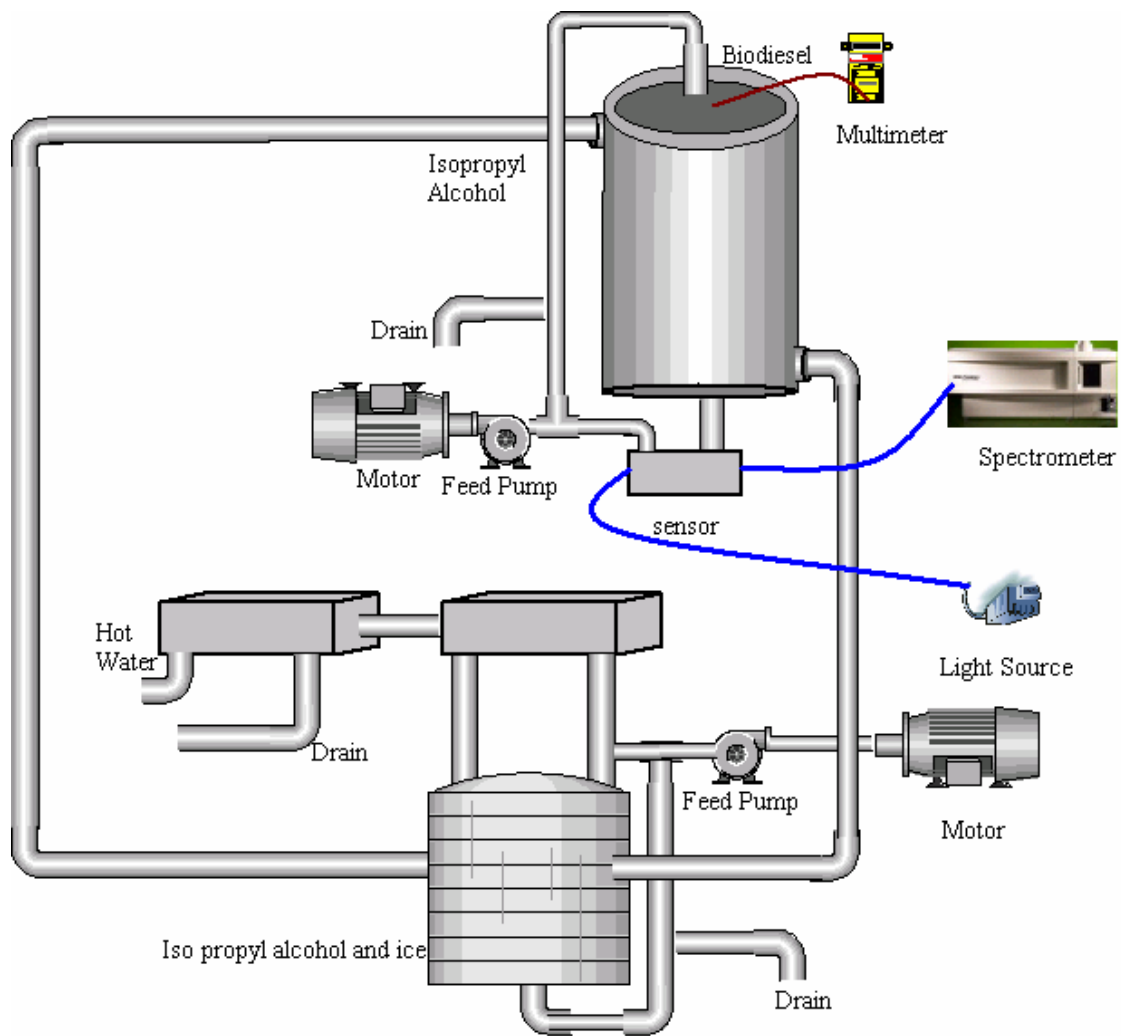


Figure 3.1 Test Stand Diagram for Testing Sensor Operation

3.1.2 BIODIESEL COOLING CYLINDER

The heat exchanger was made from two concentric circular cylinders. Isopropyl alcohol was circulated by the pump between the walls of the inner and outer cylinder. The biodiesel circulated through the inner cylinder as shown in Figure 3.2.

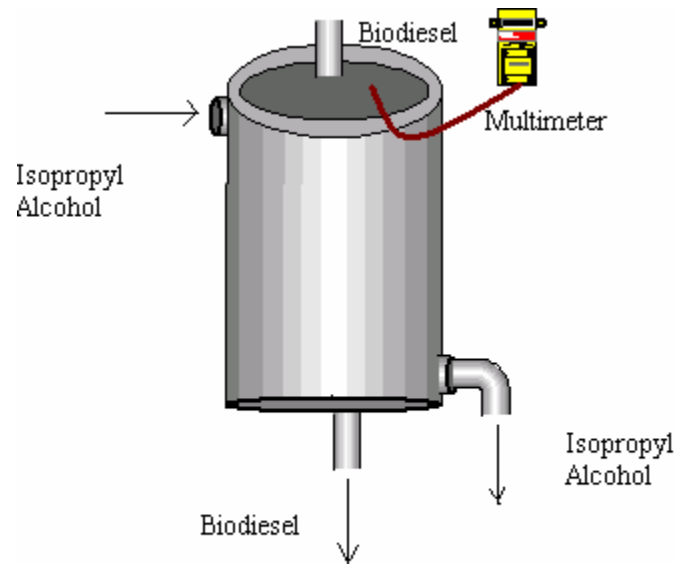


Figure 3.2 Biodiesel Cooling Cylinder

3.1.3 COOLING SYSTEM EXCHANGER

The temperature of biodiesel fuel was controlled by decreasing the flow of isopropyl alcohol in the dry ice / isopropyl alcohol bath as shown in Figure 3.3. The computer controlled the flow of isopropyl alcohol. Readings were taken at every one degree change till the cloud point was reached. The fuel in the heat exchanger froze, blocking the flow of fuel; therefore, heat exchanger was bypassed.

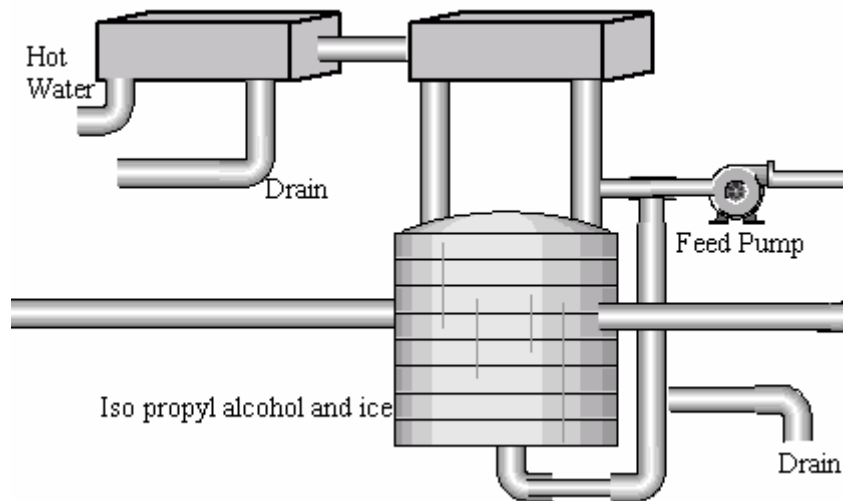


Figure 3.3: Temperature Control for the Test Stand

3.2 SENSOR

3.2.1 BASIC PRINCIPLE

The sensor used the principle of transmittance of light, as shown in Figure 3.4, to detect transmittance of light through blends of biodiesel fuel. Transmittance is given by

$$T = I_E / I_0$$

Where I_E = intensity of transmitted light

I_0 = intensity of incident light

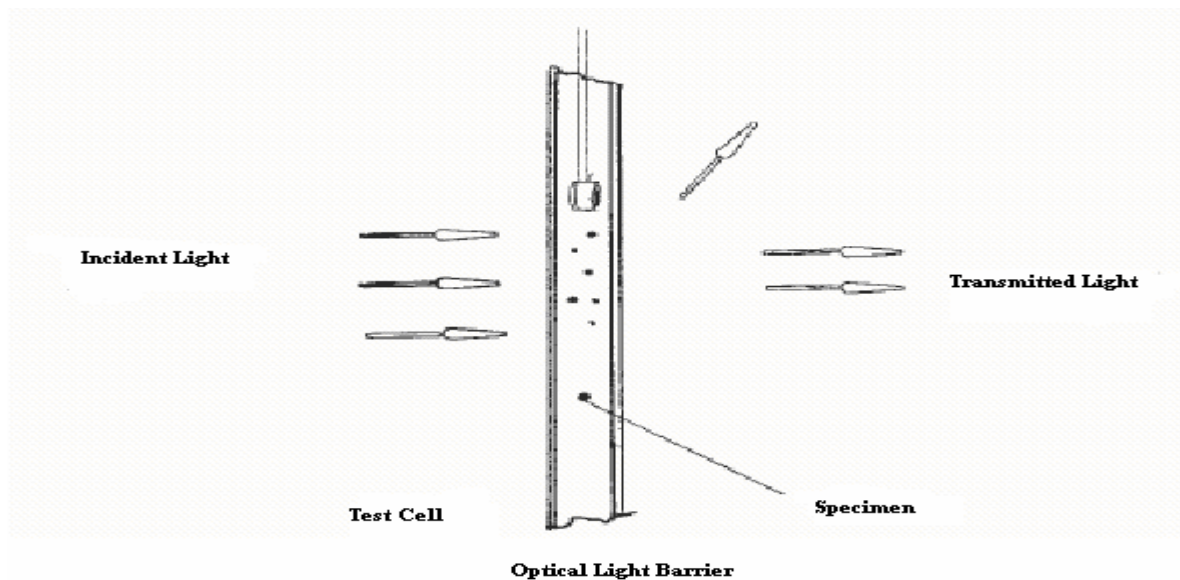


Figure 3.4: Transmittance of Light Through the Test Cell (ASTM, 2002d)

3.2.2 SENSOR CONSTRUCTION

The sensor was made from stainless steel to ensure material compatibility. The lenses were embedded inside the sensor using O-rings and internal lock rings. The ray of light was passed to one side of the sensor through the fiber cable as shown in Figure 3.5. The light ray traveled from the assembly of convex and concave lenses and was collected on the other side of the sensor. The other side of the sensor was connected to spectrometer through a fiber cable. The outer view of stainless steel is shown in Figure 3.6. Figure 3.7 shows the outside view and cross section of the sensor assembly and the direction of the light traveling through the sensor assembly. APPENDIX A contains the drawings for the sensor.

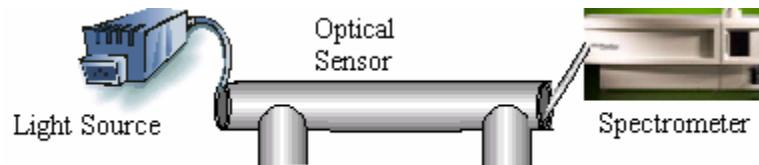


Figure 3.5: Overview of Detection of Signal Using Optical Sensor

The spectral properties of biodiesel fuel were measured using the spectrometer. With a change in temperature of biodiesel fuel, the optical properties of the fuel changed. The optical properties of biodiesel fuel were detected using an optical sensor connected to the spectrometer.

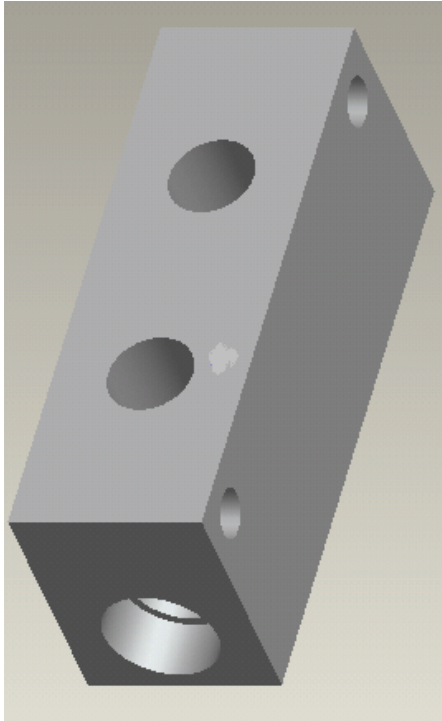


Figure 3.6: Outerview of the Sensor Housing

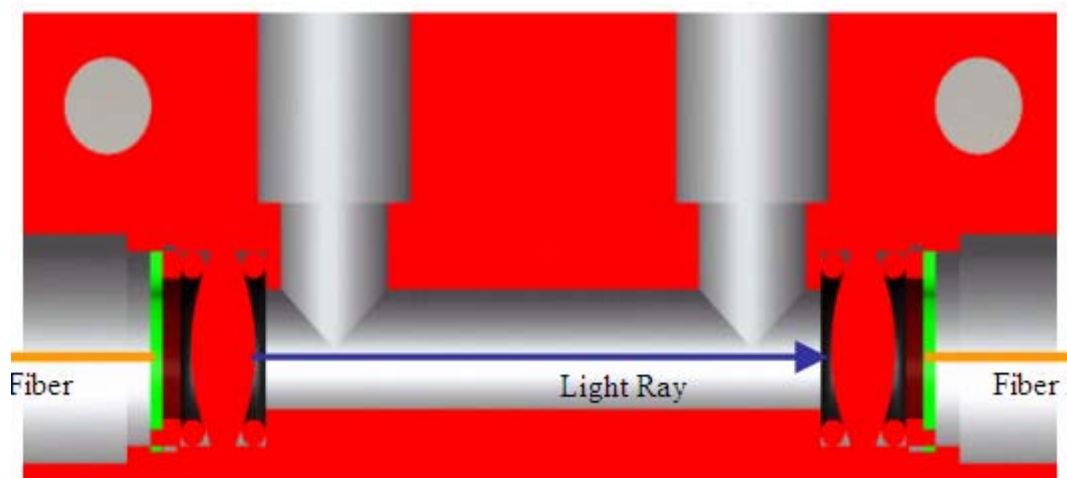


Figure 3.7: Parts Assembly Inside the Sensor

3.2.3 SNELL'S LAW

The lens assembly was based on the principle of Snell's law. It states that when a ray of light is refracted at an interface dividing two uniform media, the transmitted ray remains within the plane of incidence and the sine of the angle of refraction is directly proportional to the sine of the angle of incidence (Figure 3.8).

Snell's law is given by equation 1:

$$n_1 \sin \theta_1 = n_2 \sin \theta_2 \dots \dots \dots (1)$$

where n_1 is index of refraction in medium 1

n_2 is index of refraction in medium 2

θ_1 is the angle of incidence

θ_2 is the angle of refraction

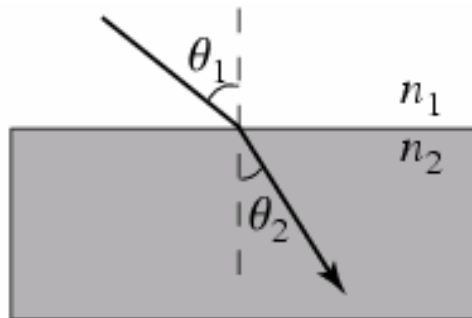


Figure 3.8: Illustration of Law of Refraction

The distance between the light coming from the fiber cable and the lens is adjusted in such a way that the fiber should lie on the focal point of biconvex lens. It is based on the principle of refraction where any incident ray traveling parallel to the principle axis of the converging lens will refract through the lens and travel through the focal point on the opposite side of the lens. Similarly, on the other side of the sensor, the fiber is kept on the focal point of the lens. It is again based on the principle of refraction where an incident ray traveling through the focal point of the way to the lens will refract through the lens and travel parallel to the principle axis as shown in Figure 3.9.

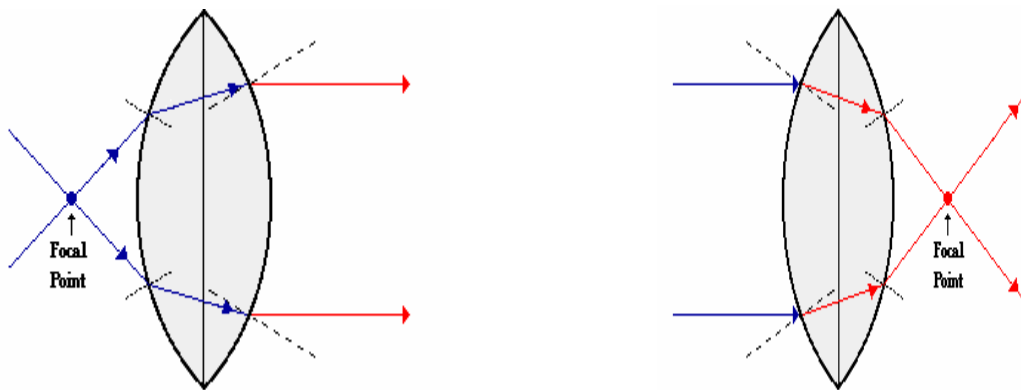


Figure 3.9: Light Source at Focal Point and Light Source at Infinity

3.3 MATERIAL REQUIRED

3.3.1 LIGHT SOURCE

A model LS-1 tungsten halogen light source was purchased from Ocean Optics (Dunedin, FL). The light source is a versatile white-light source optimized for the visible, near infrared (360-2500 nm). The light source featured the standard SMA 905 connector for attaching to the fiber optic cable. Figure 3.10 showed the graph between the wavelengths versus the power output from the light source.

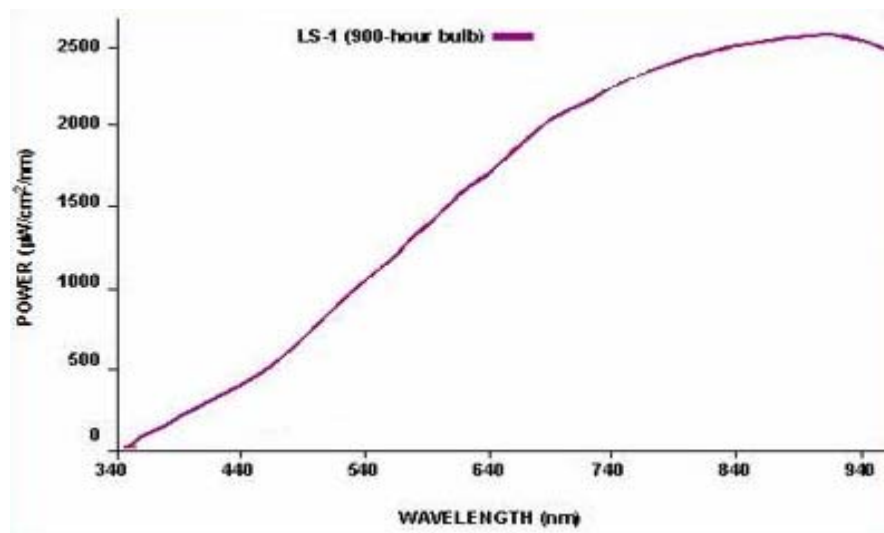


Figure 3.10: Output Power of Tungsten Halogen Light Source for Wavelength From 340nm – 940nm

3.3.2 MOTORS

- Marathon Electric (Wausau, WI)- 725 rpm, 230/460 Volts, 1.6 Amperes. It has 1-400Hz, 240 Volts, and 7 Amperes. The motor was used to control the flow of biodiesel fuel.
- General Electric- 1740 rpm, 230/460 Volts, 1.4 Ampere. It has General Electric AF-300P11 inverter 200-230 Volts, 1-120Hz, 6 Amperes for a 208 Volt system. The motor was used to control the flow of isopropyl alcohol.

3.3.3 PUMP

Two pumps were used to control the flow of fuel and isopropyl alcohol. Pumps were bought from Tuthill Pump Group (Alsip, IL) model no. 4106.

3.3.4 SPECTROMETER

Spectrometer used was Lab Spec Pro 350nm – 2500nm, portable spectrometer with visible and NIR spectral range from 350nm to 2500nm. Spectrometer was purchased from Analytical Spectral Devices (Boulder, CO). It has NiMH battery back with built-in charger. It automatically adjusts gain and offset for optimal signal.

3.3.5 MULTIMETER

A Fluke (Everett, WA) model 189 multimeter was used to take the fuel temperature inside the fuel tank of cooling system.

3.4 FUEL SAMPLE PREPARATION

3.4.1 FUEL

Diesel No. 1 and Diesel No. 2 were ultra-low sulfur diesel fuel purchased from Chevron Phillips Chemical Company (The Woodlands, TX). Biodiesel was purchased from Environmental Products, LLC (Omaha, NE).

3.4.2 BLENDING OF BIODIESEL FUEL WITH DIESEL FUEL

Different blends of biodiesel fuel were prepared by mixing diesel fuel with biodiesel on a volume per volume basis. Conversion of weight to volume was done by taking 100 mL of sample and weighing it. Ten replicates were taken and then the average of those replicates was computed. Kilogram to liter for no. 1 diesel, no. 2 diesel and biodiesel was as follows.

Diesel No.1 = 0.8055 kg/ liter

Diesel No.2 = 0.8055 kg/ liter

Biodiesel = 0.8505 kg/ liter

The weights of the diesel and biodiesel fuel were calculated by the known volume and density of the respective fuel. For example, 15 liters of B2 (2% Biodiesel and 98% Diesel) blend included 14.115 kg of diesel and 0.3193 kg of biodiesel. Therefore, the total weight of blended biodiesel fuel was 14.430 kg. This process was followed to arrive at the total calculated weights for different blends of biodiesel blended fuel in Table 3.1 and 3.2 for No.1 and No. 2 diesel fuel. We converted the volume into weight because we can measure more accurately by weight. The accuracy of the scale was 0.005 kg. The scale used was a Pennsylvania (Lancaster, PA), Model No. 7300.

Table 3.1: Biodiesel Blends Prepared With No. 1 Diesel

Blend of Biodiesel	Wt. Empty can (kg)	Wt. Diesel (kg)	Wt. Diesel (kg)	Wt. Biodiesel (kg)	Wt. Biodiesel (kg)	Wt. (can + diesel + biodiesel)
		Calculated	Measured	Calculated	Measured	
0%	1.085	14.4023	14.4	0	0	15.485
2%	1.06	14.1142	14.115	0.3178	0.32	15.495
5%	1.055	13.6821	13.685	0.7946	0.795	15.535
20%	1.09	11.5218	11.52	3.1783	3.18	15.795

Table 3.2: Biodiesel Blends Prepared With No. 2 Diesel

Blend of Biodiesel	Wt. Empty can (kg)	Wt. Diesel (kg)	Wt. Diesel (kg)	Wt. Biodiesel (kg)	Wt. Biodiesel (kg)	Wt. (can + diesel + biodiesel)
		Calculated	Measured	Calculated	Measured	
0%	1.065	15.0572	15.055	0	0	16.125
2%	1.06	14.756	14.76	0.3178	0.32	16.14
5%	1.07	14.3043	14.305	0.7946	0.795	16.17
20%	1.095	12.0457	12.045	3.1783	3.18	16.325

3.5 EXPERIMENTAL DESIGN

Experiment performed for different blends of biodiesel fuel were taken in the random order. Three replicates of each sample were performed except for D1B0 (100% No. 1 Diesel) and D1B2 (98% No. 1 Diesel and 2% Biodiesel). Only 2 replicates of D1B0 (100% No. 1 Diesel) and D1B2 (98% No. 1 Diesel and 2% Biodiesel) were taken. The reason being that cloud point of these 2 samples was too low to be detected using the experimental sensor. The order of sample performance is listed in Table 3.3. The reason three replicates were taken was that sometimes moisture would build up on the outer sides of the lenses in the sensor. Then the transmittance value read much lower than expected.

Table 3.3 Order of Experiment Performance

Replicate 1	Replicate 2	Replicate 3
100% No. 2 Diesel	100% No. 2 Diesel	95% No. 1 Diesel, 5% Biodiesel
95% No. 2 Diesel, 5% Biodiesel	100% Biodiesel	100% No. 2 Diesel
95% No. 1 Diesel, 5% Biodiesel	95% No. 2 Diesel, 5% Biodiesel	100% Biodiesel
100% Biodiesel	80% No. 1 Diesel, 20% Biodiesel	80% No. 2 Diesel, 20% Biodiesel
80% No. 2 Diesel, 20% Biodiesel	98% No. 1 Diesel, 2% Biodiesel	95% No. 2 Diesel, 5% Biodiesel
98% No. 2 Diesel, 2% Biodiesel	98% No. 2 Diesel, 2% Biodiesel	80% No. 1 Diesel, 20% Biodiesel
80% No. 1 Diesel, 20% Biodiesel	80% No. 2 Diesel, 20% Biodiesel	98% No. 2 Diesel, 2% Biodiesel
	95% No. 1 Diesel, 5% Biodiesel	100% No. 1 Diesel
	100% No. 1 Diesel	98% No. 1 Diesel, 2% Biodiesel

3.6 EXPERIMENTAL PROCEDURE

3.6.1 SETTING BASELINE

Each time the experiment was started from the beginning, after a gap of couple of hours, or if there was a beeping sound from the spectrometer, the new baseline was set. The baseline taken was from No.1 Diesel fuel as it had maximum transmittance compared to other blends of diesel and biodiesel fuel. Collection of baseline followed the same procedure as discussed in section 3.6.2 except that the motor that rotated isopropyl alcohol was not turned on. The other important thing noted was that the baseline was established at room temperature.

3.6.2 PRE EXPERIMENTAL MEASURES

To collect the optical properties of the fuel we waited till the system was at least 20 degrees above the cloud point of the sample to be measured. Measurement involved the following steps:

3.6.2.1 SYSTEM CLEANING

This was done to make sure that the sample for analysis was not contaminated with other blends of biodiesel. The system was cleaned using the same fuel that was used for analysis. System was cleaned and drained out 3 times.

3.6.2.2 SAMPLE QUANTITY

An 800 mL sample was poured into the stainless steel beaker for analysis. It was determined that as the volume of the fuel increased, it took less time to chill the fuel.

3.6.2.3 STARTING THE TEST STAND

- Turn on nitrogen gas cylinder allowing nitrogen gas to flow through fuel cooling cylinder. This was done so that the condensation of moisture in fuel system was eliminated as this served to purge the air from the fuel system.
- The motor that circulated the biodiesel was turned on. The speed of the motor was maintained at a constant 108 rpm, since increasing the speed of rotation of fuel formed air bubbles and caused transmittance to decrease.
- Once the fuel started flowing the second motor was turned on to pump isopropyl alcohol through the outer walls of stainless steel reservoir. This motor was controlled using a Dell, Pentium 4 computer equipped with software written in Visual C++.

3.6.2.4 COLLECTING READINGS

Once both the motors were turned on, the temperature of the biodiesel fuel was taken using a Fluke (Everett, WA), model 189 multimeter. For every degree change in temperature the enter button on the computer was pressed to take the spectra of the sample through the spectrometer. Once the enter key was pressed, the computer automatically stored the raw data in the hard drive of the computer in predefined folder.

CHAPTER 4

RESULTS AND DISCUSSION

4.1 FUEL ANALYSIS

Table 4.1, Table 4.2 and Table 4.3 showed the fuel analysis for No. 1 Diesel fuel; No. 2 Diesel fuel and Biodiesel fuel. It showed the physical and chemical properties of No. 1 and No. 2 Diesel fuel using ASTM D975. The biodiesel was analyzed using ASTM D6751.

Table 4.1: Fuel Analysis for No. 1 Diesel Fuel

Test	Description		Results	Range	
D-1796	Sediment & water		NIL		
D-287	API Gravity @ 60		60		
D-86	Distillation	IBP	161		°C
		10%	173		°C
		20%	181		°C
		30%	188		°C
		40%	193		°C
		50%	293		°C
		60%	213		°C
		70%	225		°C
		80%	238		°C
		90%	252		°C
		95%	261		°C
	Total recovered volume		99.0		%
	Residue		1.0		%
D-613	Cetane number		43.7		
D-93	Flash point		51		°C
D-2622	Sulfur wt. %		0.0003		%
D-130	Copper corrosion		1A		
D-482	Ash content wt. %		0.003		%
D-2500	Cloud point		26		°C
D-97	Pour point		28		°C
D-445	Viscosity @ 40°C		2.04		cSt
D-524	Carbon residue		0.042		%
D-974	Alkali or mineral acids		neutral		
D-2274	Accelerated stability				
	filterable insoluble		0.2000		mg/100 ml
	adherent insoluble		0.6000		mg/100 ml
	total insoluble		0.8000		mg/100 ml

Table 4.2: Fuel Analysis for No. 2 Diesel Fuel

Test	Description	Results	Range
D-1796	Sediment & water	NIL	
D-287	API Gravity @ 60	60	
D-86	Distillation IBP	197	°C
	10%	214	°C
	20%	225	°C
	30%	232	°C
	40%	239	°C
	50%	248	°C
	60%	253	°C
	70%	259	°C
	80%	268	°C
	90%	287	°C
	95%	310	°C
	Total recovered volume	99.0	%
	Residue	1.0	%
D-613	Cetane number	57.7	
D-93	Flash point	53	°C
D-2622	Sulfur wt. %	0.0018	%
D-130	Copper corrosion	1A	
D-482	Ash content wt. %	0.005	%
D-2500	Cloud point	-67	°C
D-97	Pour point	-70	°C
D-445	Viscosity @ 40°C	2.31	cSt
D-524	Carbon residue	0.063	%
D-974	Alkali or mineral acids	neutral	
D-2274	Accelerated stability		
	filterable insoluble	0.2285	mg/100 ml
	adherent insoluble	0.6286	mg/100 ml
	total insoluble	0.8571	mg/100 ml

Table 4.3: Fuel Analysis for Biodiesel Fuel

Test	Description	Results	Range
D-2709	Sediment & water	NIL	
D-1160	Distillation IBP	202	°C
	at reduced 10%	345	°C
	pressure 20%	345	°C
	(10mm Hg) 30%	346	°C
	40%	348	°C
	50%	349	°C
	60%	349	°C
	70%	350	°C
	80%	350	°C
	90%	351	°C
	95%	354	°C
	End point	407	°C
	Total recovered volume	99.0	%
	Residue	1.0	%
D-613	Cetane number	62.4	
D-93	Flash point	135	°C
D-5453	Sulfur wt. %	0.0052	%
D-130	Copper corrosion	1A	
D-874	Sulfated ash	0.005%	%
D-2500	Cloud point	1	°C
D-445	Viscosity @ 40°C	3.12	cSt
D-4530	Carbon residue	0.081	%
D-664	Alkali or mineral acids	0.02	mg/KOH/g
D-6584	Free & total Glycerin wt. %		
	Free glycerin	0.002	%
	Monoglyceride	0.408	%
	Diglyceride	0.183	%
	Triglyceride	0.020	%
	Total glycerin	0.137	%

4.2 FUEL PROPERTIES

The cloud point temperatures of different blends of diesel and biodiesel fuel were reported by MAGELLAN Labs (Kansas City, KS). Magellan Labs used cloud point detection procedure ASTM D2500 (Table 4.1). The repeatability of the test was 2 degrees Celsius. It also showed that the cloud point temperature of D2B5 (95% No.2 Diesel and 5% Biodiesel) was the same as 100% No. 2 Diesel. The reason explained was that a cloud point depression was observed going from a D2B0 (100% No. 2 Diesel) to a D2B2 (98% No. 2 Diesel and 2% Biodiesel). The cloud point of a D2B5 (95% No. 2 Diesel and 5% Biodiesel) increased back to the cloud point temperature of the D2B0 (100% No. 2 Diesel). This depression indicated that biodiesel may be added to diesel fuel as a cloud point suppressant at low level blends.

Table 4.4: Cloud Point Temperature of Different Blends of Biodiesel Fuel

Biodiesel	No. 1 Diesel	No. 2 Diesel
0%	-67*	-27*
2%	-45	-26
5%	-36	-27
20%	-22	-20
100%	1	1

* ANA Labs (Bellmawr, New Jersey) for fuel analysis, conducted on ASTM D975.

4.3 DATA COLLECTION

The data taken from the spectrometer is raw data from a range of 350nm to 1600nm. The baseline taken was from No.1 Diesel fuel as it had the maximum transmittance compared to other blends of diesel and biodiesel fuel. Increasing the speed of rotation of the fuel led to a decrease in raw data intensity as shown in Figure 4.1, so the speed of rotation was held constant at 108 rpm.

The raw data for B100 (100% Biodiesel) for different temperatures is shown in Figure 4.2. The baseline is shown in Figure 4.3. Transmittance was obtained from ratio of transmitted power to baseline power. Statistical Analysis Software program (SAS, 1990) was written to convert raw data into transmitted data (Appendices B) and then data was exported to Grapher 2.0 to plot the graph. Figure 4.4 showed the result of transmitted data of B100 (100% Biodiesel) at different temperatures.

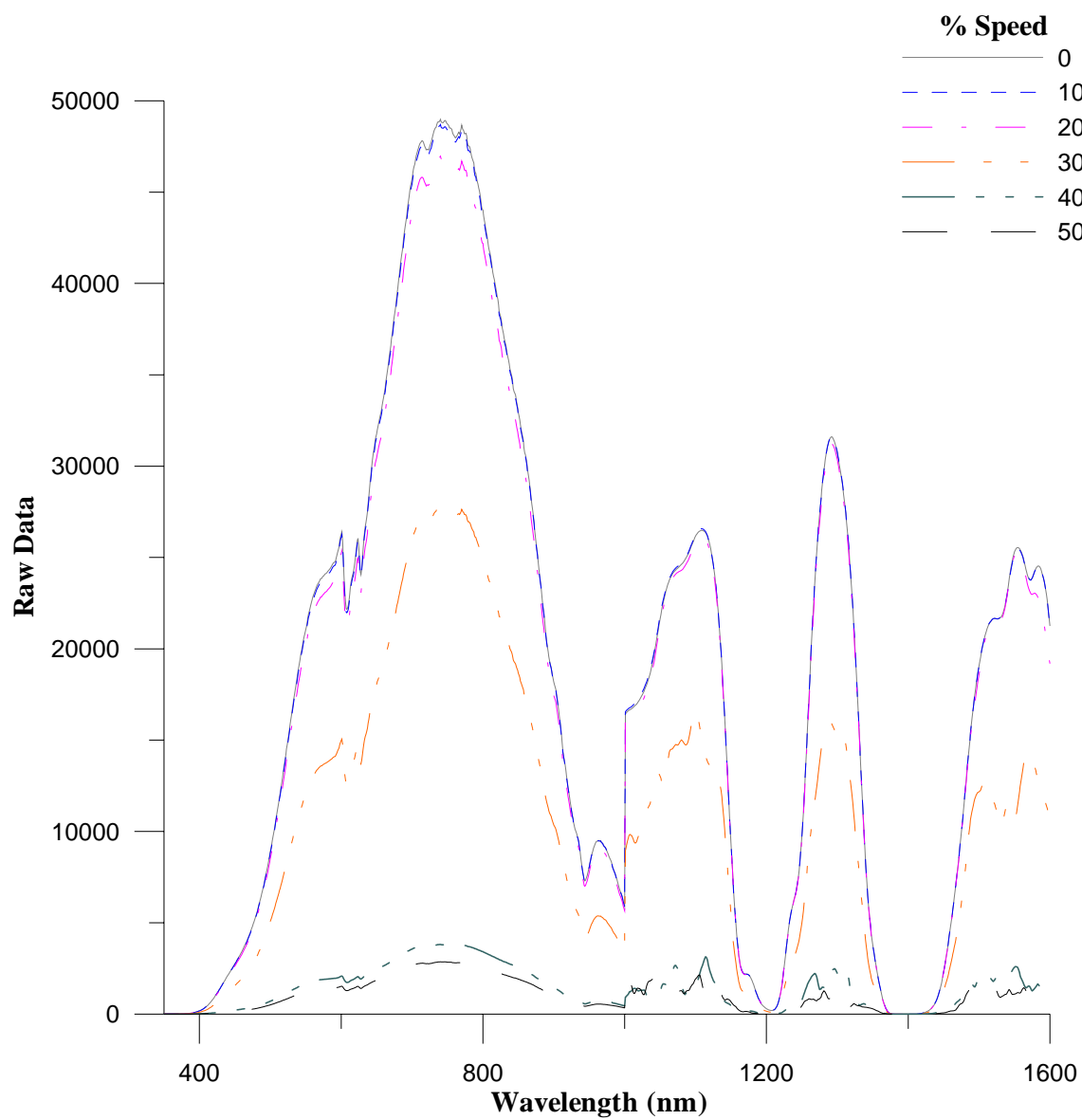


Figure 4.1: Raw Data Vs Wavelength with Change in Speed

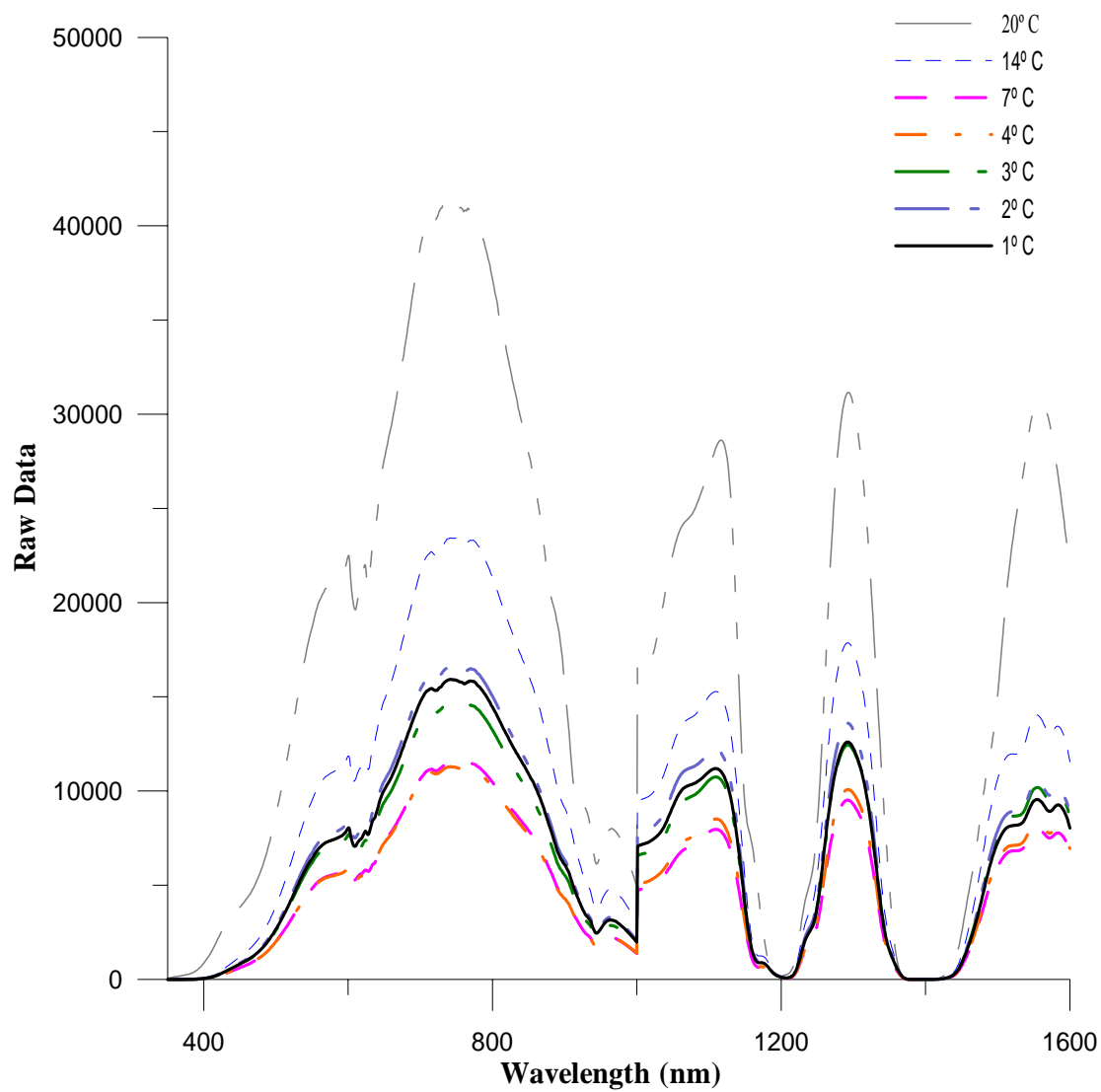


Figure 4.2: Raw Data Vs Wavelength (nm) for B100 (100% Biodiesel) at Different Temperatures (°C)

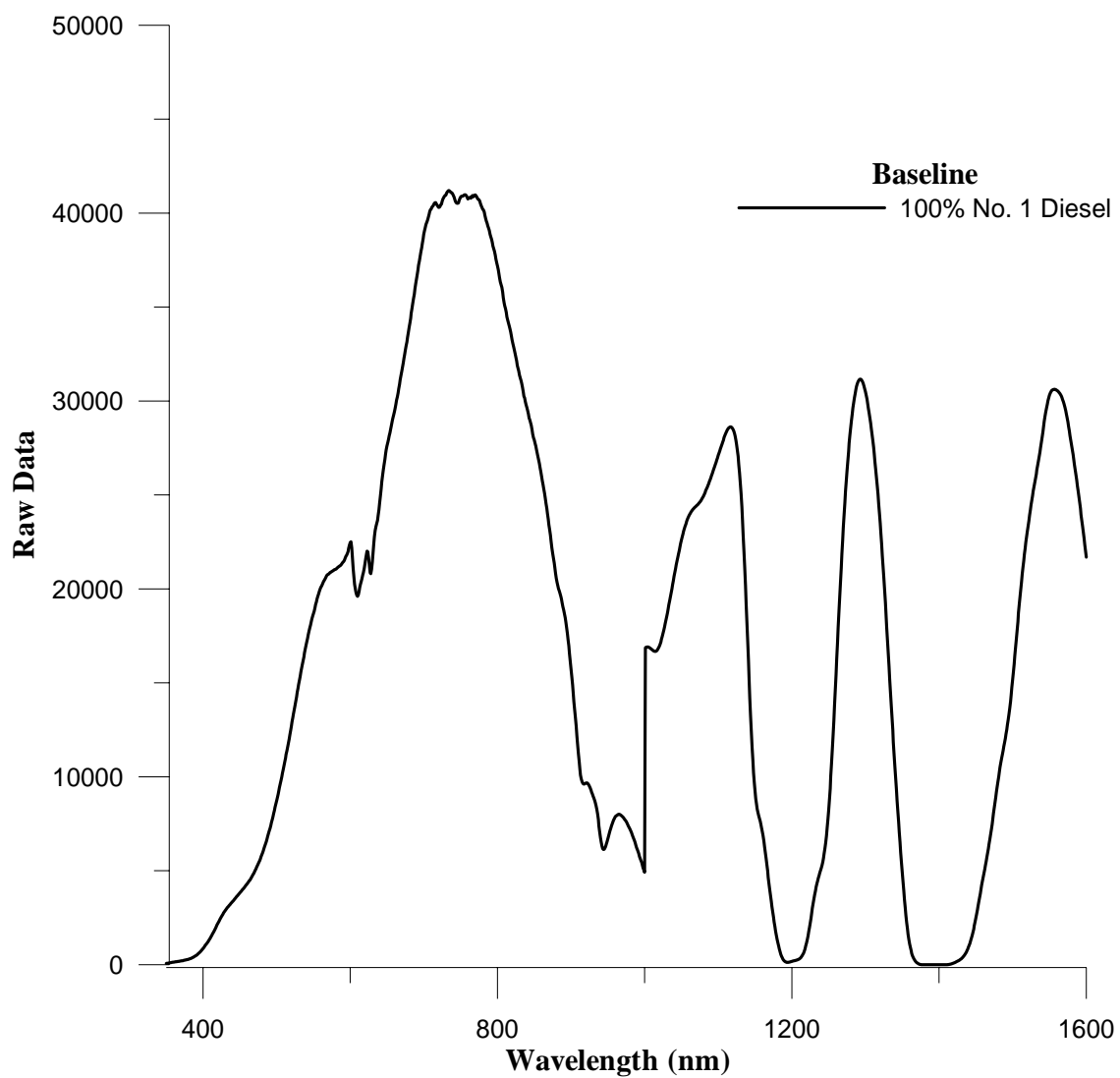


Figure 4.3: Baseline (No.1 Diesel) Vs Wavelength (nm) for D1B5 (95% Diesel and 5% Biodiesel)

4.4 BLENDS OF BIODIESEL

Nine different blends of diesel and biodiesel fuel were examined along with their plots. Figures 4.4 through 4.12 showed the plots drawn between transmittance and wavelength for the one replicate of biodiesel fuel. The other 2 replicates of nine different blends of biodiesel are shown in APPENDIX C. The other temperatures were also shown where there were distinct changes in transmittance.

It was noted that four replicates were taken for D2B20 (80% No. 2 Diesel and 20% Biodiesel) and B100 (100% Biodiesel). The reason being, one of the replicate of these 2 samples was bad. Moisture in the atmosphere condensed on the outer part of convex lenses of the sensor. This resulted in low transmittance of light sources through the sensor and hence wrong data.

4.4.1 B100 (100% BIODIESEL)

Spectral analysis for B100 (100% Biodiesel) showed interesting observations. A small spike was seen at 900nm; at 1180nm another big spike was noted. Noise was observed at about 1400nm. The plot is shown in Figure 4.4.

- At 20° C, transmittance reached to about 0.8 as wavelength increased from 350nm to 800nm. From 800nm to 1600nm there was a presence of noise.
- At 14° C, transmittance was about 0.45 until 1000nm and then decreased to about 0.38.
- At 7° C, transmittance was about 0.2 until 1000nm and then decreased to about 0.18 at 1000nm to 1600nm.
- At 4° C, transmittance was increased to about 0.35 from 350nm to 850nm with small noise at 600nm. From 850nm to 1600nm there was a presence of noise.
- At 3° C, transmittance was almost 0.45 between 550nm to 1000nm and then increased to about 0.5 at 1000nm to 1600nm.
- At 2° C, transmittance again went down to about 0.32 between 550nm to 850nm. From 850nm to 1600nm there was presence of noise.
- At the cloud point temperature (1° C) transmittance again went up a little to 0.38 between 550nm to 850nm. From 850nm to 1600nm there was a presence of noise.

Overall, the plot showed that the transmittance decreased as the temperature decreased from 20° C to 7° C, and then it started increasing until 3° C. As it neared the cloud point, the transmittance was about 0.4

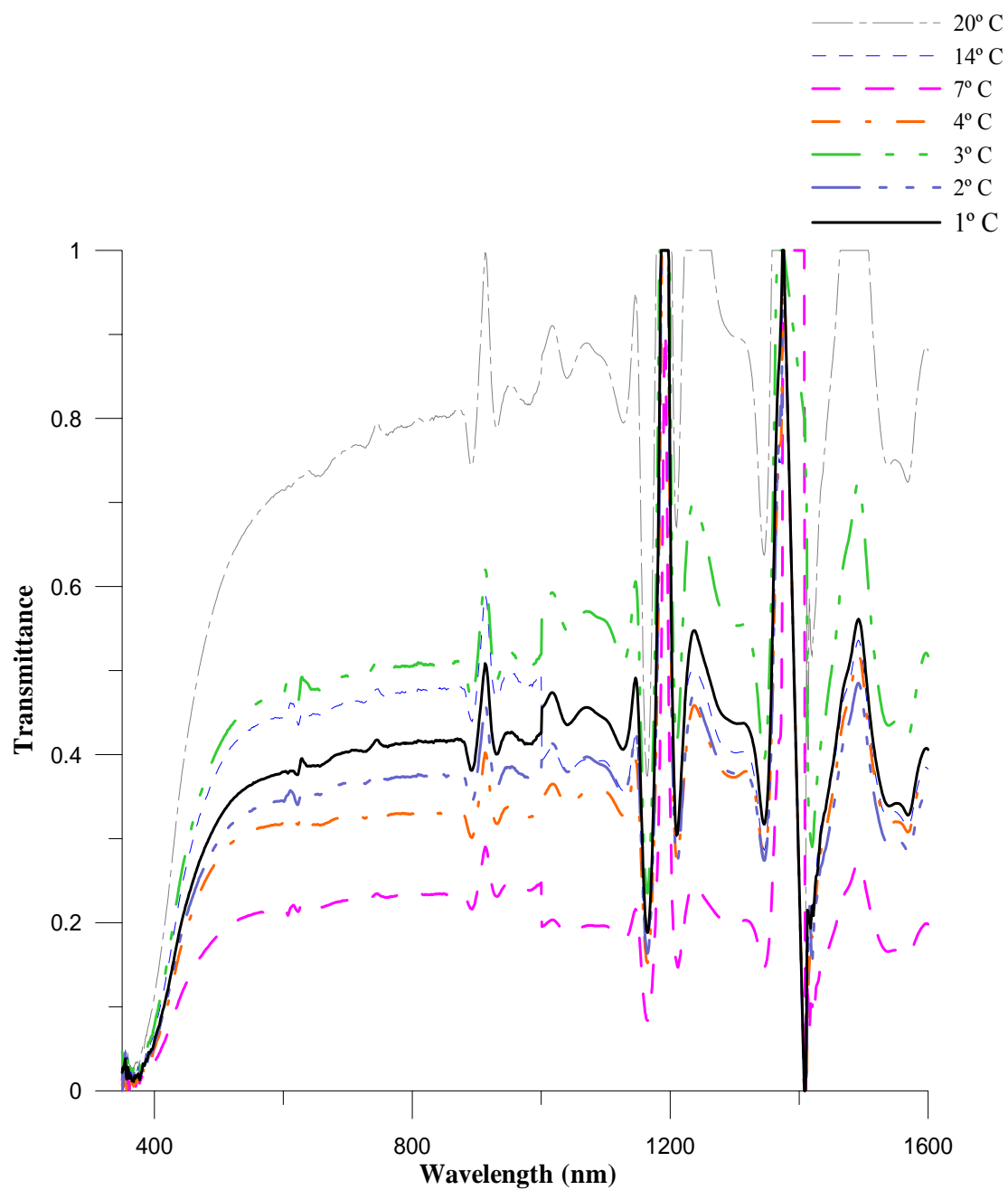


Figure 4.4: Transmittance Vs Wavelength (nm) for B100 (100% Biodiesel) at Different Temperatures (°C). The dark black line indicates the spectrum at the cloud point of the fuel

4.4.2 D2B0 (100% No. 2 DIESEL)

Spectral analysis for D2B0 (100% No. 2 Diesel) showed a small peak at 1150nm and sudden down peak from 1200nm to 1250nm. There was also a small noise observed at 610nm. Noise was observed at 1400nm. The plot is shown in Figure 4.5.

- At 7° C, transmittance was about 0.68 from 450nm to 900nm. Transmittance was decreased to 0.65 from 450nm to 1000nm. At 1000nm there was sudden increase in transmittance to 0.84 from 1000nm to 1400nm. From 1400nm to 1600nm transmittance was back to 0.7.
- At 0° C, transmittance was 0.4 from 450nm to 1000nm and then it suddenly decreased to 0.26 at 1000nm onwards.
- At -13° C, transmittance was decreased to 0.18 from 450nm to 1000nm and then it suddenly decreased to 0.12 at 1000nm and onwards.
- At -19° C transmittance was 0.26 from 450nm to 1000nm and then suddenly decreased to 0.22 from 1000nm onwards.
- At -23 degrees, transmittance was 0.55 from 450nm to 1400nm. At 1400nm transmittance was suddenly decreased to 0.14.
- At Cloud point temperature (-27° C), transmittance was 0.74 from 450nm to 1200nm.
- At -28° C, transmittance was 8.0 from 450nm to 1200nm.

Overall, the plot showed that the transmittance decreased as the temperature decreased from 7° C to -13° C, and then it started increasing until it reached the cloud point at -27° C. After it passed the cloud point, transmittance again decreased.

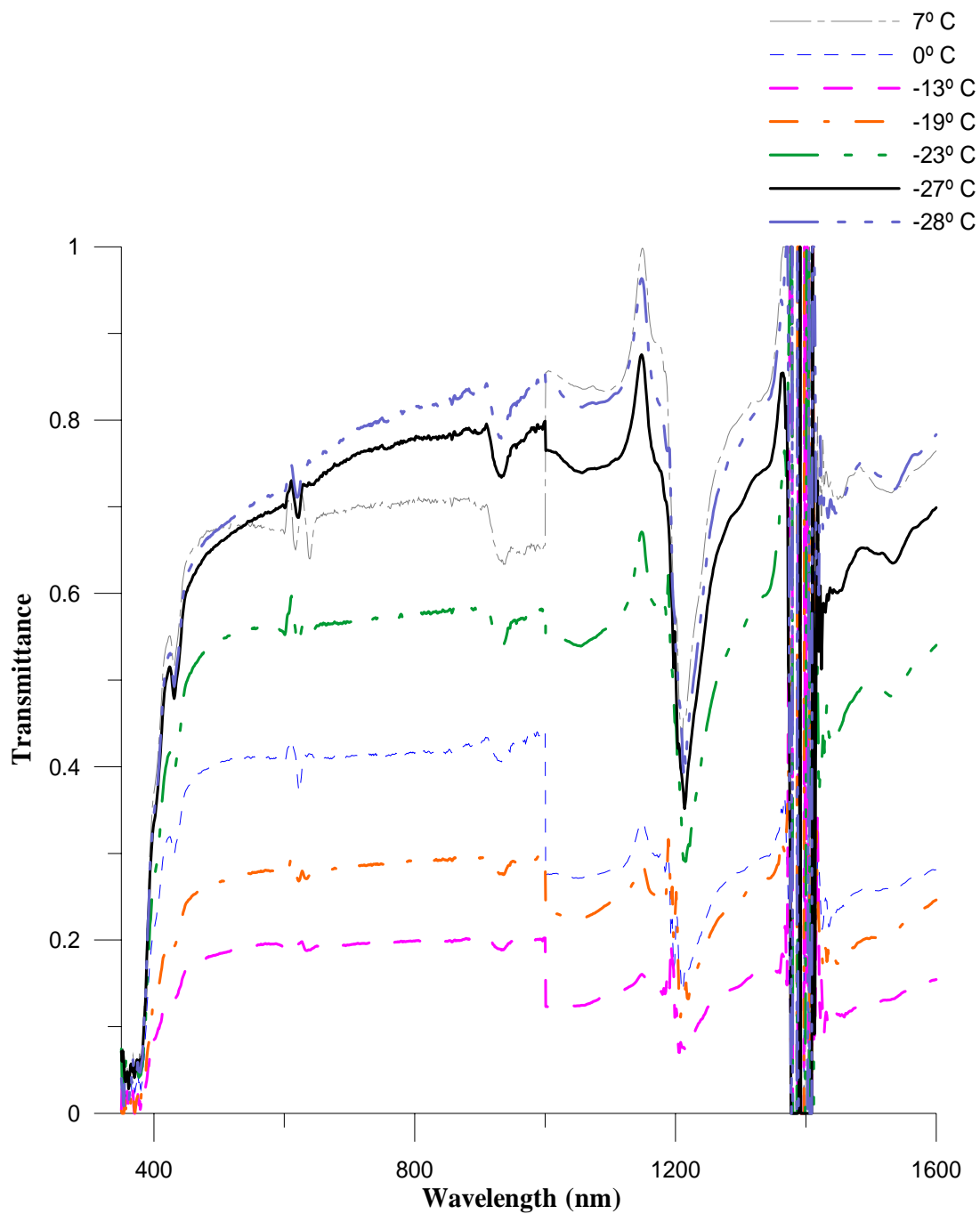


Figure 4.5: Transmittance Vs Wavelength (nm) for D2B0 (100%No. 2 Diesel and 0% Biodiesel) at Different Temperatures (°C). The dark black line indicates the spectrum at the cloud point of the fuel

4.4.3 D2B2 (98% No. 2 DIESEL AND 2% BIODIESEL)

Spectral analysis for D2B2 (98% No. 2 Diesel and 2% Biodiesel) showed that at all temperature ranges there was a little peak at 1150nm and then there was a downward slope at 1200nm. Noise was observed at 1400nm. The plot is shown in Figure 4.6.

- At 4° C, transmittance was about 0.95 from 450nm to 1000nm and then from 1400nm to 1600nm.
- At -3° C, transmittance was about 0.55 from 450nm to 1100nm and then from 1400nm to 1600nm.
- At -10° C, transmittance was lowest to about 0.3 from 450nm to 1100nm and then from 1400nm to 1600nm.
- At -15° C, transmittance rose to about 0.38 from 450nm to 1000nm and suddenly transmittance value shoot to 0.42 at 1000nm.
- At -20° C, transmittance was 0.62 from 450nm to 1100nm with slightly lower transmittance between the wavelengths 900nm to 1000nm.
- At -23° C transmittance went to about 0.86 from 450nm to 1150nm with small noise at 600nm.
- At cloud point temperature (-26° C), transmittance was about 0.84 from 450nm to 1150n with small noise at 600nm.

Overall, the plot showed that the transmittance decreased as the temperature was decreased from 4° C to -10° C and then it started increasing until it reached -23° C.

Transmittance decreased a little as temperature approached to its cloud point at -26° C.

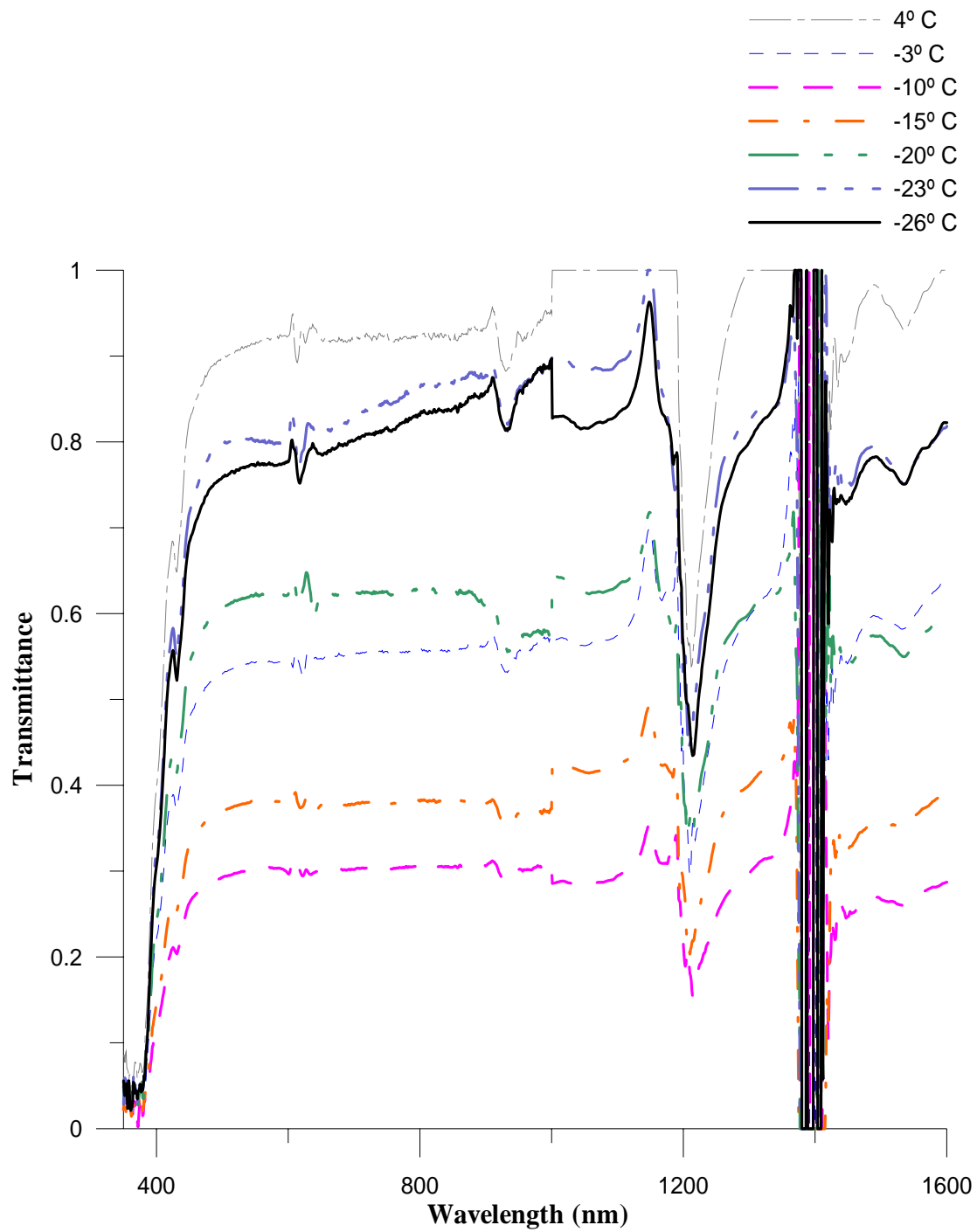


Figure 4.6: Transmittance Vs Wavelength (nm) for D2B2 (98%No. 2 Diesel and 2% Biodiesel) at Different Temperatures (°C). The dark black line indicates the spectrum at the cloud point of the fuel

4.4.4 D2B5 (95% No. 2 DIESEL AND 5% BIODIESEL)

Spectral analysis for D2B5 (95% No. 2 Diesel and 5% Biodiesel) showed a small peak at 1150nm and a sudden decrease of transmittance between wavelengths 1180nm to 1220nm. Noise was observed at 1400nm. The plot is shown in Figure 4.7.

- At 0° C, transmittance was found to be 0.3 from 450nm to 1000nm with small noise at 600nm but suddenly decreased to 0.25 at 1000nm to 1600nm.
- At -8° C, transmittance went to about 0.14 from 450nm to 1000nm with small noise at 600nm and further decreased to 0.1 at 1000nm to 1600nm.
- At -15° C, transmittance went up to about 0.28 from 450nm to 1000nm with little noise at 600nm and 1100nm.
- At -19° C, transmittance was 0.46 from 450nm to 1000nm with little noise at 600nm and 1100nm.
- At -22° C, transmittance was the highest, about 0.65 from 450nm to 1000nm with small noise at 600nm.
- At -24° C, transmittance was down to about 0.45 from 450nm to 1000nm with small noise at 600nm.
- At cloud point temperature (-27° C) transmittance was about 0.48 from 450nm to 1000nm and then transmittance shoot down to 0.45.

Overall, the plot showed that the transmittance decreased as the temperature was decreased from 0° C to -8° C and then it started increasing from -15° C until it reached the cloud point at -27° C.

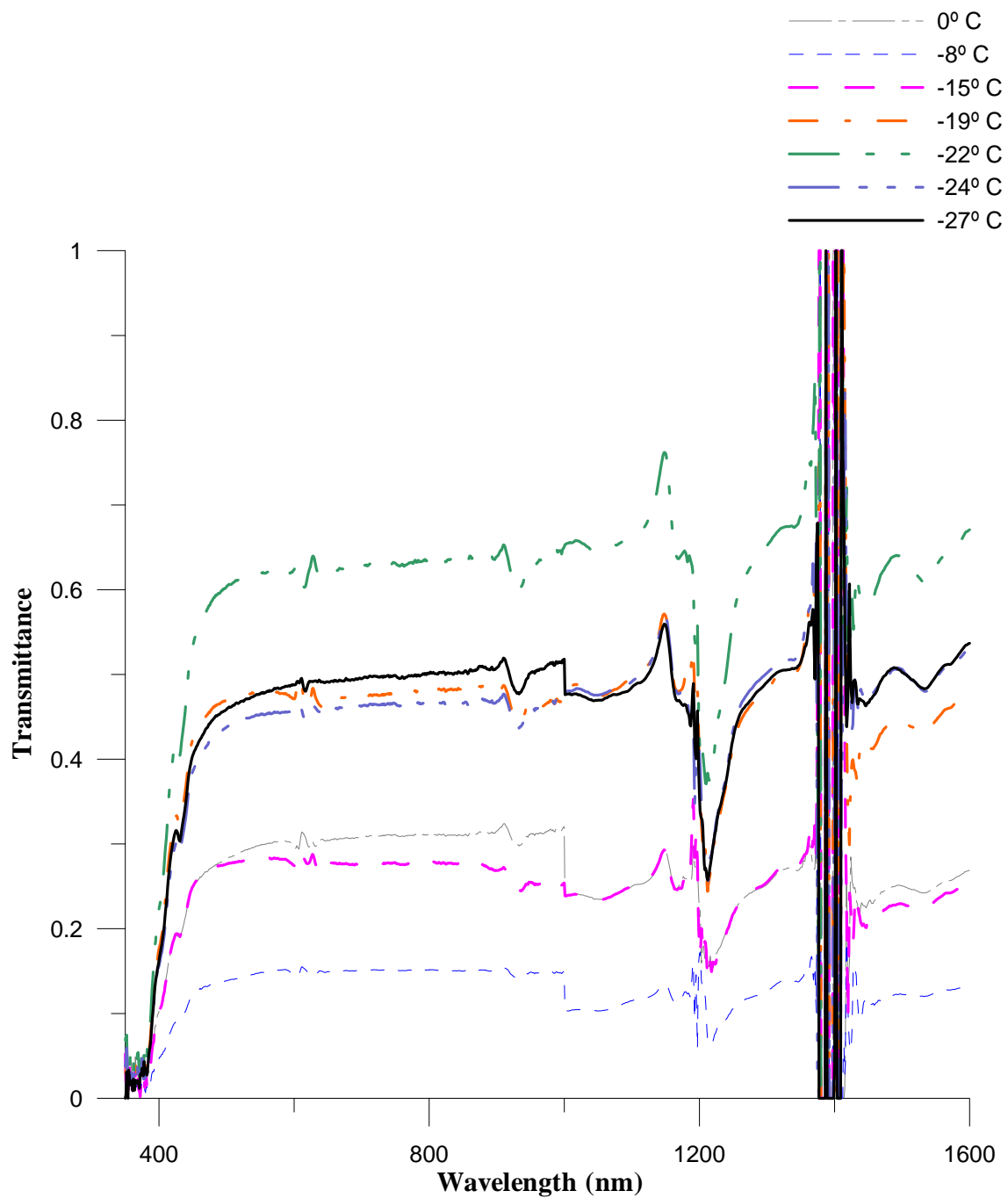


Figure 4.7: Transmittance Vs Wavelength (nm) for D2B5 (95% No. 2 Diesel and 5% Biodiesel) at Different Temperatures (°C). The dark black line indicates the spectrum at the cloud point of the fuel

4.4.5 D2B20 (80% No. 2 DIESEL AND 20% BIODIESEL)

Spectral analysis of D2B20 (98% No. 2 Diesel and 2% Biodiesel) observed a small peak at 1150nm, then a peak at 1190nm and then it went down at 1200nm came back at 1250nm. Noise was observed at 1400nm. The plot is shown in Figure 4.8.

- At 8° C, transmittance was about 0.8 from 450nm to 1600nm and then it increased suddenly to 1 at 1000nm to 1600nm.
- At 0° C, transmittance was 0.28 from 450nm to 1000nm and then it shoot down to 0.25 at 1000nm to 1600nm.
- At -10° C, transmittance was about 0.22 from 450nm to 1000nm and then shoot down to 0.18 at 1000nm to 1600nm.
- At -16° C, transmittance was increased to about 0.38 from 450nm to 1200nm with small noise at 600nm and 950nm.
- At -18° C, transmittance was 0.8 from 450nm to 1200nm with noise at 600nm and 950nm..
- At cloud point temperature (-20° C), transmittance rose to about 0.84 from 450nm to 950nm with noise at 950nm to 1600nm.
- At -21° C, transmittance was again decreased a little to 0.82 from 450nm to 950nm with noise at 950nm to 1600nm.

Overall, the plot showed that the transmittance decreased as the temperature was decreased from 8° C to -10° C and then it started increasing from -16° C until it reached the cloud point at -20° C. Transmittance decreased slightly as temperature went above the cloud point.

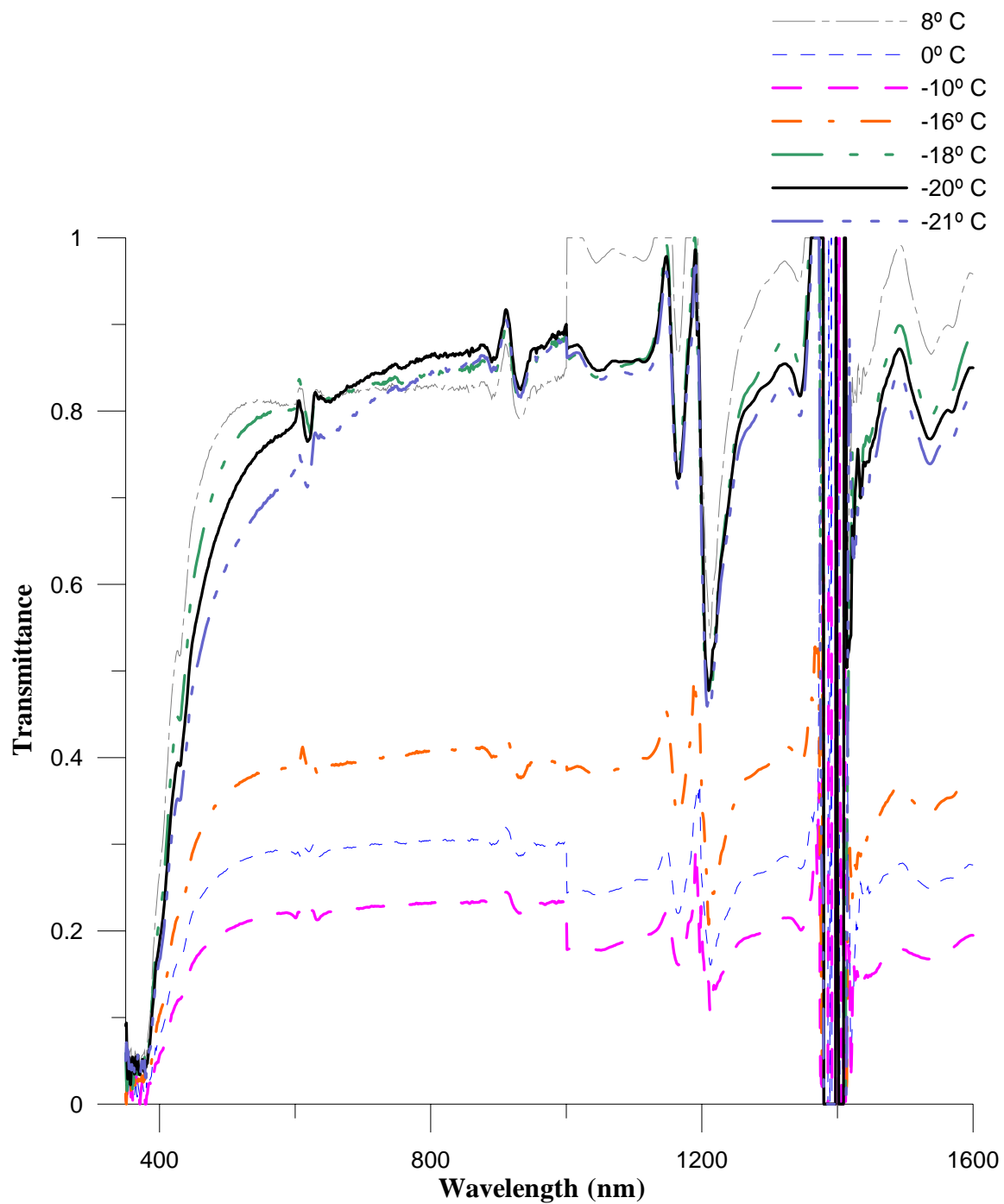


Figure 4.8: Transmittance Vs Wavelength (nm) for D2B20 (80%No. 2 Diesel and 20% Biodiesel) at Different Temperatures (°C). The dark black line indicates the spectrum at the cloud point of the fuel

4.4.6 D1B0 (100% No. 1 DIESEL)

Spectral analysis for D1B0 (100% No. 1 Diesel) observed interesting data that transmittance at 350nm did not start at 0 value compared to other spectral analysis. A small spike was observed at 1200nm. Noise was observed at 1400nm. The plot is shown in Figure 4.9.

- At 6° C, transmittance was found to be 0.9 from 400nm to 1200nm with little noise at 600nm and 950nm.
- At 0° C transmittance was found be to 0.8 from 350nm to 1000nm and then decreased to 0.75 at 1000nm to 1600nm.
- At -10° C, transmittance was transmittance was about 0.55 from 350nm to 1000nm and then decreased to about 0.5 at 1000nm to 1600nm.
- At -17° C, transmittance was about 0.37 with a very slight decrease in transmittance at 1000nm.
- At -28° C transmittance was 0.24 from 400nm to 1400nm with little noise at 600nm and 1200nm.
- At -35° C, transmittance at 0.16 from 350nm to 1000nm and then decreased to about 0.1 at 1000nm to 1600nm.
- At -40° C, transmittance remained at 0.16 from 400nm to 950nm and then decreased to about 0.13 at 1000nm to 1600nm.

Overall, the plot showed that the transmittance decreased as the temperature decreased from 6° C to -35° C. There was a slight increase in transmittance as the temperature went to -40° C.

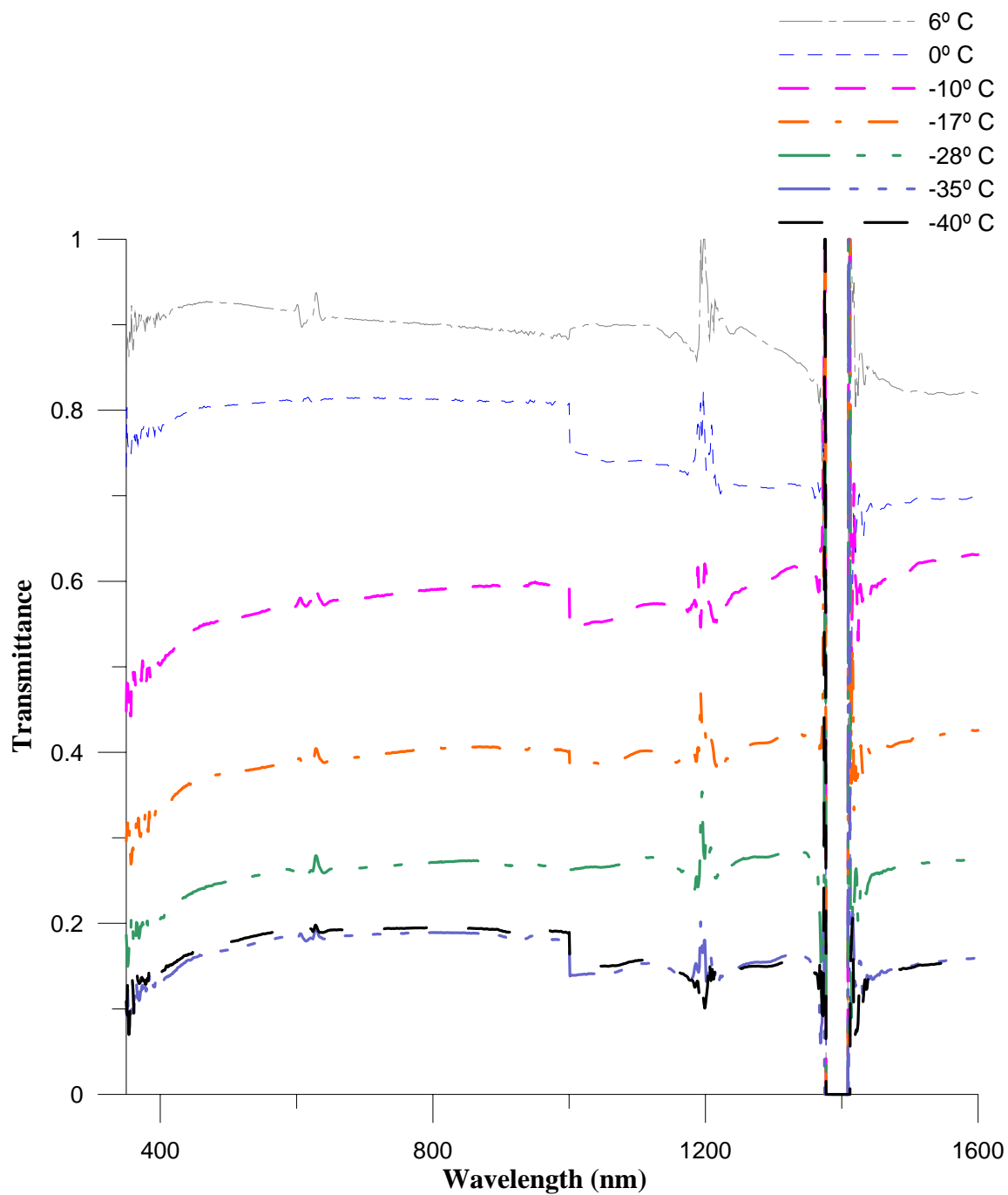


Figure 4.9: Transmittance Vs Wavelength (nm) for D1B0 (100%No. 1 Diesel and 0% Biodiesel) at Different Temperatures (°C). No cloud point obtained for D1B0 (100%No. 1 Diesel and 0% Biodiesel) because experimental set up does not go beyond -40° C

4.4.7 D1B2 (98% No. 1 DIESEL AND 2% BIODIESEL)

Spectral analysis of D1B2 (98% No. 1 Diesel and 2% Biodiesel) showed transmittance value even at 350nm is not zero (same as for 100% No. 1 Diesel) compared to other blends of biodiesel fuel. A small spike was observed at 600nm and 1200nm. Noise was observed at 1400nm. The plot is shown in Figure 4.10.

- At 2° C, transmittance rose to about 0.74 from 350nm to 450nm and then decreased to 0.65 from 450nm to 1200nm.
- At -7° C, transmittance was about 0.45 from 350nm to 1000nm and decreased to 0.4 from 1000nm to 1600nm.
- At -15° C, transmittance increased to about 0.64 from 450nm to 1200nm with little noise at 600nm.
- At -19° C, transmittance was 0.65 from 450nm to 1200nm with little noise at 600nm and 950nm.
- At -23° C, transmittance was about 0.38 from 400nm to 1000nm and increased to 0.42 from 1000nm to 1600nm.
- At -28° C, transmittance was 0.24 from 400nm to 1000nm and then decreased to 0.2 from 1000nm to 1600nm.
- At -39° C, transmittance was 0.18 from 400nm to 1200nm with noise at 600nm and 950nm.

Overall, the plot showed that the transmittance decreased as the temperature was decreased from 2° C to -7° C, but again increased as the temperature was decreased to -28° C. Transmittance increased a little as temperature was further decreased to -39° C.

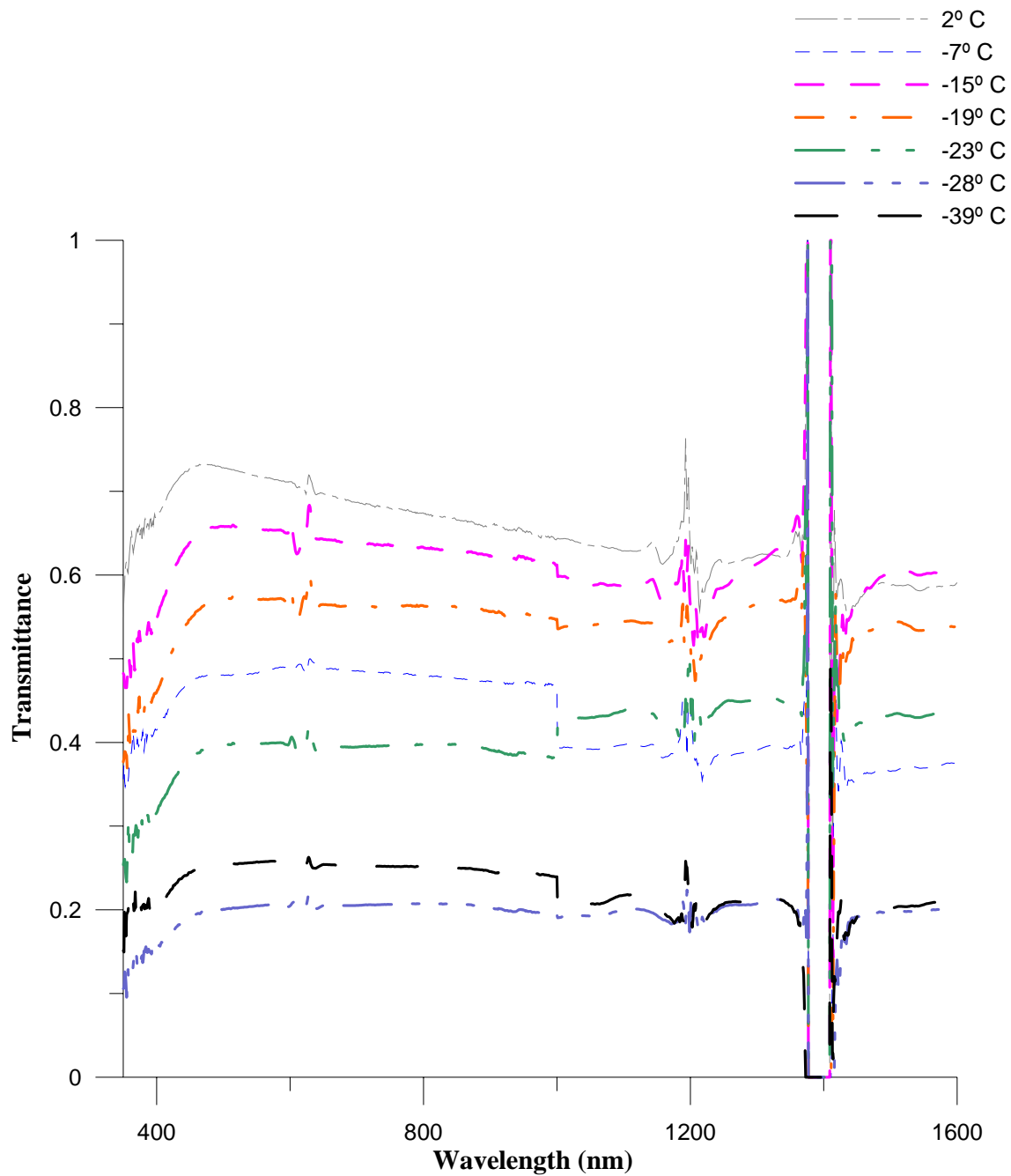


Figure 4.10: Transmittance Vs Wavelength (nm) for D1B2 (98%No. 1 Diesel and 2% Biodiesel) at Different Temperatures (°C). No cloud point obtained for D1B2 (98%No. 1 Diesel and 2% Biodiesel) because experimental set up does not go beyond -40° C

4.4.8 D1B5 (95% No. 1 DIESEL AND 5% BIODIESEL)

Spectral analysis for D1B5 (95% No. 1 Diesel and 5% Biodiesel) showed a small spike at 1200nm. Noise was observed at 1400nm. The plot is shown in Figure 4.11.

- At -1° C, transmittance was about 0.53 from 450nm to 1200nm with little noise at 600nm.
- At -10° C, transmittance went slightly up by 0.57 from 450nm to 1200nm with little noise at 600nm.
- At -23° C, transmittance was found to be about 0.3 from 450nm to 1000nm, but suddenly transmittance went down to about 0.23 from 1000nm to 1600nm.
- At -30° C, transmittance was about 0.14 from 450nm to 1000nm and decreased to 0.1 from 1000nm to 1600nm.
- At -34° C, transmittance was about 0.1 from 450nm to 1000nm and decreased to about 0.08 from 1000nm to 1600nm.
- At cloud point temperature (-36° C), transmittance was almost same as at -34° C i.e. 0.1 from 450nm to 1000nm but slightly increased to 0.12 at 1000nm to 1600nm.
- At -37° C, transmittance was almost same as at -36° C from 450nm to 1000nm, but transmittance was about 0.14 from 1000nm to 1600nm.

Overall, the plot showed that the transmittance increased a little as the temperature was decreased from -1° C to -10° C, but then decreased as temperature was decreased to -34° C. Transmittance was slightly increased as temperature approached to its cloud point at -36° C.

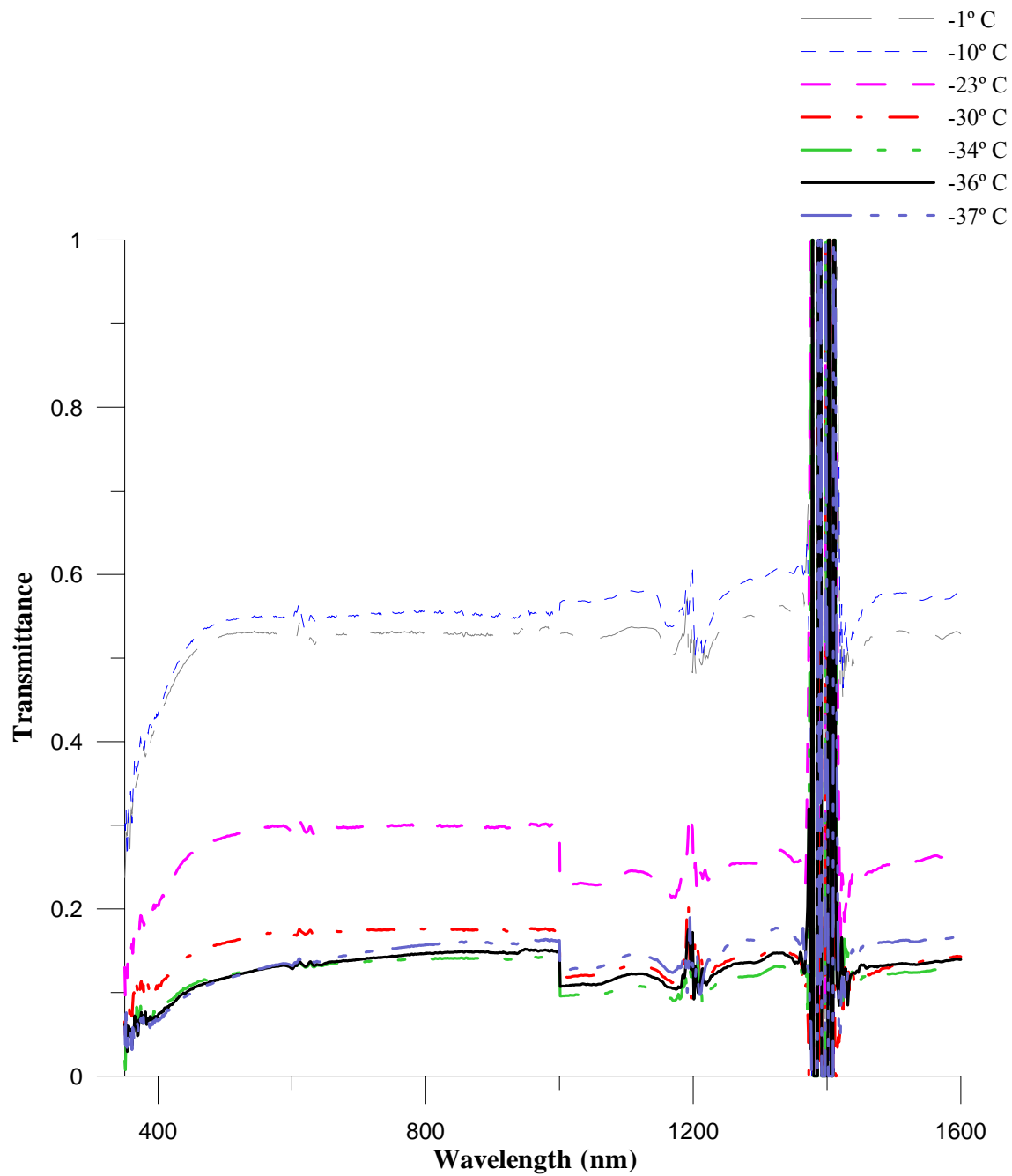


Figure 4.11: Transmittance Vs Wavelength (nm) for D1B5 (95%No. 1 Diesel and 5% Biodiesel) at Different Temperatures (°C). The dark black line indicates the spectrum at the cloud point of the fuel

4.4.9 D1B20 (80% No. 1 DIESEL AND 20% BIODIESEL)

Spectral analysis for D1B20 (80% No. 1 Diesel and 20% Biodiesel) showed a slight spike at about 910nm and then a big spike at 1200nm. Noise was observed at 1400nm.

The plot is shown in Figure 4.12.

- At 3° C, transmittance about 0.71 from 450nm to 1150nm with noise at 600nm and 900nm.
- At -10° C, transmittance was about 0.61 from 450nm to 1150nm with noise at 600nm and 900nm.
- At -13° C, transmittance was about 0.43 from 450nm to 1150nm with very small noise at 600nm and 900nm..
- At -17° C transmittance was 0.39 from 450nm to 1000nm with small noise at 600nm, but decreased to 0.36 from 1000nm to 1600nm.
- At -21° C, transmittance was decreased to about 0.28 from 600nm to 1200nm with small noise at 900nm.
- At cloud point (-22° C), transmittance went up to about 0.29 from 600nm to 1200nm with small noise at 850nm.
- At -23° C, transmittance was increased from 0.28 to 0.38 as wavelength increased from 600nm to 1000nm and at 1000nm transmittance was decreased to 0.36

Overall, the plot showed that the transmittance decreased as temperature was decreased from 3° C to -21° C, but then increased as temperature approached the cloud point of the fuel.

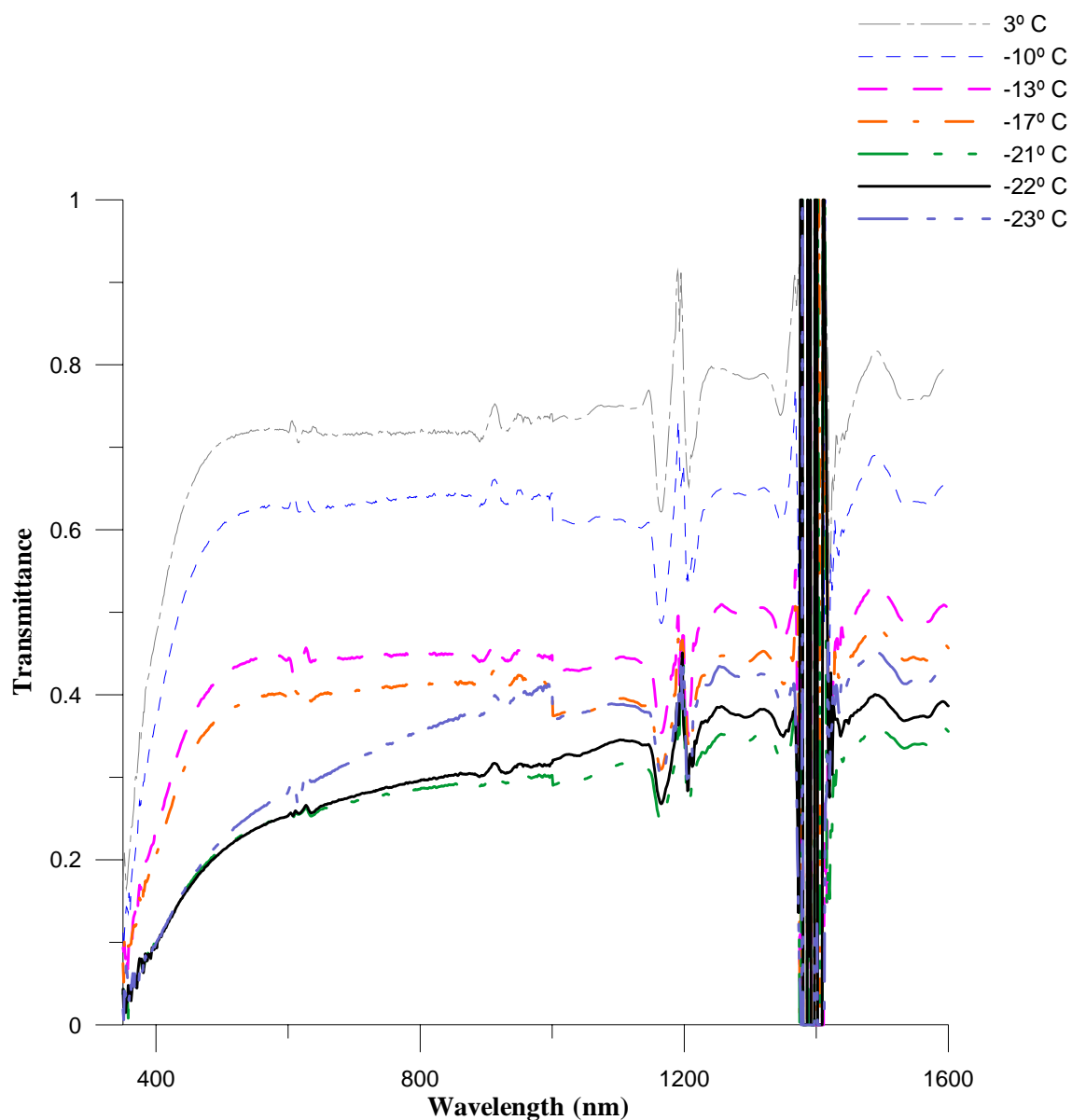


Figure 4.12: Transmittance Vs Wavelength (nm) for D1B20 (80%No. 1 Diesel and 20% Biodiesel) at Different Temperatures (°C). The dark black line indicates the spectrum at the cloud point of the fuel

4.5 TRANSMITTANCE VS WAVELENGTH-CLOUD POINT

Transmittance vs. wavelength for different blends of biodiesel fuel at their respective cloud-point temperatures were plotted in Figure 4.13. The plots were the average of cloud point temperature of the 3 replicates for each blend of biodiesel fuel. A Statistical Analysis Software program (SAS, 1990) was written (Appendices D) and then exported to Grapher 2.0 to plot the graph. The plot did not contain cloud point temperature of D1B0 (100% No.1 Diesel) and D1B2 (98% No.1 Diesel and 2% Biodiesel) because the equipment did not allow us to go below -40°C.

The results report the transmittance for all the blends of biodiesel fuel. It was interesting to note that there was no specific transmittance value at cloud point temperatures. Transmittance values varied from 0.1 to 0.6 for different blends of biodiesel fuel. This led to the conclusion that it was difficult to determine the cloud point temperature of a fuel using our optical sensor.

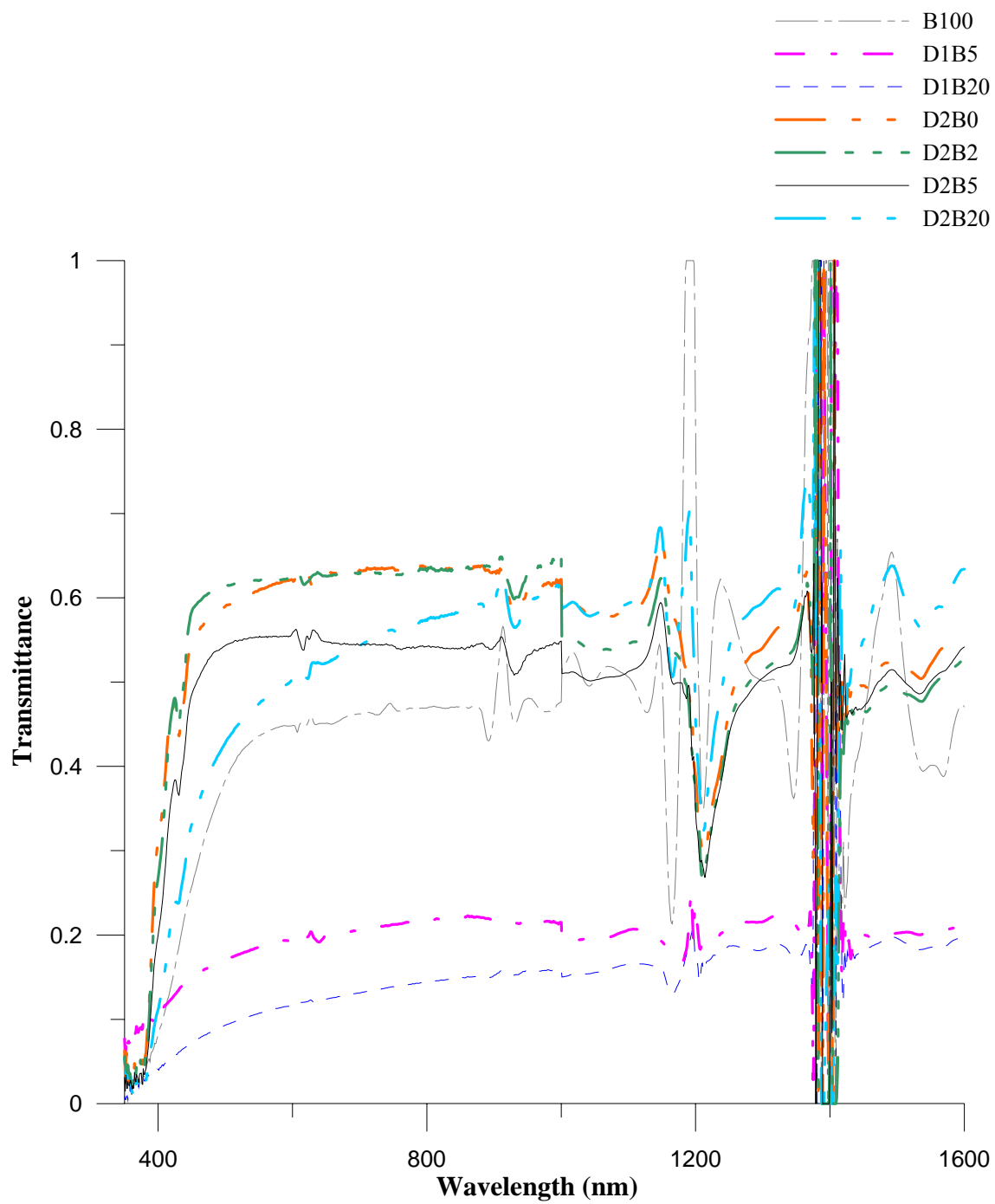


Figure 4.13: Transmittance Vs Wavelength for Different Blends of Diesel and Biodiesel Fuel at Their Respective Cloud Point Temperatures

4.6 TRANSMITTANCE VS TEMPERATURE

Graphs were a plot between transmittance and temperature at different wavelengths. The plots are the average of particular wavelengths of 3 replicates for each blend of biodiesel fuel. Statistical Analysis Software program (SAS, 1990) was written (Appendices E) and then exported to Grapher 2.0 to plot the graphs.

The wavelengths taken into consideration were 660nm, 750nm and 1600nm. The wavelength at 660nm was considered because it was used in ASTM D5773-02 (Figure 4.14). 750nm and 1600nm were used because there was a peak transmittance at each wavelength (Figures 4.15 and 4.16).

- Results showed that the transmittance was higher at higher temperatures but transmittance decreased as the temperature of blend of biodiesel was reduced. The temperature continued to decrease until about 2° C to 10° C above the cloud point of respective blend of biodiesel fuel. The reason was that cold temperatures cause crystal formation. The crystal particles froze on the sides of the container while rest of the fuel became clear. Therefore sometime before cloud point was reached, transmittance decreased. But once fuel was clear, transmittance again increased.
- It was observed that all the blends of fuel went to at least the transmittance value of 0.3 before they reached the cloud point.
- It was also noted that transmittance of different blends of biodiesel started decreasing once it reached its cloud point.

- It was also observed that for 660nm, the transmittance value for D1B20 (80% No. 1 Diesel and 20% Biodiesel), almost dipped to zero after it reached the cloud point. However it was not the case with 750nm and 1600nm.
- It was also observed that the transmittance value for B100 (100% Biodiesel) at 660nm did not go as low as it went for other blends of biodiesel fuel. However, B100 (100% Biodiesel) behaved same way as other blends of biodiesel fuel at 750nm and 1600nm.

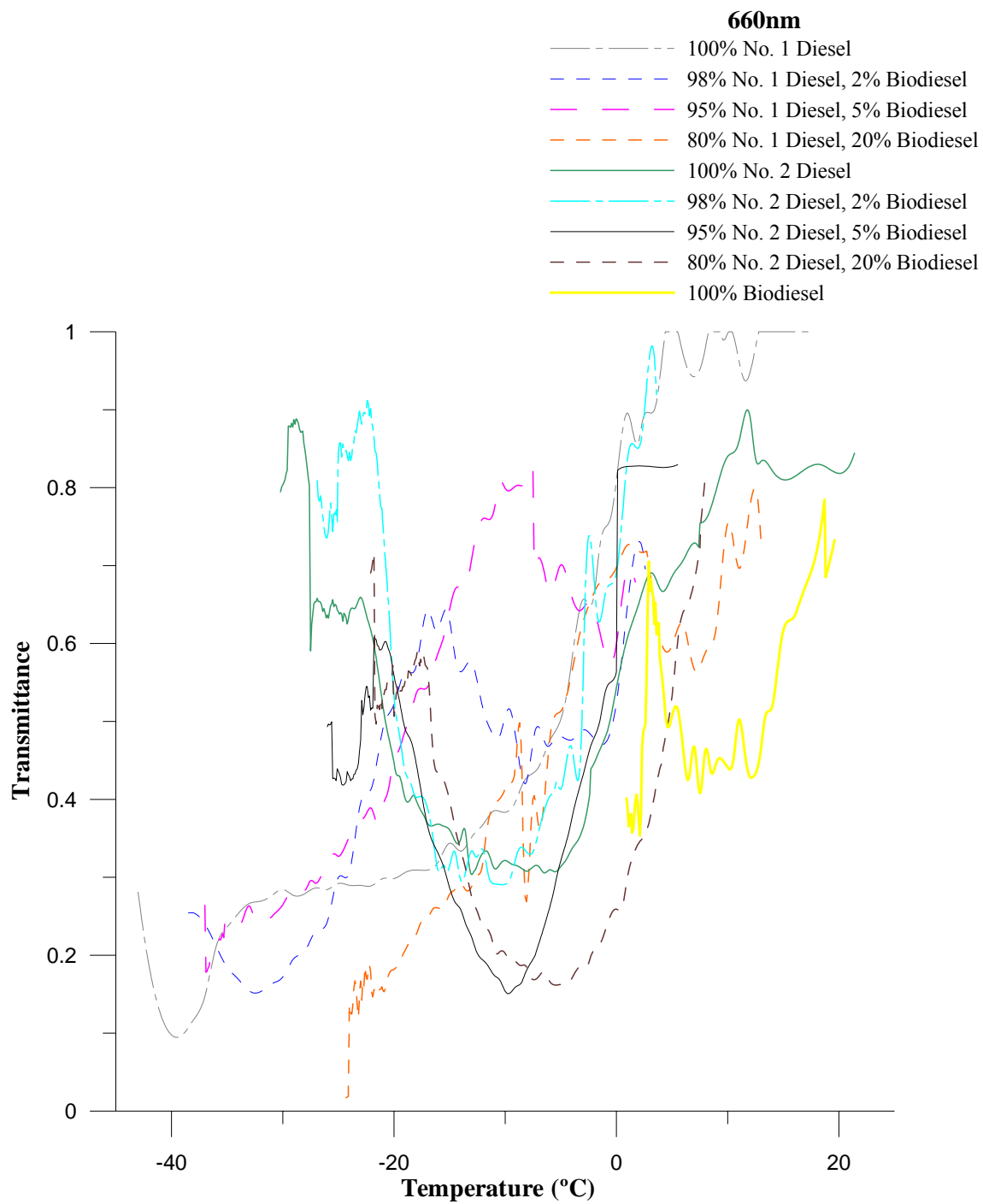


Figure 4.14: Transmittance Vs Temperature for Different Blends of Diesel and Biodiesel Fuel at 660nm

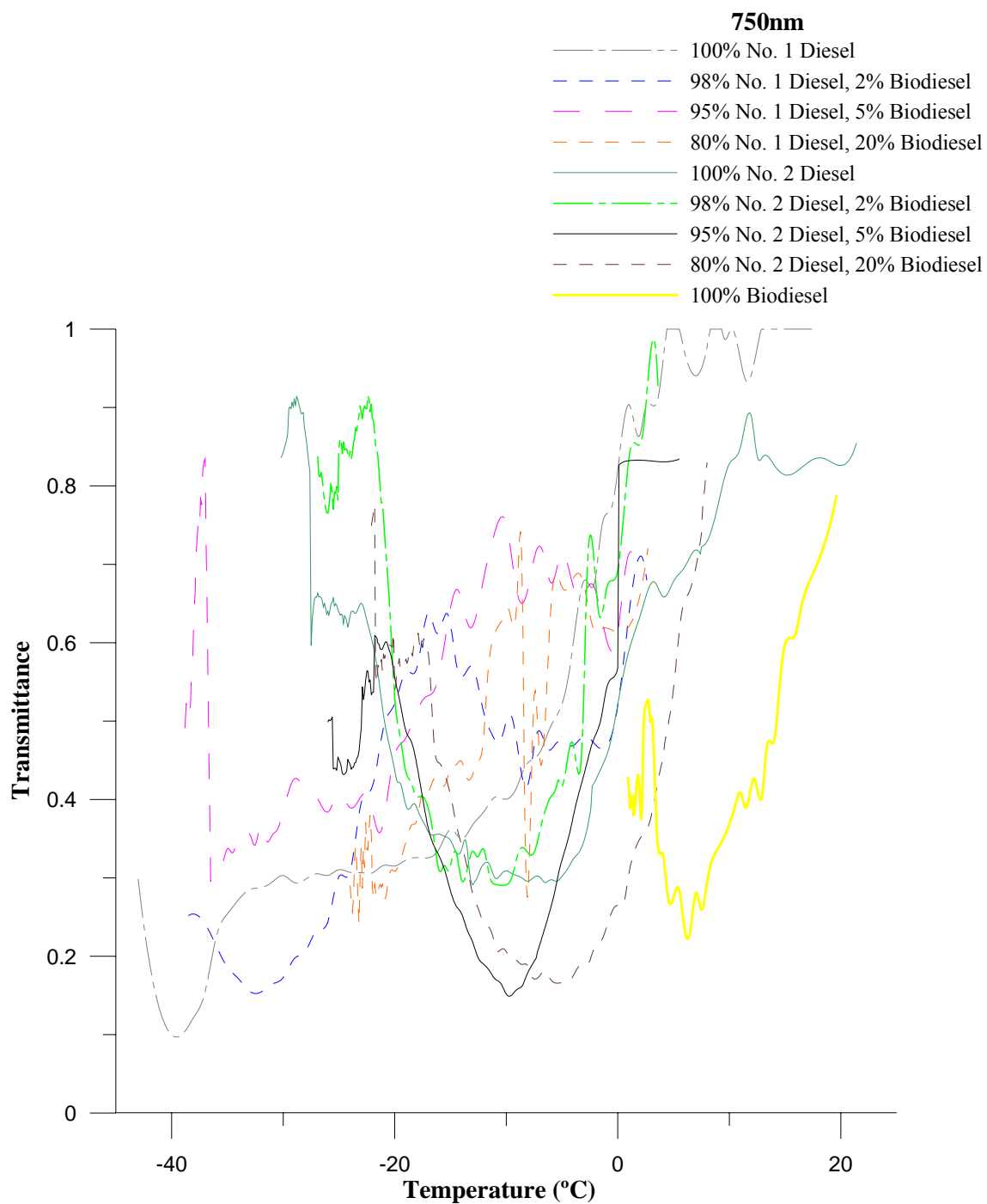


Figure 4.15: Transmittance Vs Temperature for Different Blends of Diesel and Biodiesel Fuel at 750nm

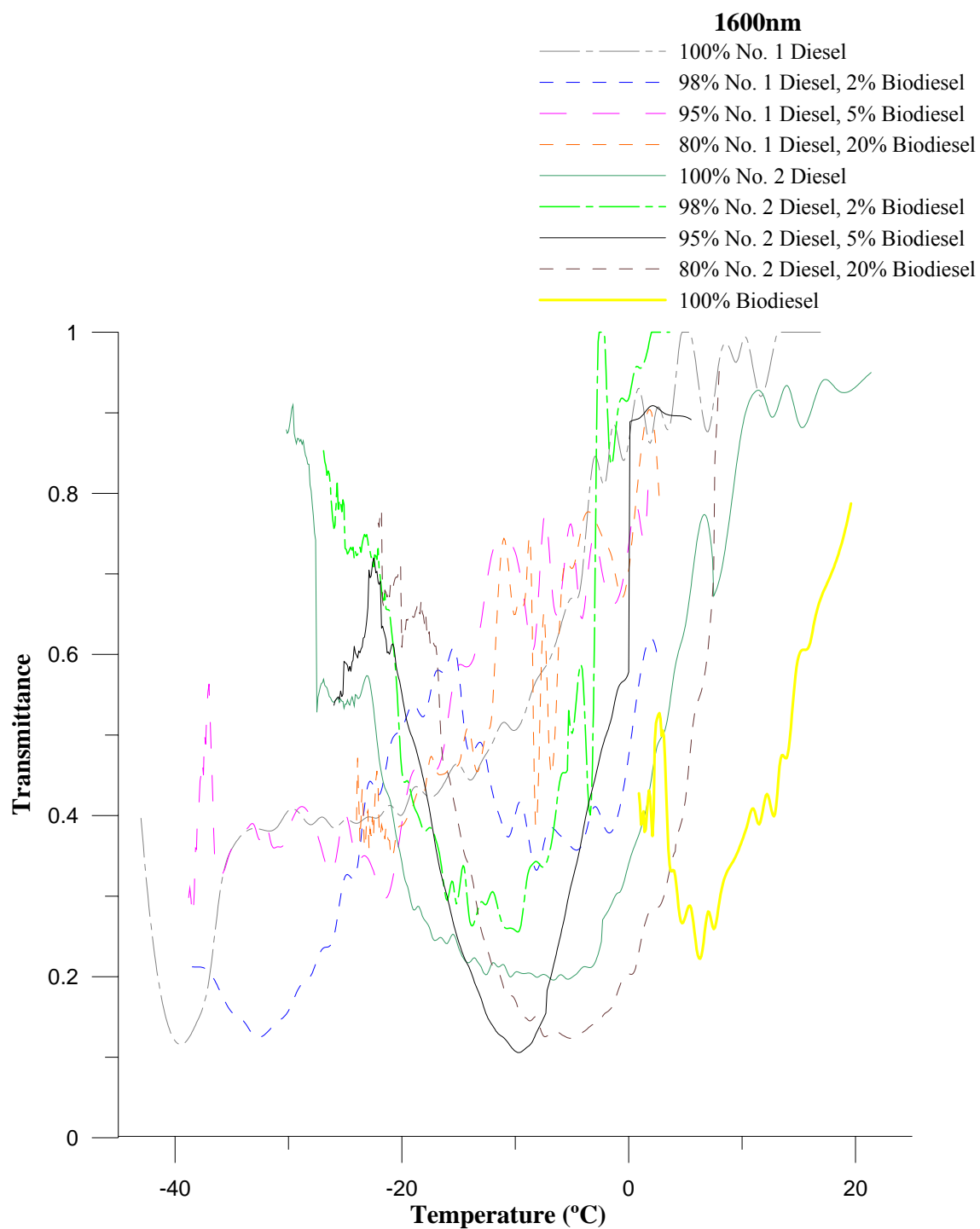


Figure 4.16: Transmittance Vs Temperature for Different Blends of Diesel and Biodiesel Fuel at 1600nm

CHAPTER 5

CONCLUSIONS

- Speed of flow of fuel was maintained constant since the transmittance decreased with a increase in speed of the flow of fuel.
- Minimum transmittance of different blends of biodiesel was reached at about 2-10° C above the cloud point, depending on the respective biodiesel blended fuel.
- The lowest value of transmittance for all blends of biodiesel was 0.3 or less, a time when crystal particles formed in biodiesel fuel even before the fuel reached its cloud point.
- The new optical sensor was helpful in determining the spectral properties of biodiesel fuel.
- Optical properties of D1B0 (100% No. 1 Diesel) and D1B2 (98% No. 1 Diesel and 2% Biodiesel) could not be observed at their cloud point. The reason being, our system was not able to obtain a reading at temperatures below -40° C.
- For all blends of biodiesel it was noted that transmittance started to decrease once it reached its cloud point.
- Cloud point detection of biodiesel fuel could not be determined using the developed optical sensor. The reason was that cold temperatures caused some crystal formation of blends of biodiesel fuel even before it reached the cloud point. After some time, those crystal particles froze on the sides of the container while rest of the fuel remained clear. Therefore even before the cloud point was reached, transmittance value became low.

CHAPTER 6

RECOMMENDATIONS

When the temperature of the biodiesel fuel goes much below freezing, moisture in the atmosphere condenses on the outer part of convex lenses of the sensor. This results in low transmittance of light through the sensor and hence wrong data. This problem can be overcome by passing nitrogen gas, as it eliminates the condensation of moisture in the lenses by purging the air from the lenses.

Future recommendation will be to use an optical sensor in an automobile. The sensor should be designed such that an LED of 750nm can be used as a light source and a photodiode can be used to detect the transmittance through the sensor. Sensor should be installed in the fuel line just after the fuel tank in the automobile. Sensor will not be able to detect the cloud point. But our result showed that freezing of the long chains of fatty acids can be detected. One standard value of transmittance should be considered and our result showed that all the blends of biodiesel fuel went to at least 0.3. Process should be such that once the transmittance value of 0.3 was reached the system should activate an automatic mechanism to maintain the fuel in liquid state, hence ensuring the engine operation.

Further research is recommended to find the reason why cloud point depressions occurred when using low level blends (less than 5%) of biodiesel with diesel fuel.

APPENDIX A

SENSOR DRAWINGS

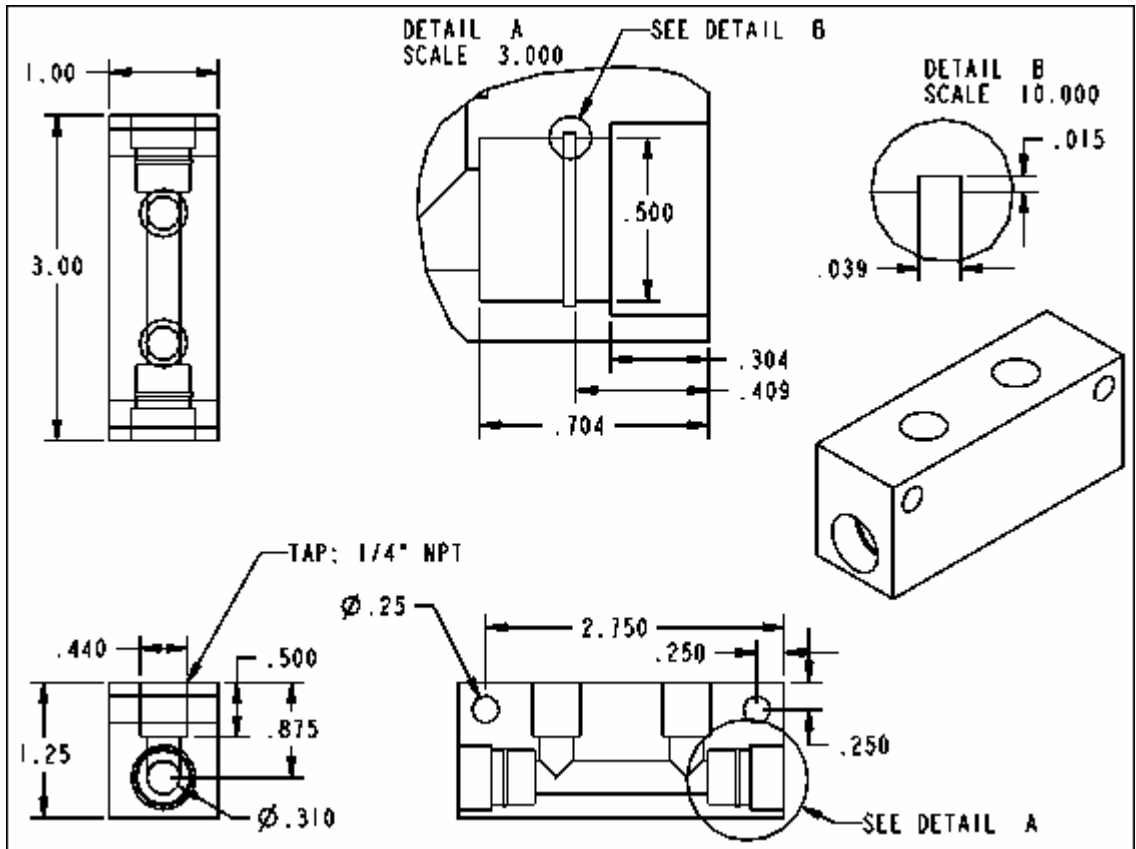


Figure A.1: Sensor Drawings

The one side of the sensor is to the light source through SMA connector, shown in figure 3.9 which is connected to the light source through the fiber cable.

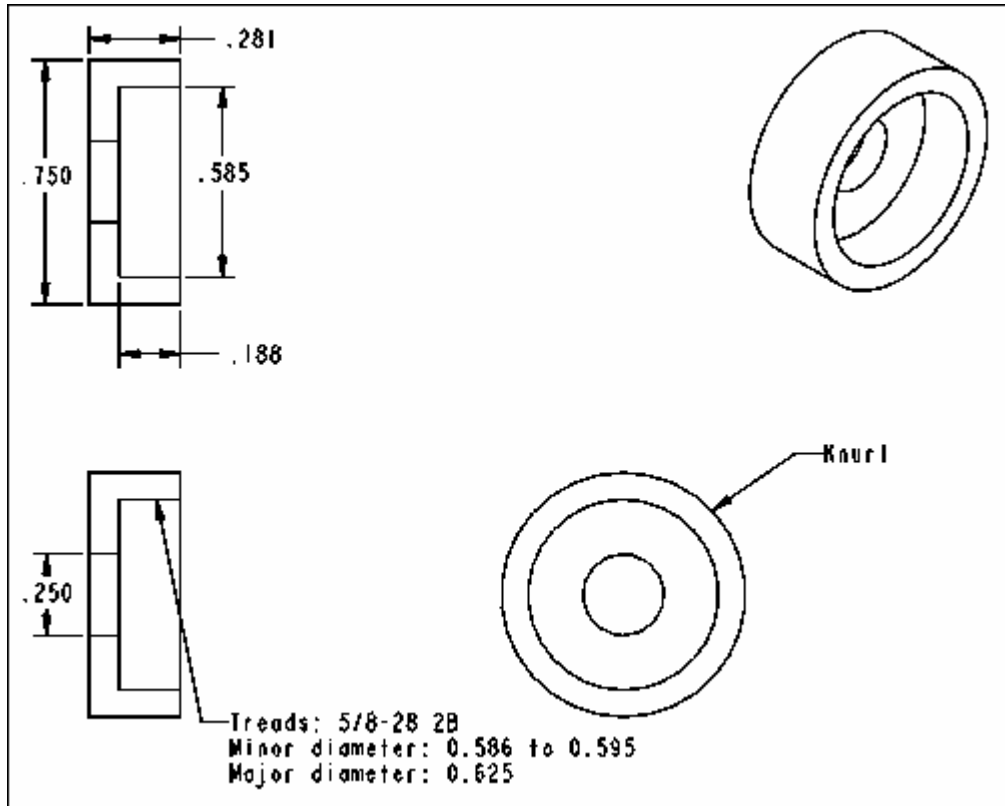


Figure A.2: Drawings for Connection Between SMA Connector of Fiber Cable to the Sensor

The other side is connected the spectrometer with the no screw at the connector side. This side is connected to the spectrometer through the fiber optic cable, which is permanently attached to the spectrometer.

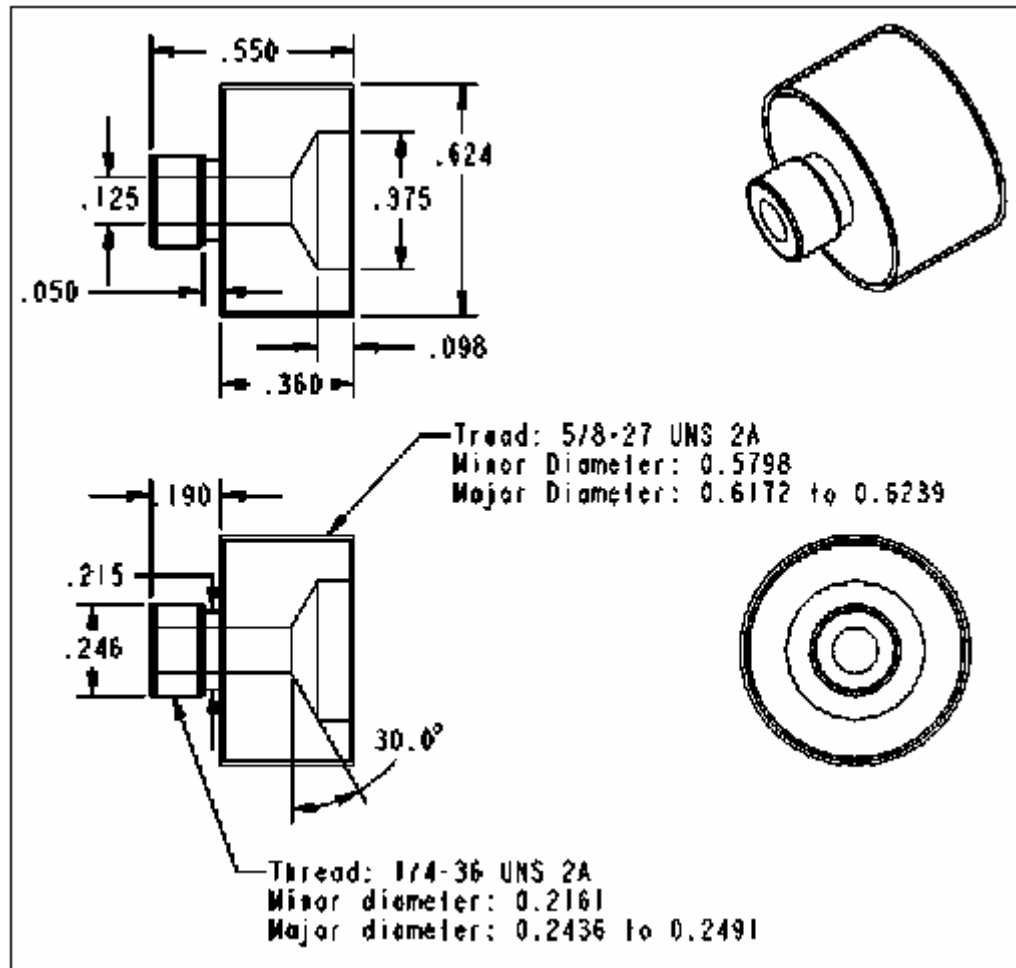


Figure A.3: Drawings for the Connection Between the Sensor and No Screw Connector of Fiber Cable

APPENDIX B

SAS program (SAS, 1990) to convert raw data into the transmittance for B100 (100% Biodiesel)

```
goptions reset=all;
data r1_b100;
infile 'C:\Documents and Settings\sumit_2\Desktop\rep-1\B100-IV.txt'
trunccover dsd firstobs=2 dlm='09'x lrecl=3000;
input Wavelength baseline t1-t92;
array tt{92} t1-t92;
array trans{92};
do i=1 to 92;
trans{i}=tt{i}/baseline;
end;

data r1_b100_small;
set r1_b100(keep=Wavelength trans1 trans5 trans11 trans15 trans23
trans31 trans36);
array tt{7} trans1 trans5 trans11 trans15 trans23 trans31 trans36;
do i=1 to 7;
if i=1 then Temperature=1;
if i=2 then Temperature=5;
if i=3 then Temperature=11;
if i=4 then Temperature=15;
if i=5 then Temperature=23;
if i=6 then Temperature=31;
if i=7 then Temperature=36;
trans=tt{i};
if trans>1 then trans=1;
if trans<0 then trans=0;
output;
end;

proc print;
run;
symbol1 i=j l=1 c=black;
symbol2 i=j l=2 c=black;
symbol3 i=j l=3 c=orange;
symbol4 i=j l=1 c=magenta;
symbol5 i=j l=2 c=magenta;
symbol6 i=j l=1 c=blue;
symbol7 i=j l=2 c=blue;

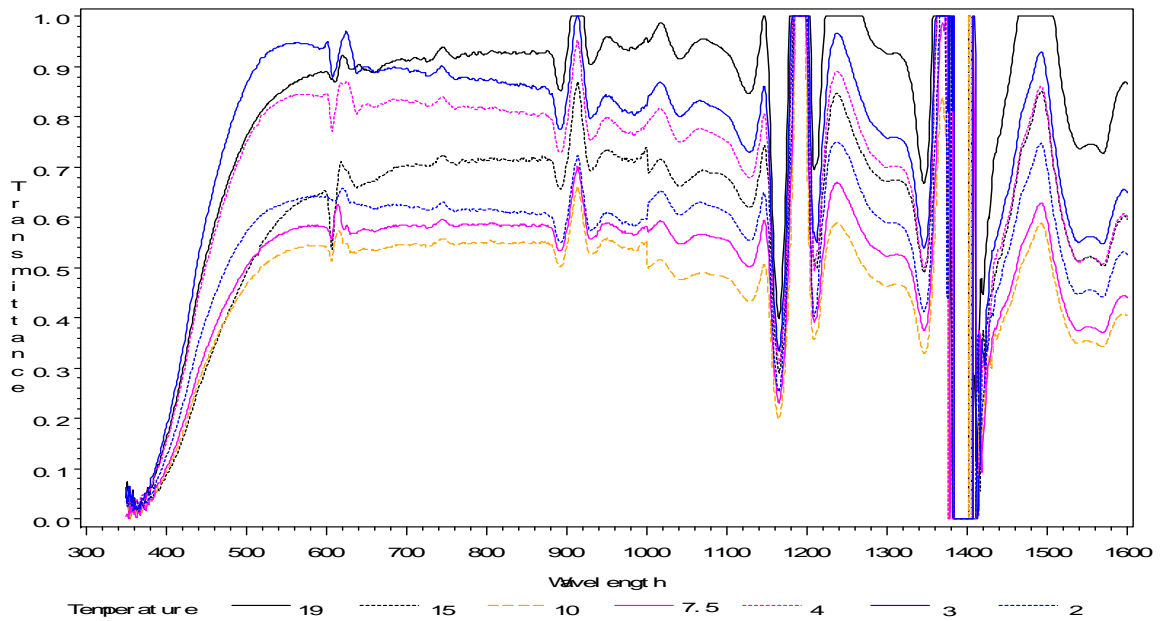
proc gplot;
plot trans*Wavelength=Temperature/haxis=300 to 1600 by 100;

run;
```

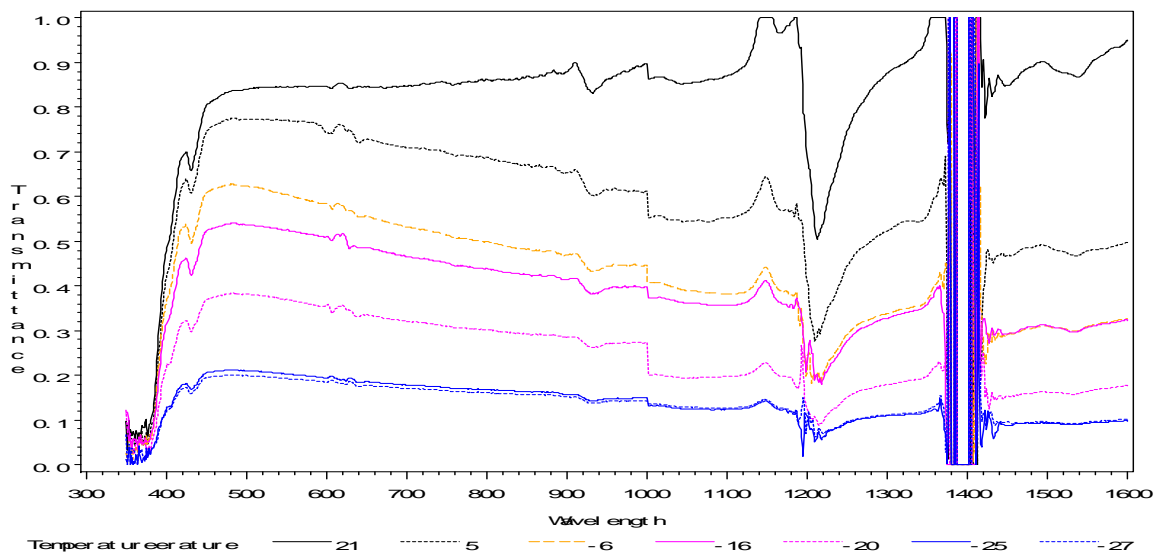
APPENDIX C

REPLICATE 2

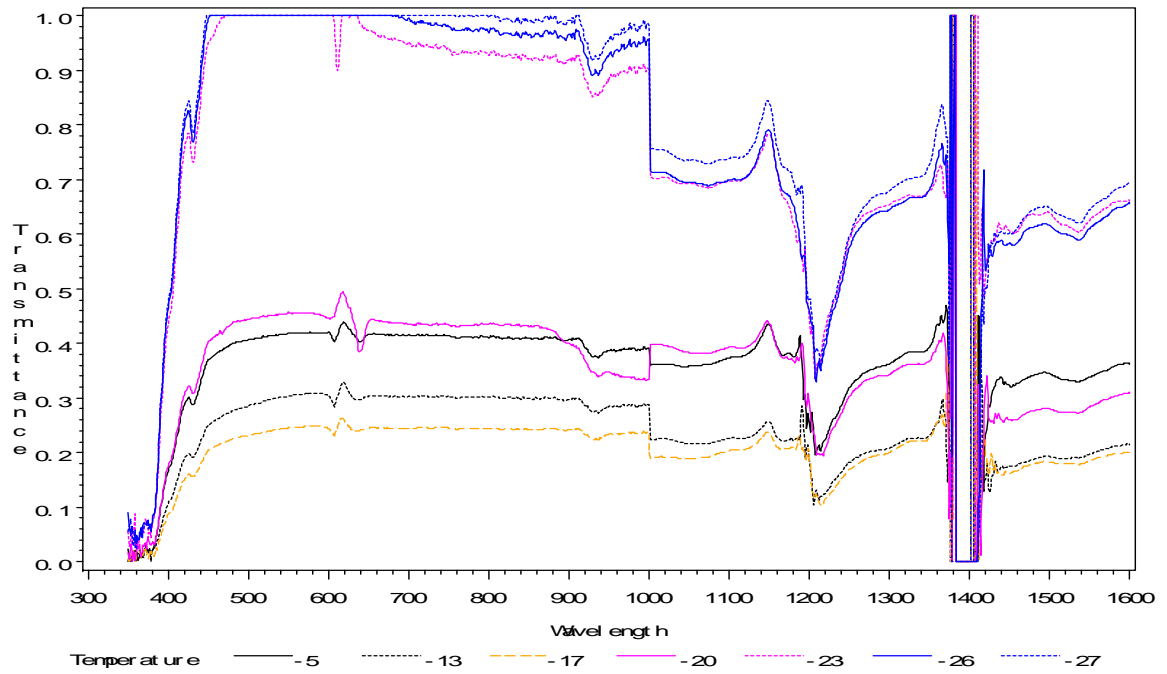
B100 (100% BIODIESEL)



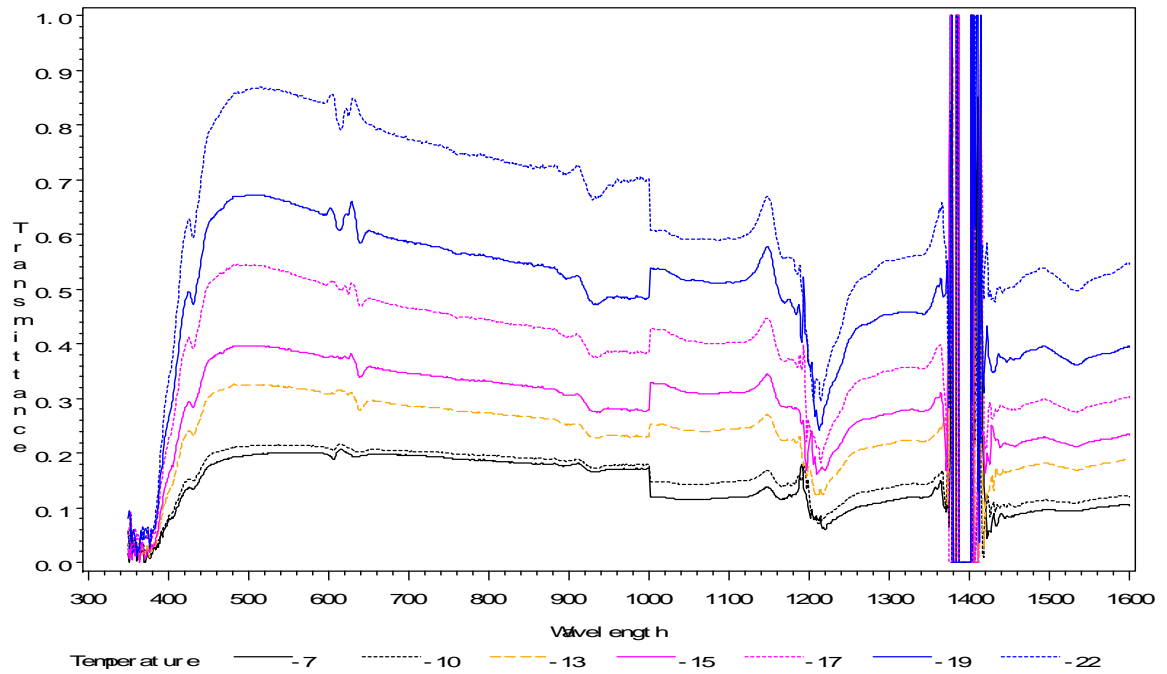
D2B0 (100% No. 2 DIESEL)



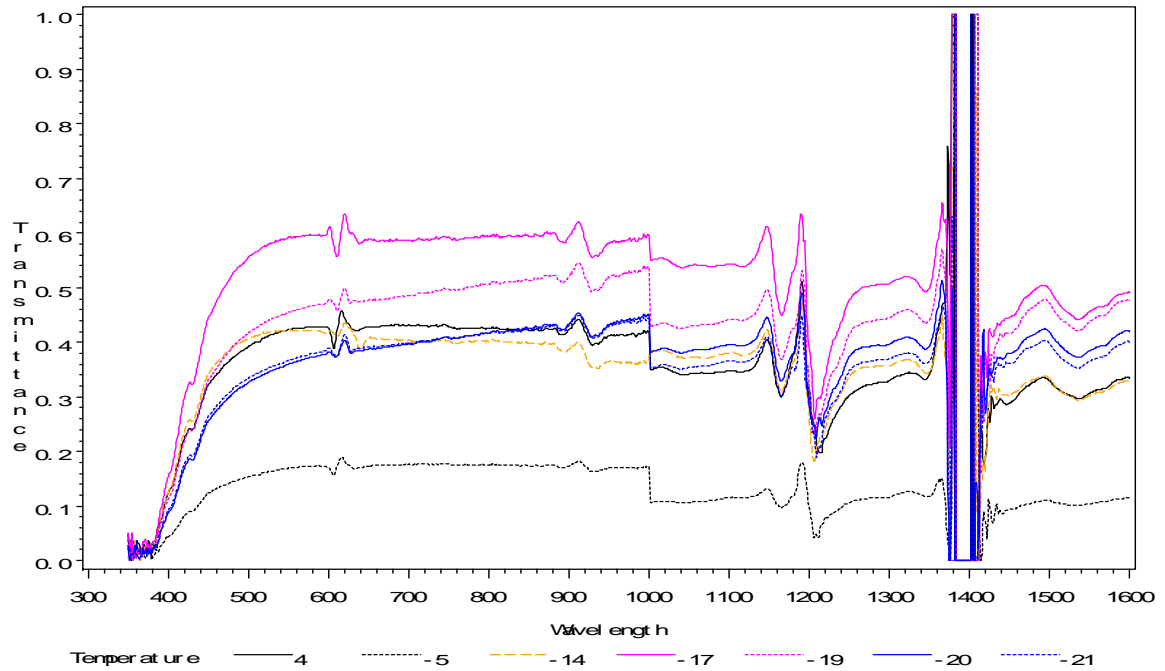
D2B2 (98% No. 2 DIESEL and 2% BIODIESEL)



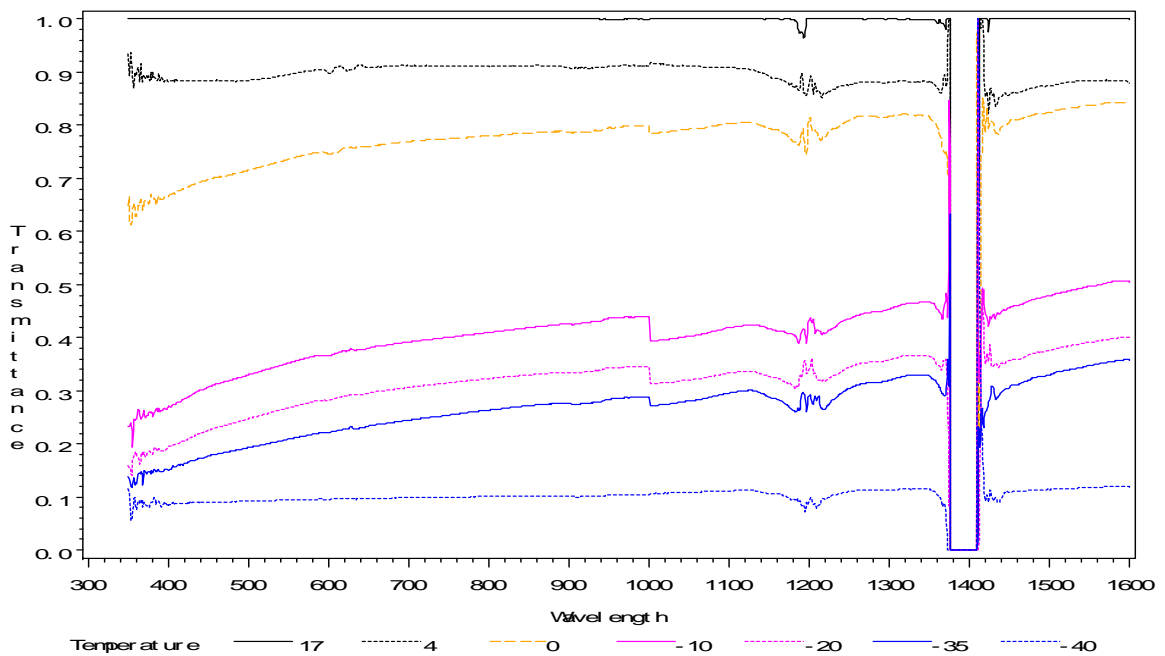
D2B5 (95% No. 2 DIESEL and 5% BIODIESEL)



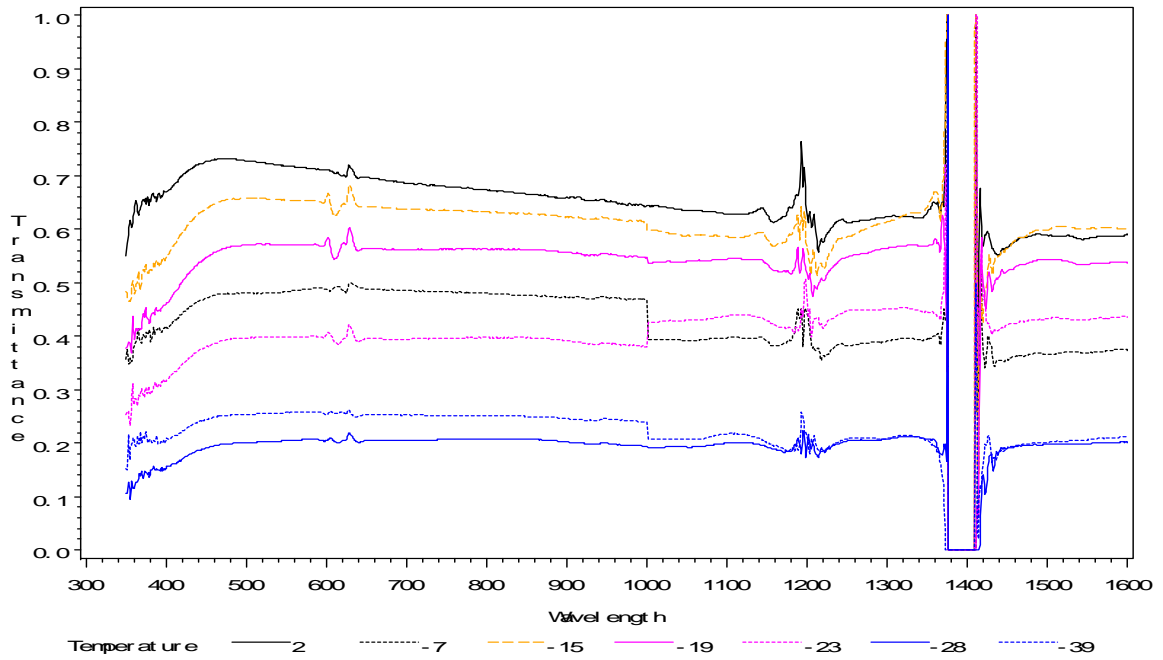
D2B20 (80% No. 2 DIESEL and 20% BIODIESEL)



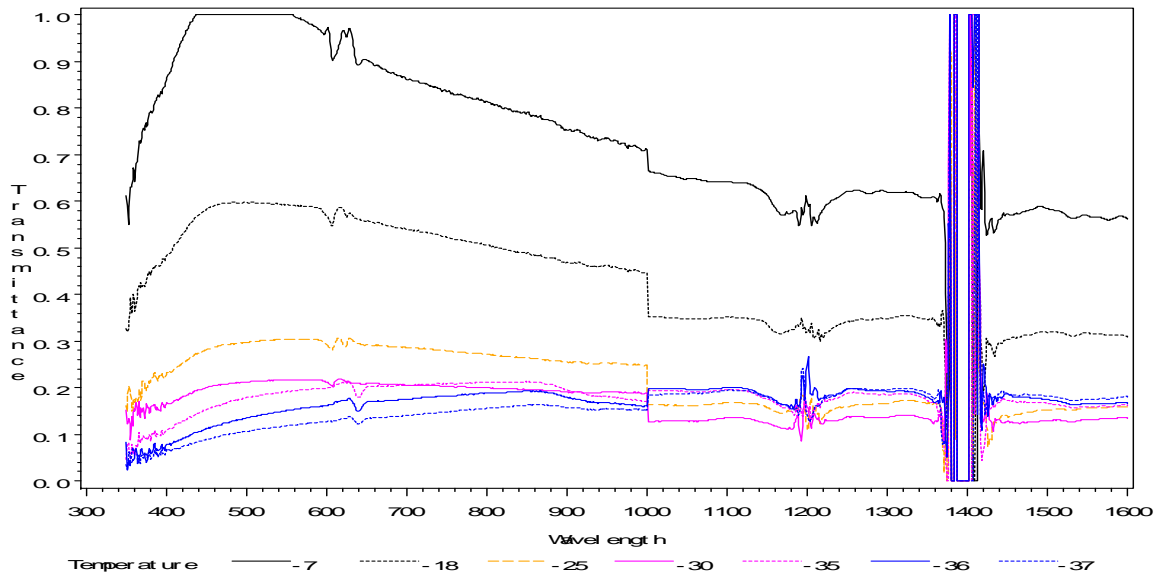
D1B0 (100% No. 1 DIESEL)



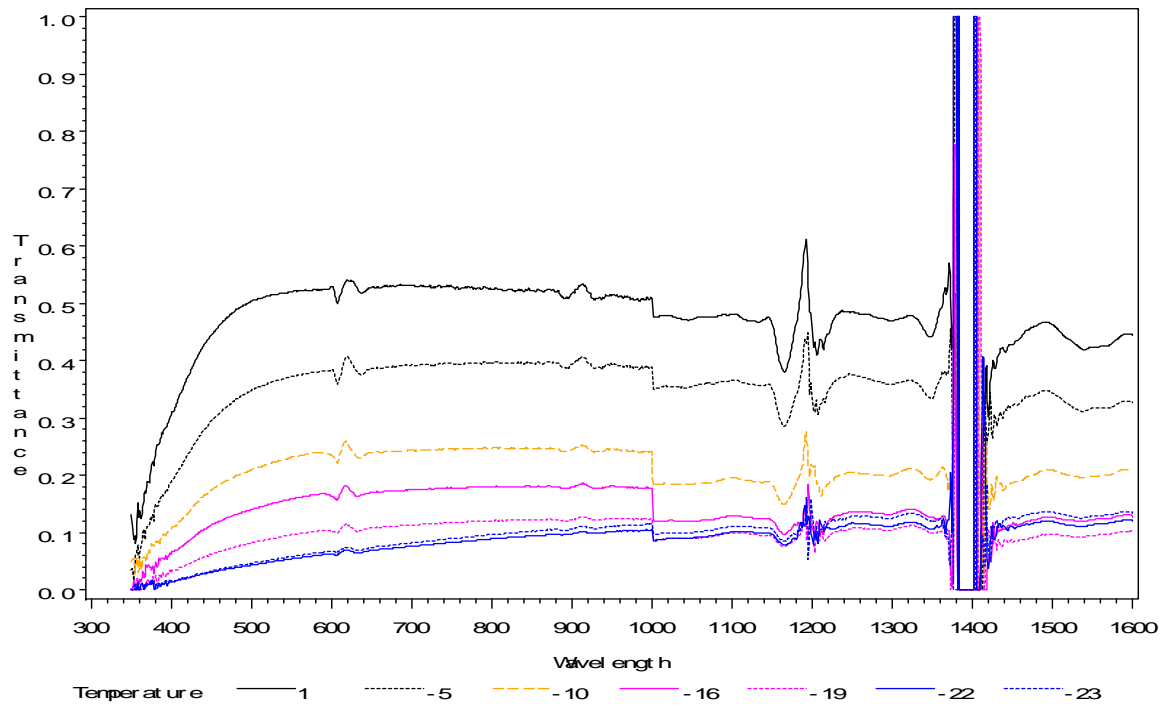
D1B2 (98% No. 1 DIESEL and 2% BIODIESEL)



D1B5 (95% No. 1 DIESEL and 5% BIODIESEL)

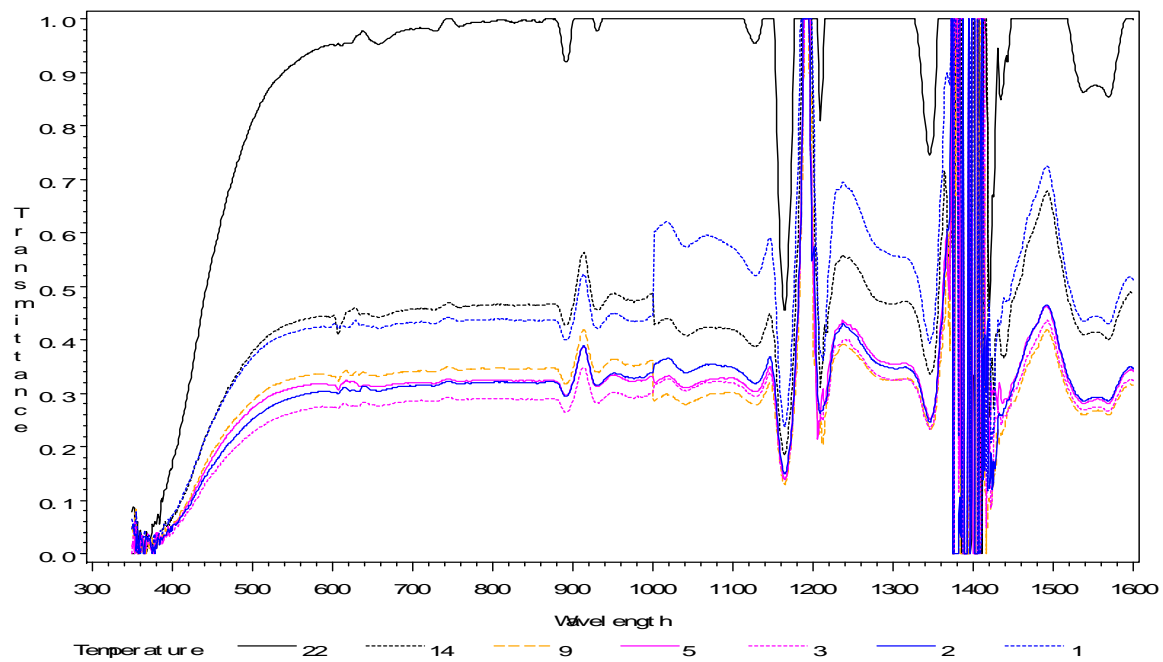


D1B20 (80% No. 1 DIESEL and 20% BIODIESEL)

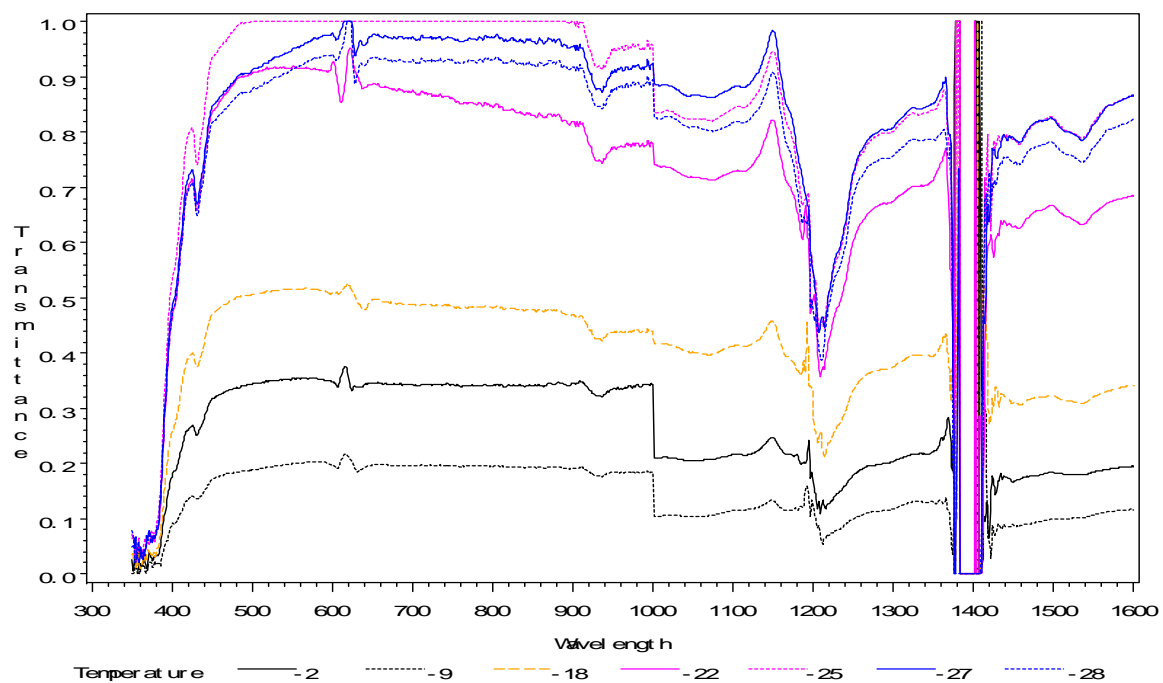


REPLICATE 3

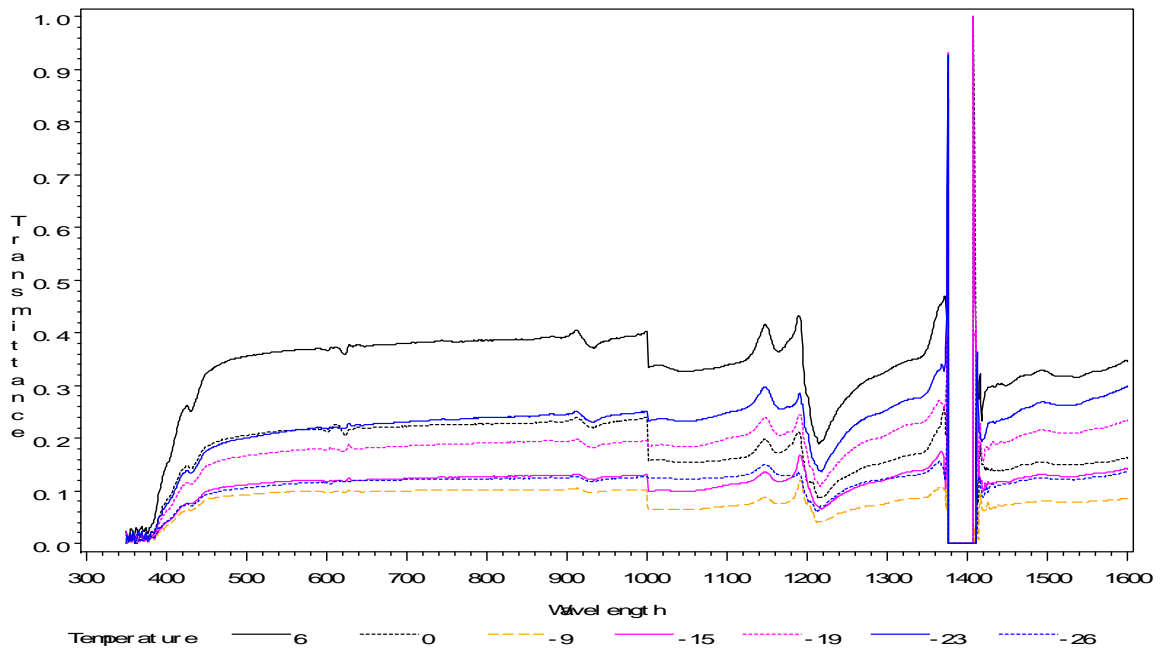
B100 (100% BIODIESEL)



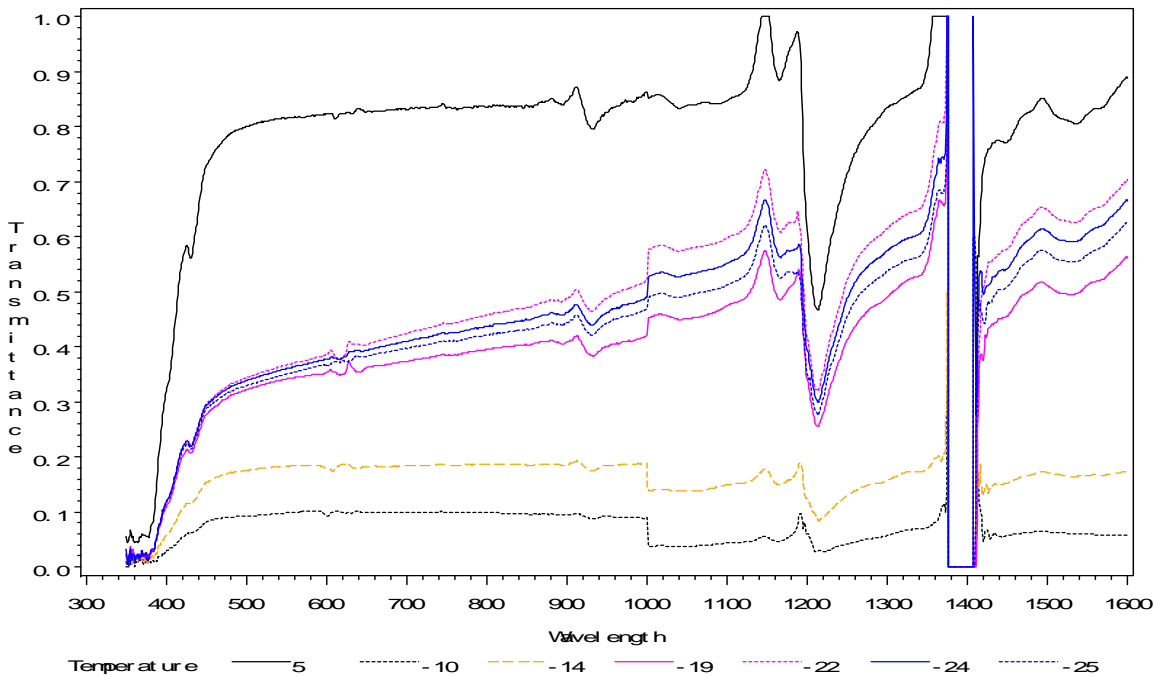
D2B0 (100% No. 2 DIESEL)



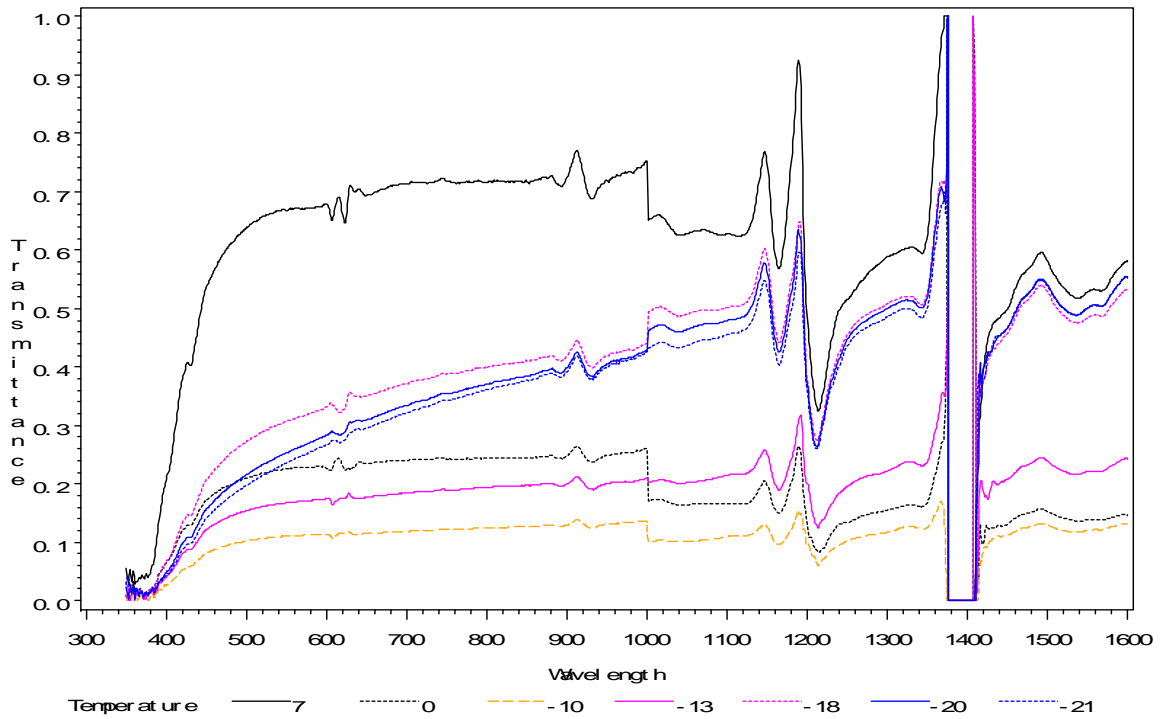
D2B2 (98% No. 2 DIESEL AND 2% BIODIESEL)



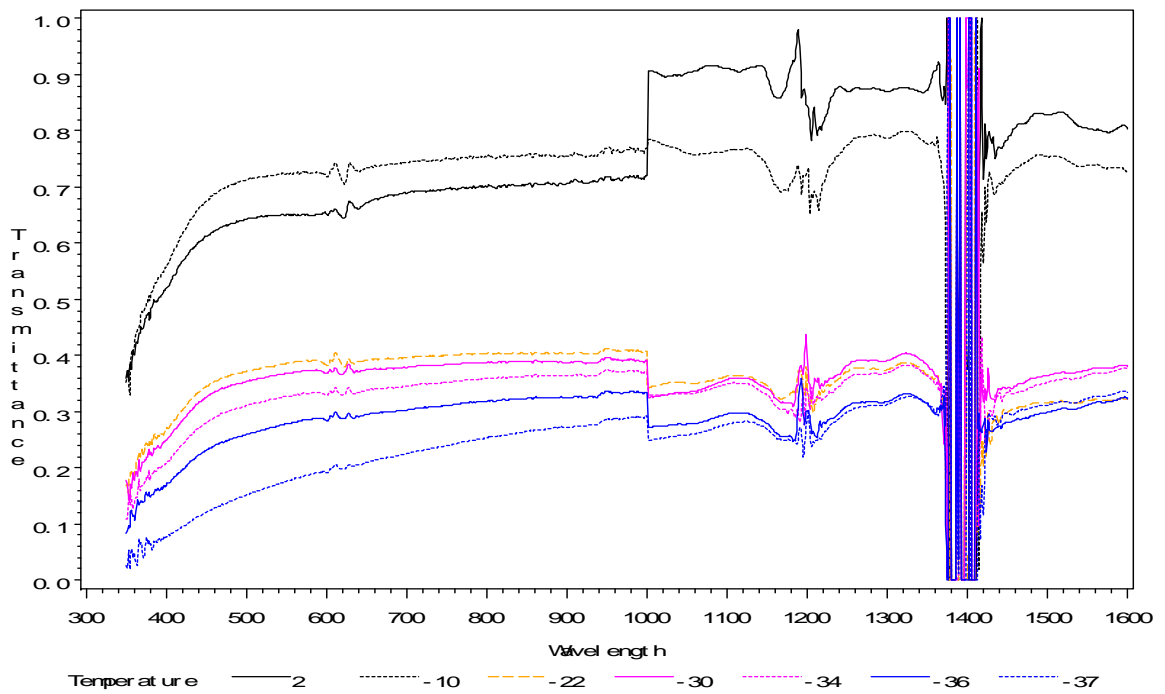
D2B5 (95% No. 2 DIESEL AND 5% BIODIESEL)



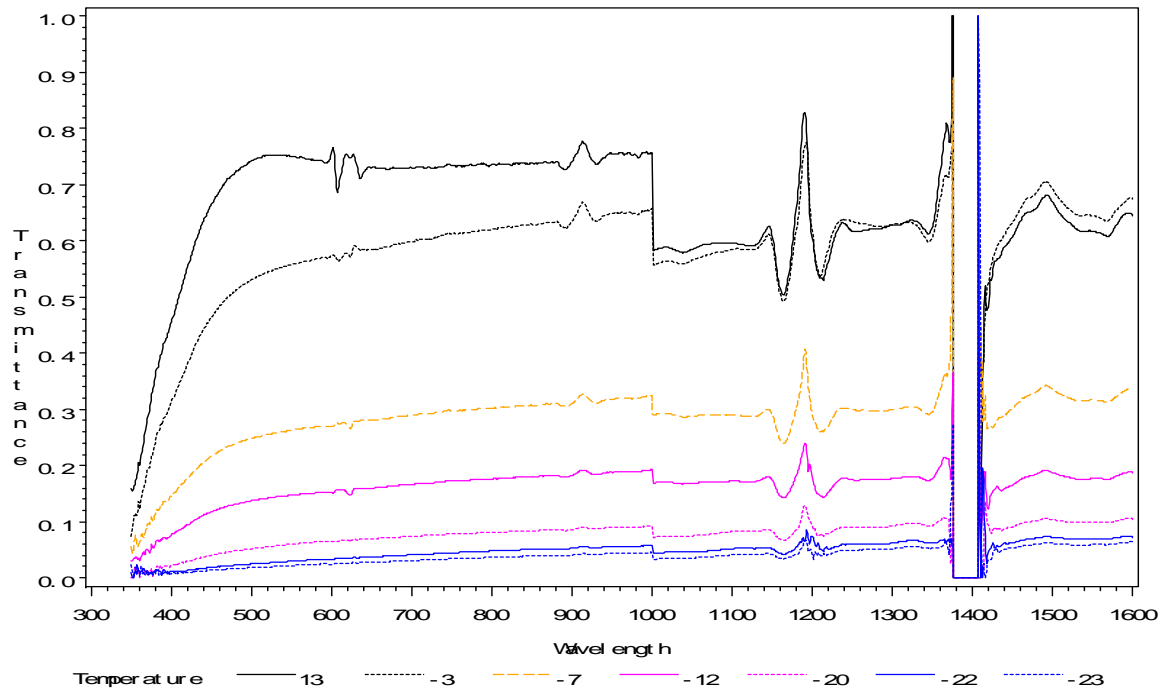
D2B20 (80% No. 2 DIESEL AND 20% BIODIESEL)



D1B5 (95% No. 1 DIESEL AND 5% BIODIESEL)



D1B20 (80% No. 1 DIESEL AND 20% BIODIESEL)



APPENDIX D

SAS program (SAS, 1990) was written to get the data to plot Transmittance Vs Wavelength for different blends of biodiesel fuel at their respective cloud point temperatures. The program first converts the 3 replicates for each blend of biodiesel fuel and then evaluates out the average of their cloud point temperature.

The program shown is for B100 (100% Biodiesel) and the other 6 were written in the same way.

```
goptions reset=all;
data r1_b100;
infile 'C:\Documents and Settings\st638\Desktop\rep-1\B100-IV.txt'
trunccover dsd firstobs=2 dlm='09'x lrecl=3000;
input wavelength baseline t1-t92;
array tt{92} t1-t92;
array trans{92};
do i=1 to 92;
trans{i}=tt{i}/baseline;
end;
rep=1;
transfer=trans36;
keep wavelength rep transfer;

proc print;
run;

data r2_b100;
infile 'C:\Documents and Settings\st638\Desktop\rep-2\B100-IX.txt'
trunccover dsd firstobs=2 dlm='09'x lrecl=3000;
input wavelength baseline t1-t92;
array tt{92} t1-t92;
array trans{92};
do i=1 to 92;
trans{i}=tt{i}/baseline;
end;
rep=2;
transfer=trans61;
keep wavelength rep transfer;

proc print;
run;
data r3_b100;
infile 'C:\Documents and Settings\st638\Desktop\rep-3\B100-XVII.txt'
trunccover dsd firstobs=2 dlm='09'x lrecl=3000;
input wavelength baseline t1-t92;
```

```

array tt{92} t1-t92;
array trans{92};
do i=1 to 92;
trans{i}=tt{i}/baseline;
end;
rep=3;
transfer=trans40;
keep wavelength rep transfer;

data cloud_point;

set r1_b100 r2_b100 r3_b100;
if transfer>1 then transfer=1;

proc print;
run;

proc means nway data=cloud_point;
class wavelength;
var transfer;
output out=b100 mean=;
libname abc 'd:\';
data abc.b100_cp;
set b100;
blend ='b100';
symbol1 i=j l=1 c=black;
symbol1 i=j l=1 c=red;
symbol1 i=j l=1 c=green;

proc gplot data=groovy;
plot transfer*wavelength/haxis=300 to 1600 by 100;

run;

quit;

```

A different program was used to merge all the plots for different blends of biodiesel fuel

```
libname abc 'D:\';
```

```
data one;
```

```
length blend $8;
```

```
set abc.b100_cp abc.d1b5_cp abc.d1b20_cp abc.d2b0_cp abc.d2b2_cp
```

```
abc.d2b5_cp abc.d2b20_cp;
```

```
symbol1 i=j c=blue w=2;
```

```
symbol2 i=j c=black w=2;
```

```
symbol3 i=j c=yellow w=2;
```

```
symbol4 i=j c=gray w=2;
```

```
symbol5 i=j c=green w=2;
```

```
symbol6 i=j c=purple w=2;
```

```
symbol7 i=j c=orange w=2;
```

```
proc gplot data=one;
```

```
plot transfer*wavelength=blend;
```

```
run;
```

APPENDIX E

SAS program (SAS, 1990) was written to get the data for the plot between Transmittance and Temperature at different wavelengths. The data is the average of particular wavelengths of 3 replicates for each blend of biodiesel fuel. Program showed for B100 (100% Biodiesel). Other 8 replicates follow the same pattern.

```
data r1_B100;

infile 'C:\Documents and Settings\st638\Desktop\rep-1\B100-IV.txt'
truncover dsd firstobs=2 dlm='09'x lrecl=3000;

input wavelength baseline t1-t130;

array tt{130} t1-t130;

array trans{130};

do i=1 to 130;

trans{i}=tt{i}/baseline;

end;

m=1;

if wavelength in(660, 750, 1650);

*proc print;

*var baseline trans1-trans40;

*id wavelength;

*run;

data r1_B100_temps;

infile 'C:\Documents and Settings\st638\Desktop\Replicates-temp-
excel\rep1_temp\B100_temp\B100-4.txt' dlm='09'x firstobs=2;

input temp1-temp130;

m=1;
```

```

data r1_B100_t;

merge r1_B100 r1_B100_temps;

by m;

rep=1;

array t{130} trans1-trans130;

array tmp{130} temp1-temp130;

do i=1 to 130;

temp=tmp{i};

trans=t{i};

output;

end;

keep wavelength rep temp trans;

run;

proc print;

run;

data r2_B100;

infile 'C:\Documents and Settings\st638\Desktop\rep-2\B100-IX.txt'
trunccover dsd firstobs=2 dlm='09'x lrecl=3000;

input wavelength baseline t1-t130;

array tt{130} t1-t130;

array trans{130};

do i=1 to 130;

trans{i}=tt{i}/baseline;

end;

m=1;

if wavelength in(660, 750, 1650);

*proc print;

*var baseline trans1-trans40;

```

```

*id wavelength;

*run;

data r2_B100_temps;

infile 'C:\Documents and Settings\st638\Desktop\Replicates-temp-
excel\rep2_temp\B100_temp\B100-9.txt' dlm='09'x firstobs=2;

input temp1-temp130;

m=1;


data r2_B100_t;

merge r2_B100 r2_B100_temps;

by m;

rep=2;

array t{130} trans1-trans130;

array tmp{130} temp1-temp130;

do i=1 to 130;

temp=tmp{i};

trans=t{i};

output;

end;

keep wavelength rep temp trans;

run;

proc print;

run;

data r3_B100;

infile 'C:\Documents and Settings\st638\Desktop\rep-3\B100-XVII.txt'
trunccover dsd firstobs=2 dlm='09'x lrecl=3000;

input wavelength baseline t1-t130;

array tt{130} t1-t130;

```

```

array trans{130};

do i=1 to 130;

trans{i}=tt{i}/baseline;

end;

m=1;

if wavelength in(660, 750, 1650);

*proc print;

*var baseline trans1-trans40;

*id wavelength;

*run;

data r3_B100_temps;

infile 'C:\Documents and Settings\st638\Desktop\Replicates-temp-
excel\rep3_temp\B100_temp\B100-17.txt' dlm='09'x firstobs=2;

input temp1-temp130;

m=1;


data r3_B100_t;

merge r3_B100 r3_B100_temps;

by m;

rep=3;

array t{130} trans1-trans130;

array tmp{130} temp1-temp130;

do i=1 to 130;

temp=tmp{i};

trans=t{i};

output;

end;

keep wavelength rep temp trans;

```

```

run;

proc print;

run;


data w660;
set r1_B100_t r2_B100_t r3_B100_t;
temp=round(temp,.1);
if wavelength=660;
run;


proc sort data=w660 nodupkey;
by rep temp;

run;


data full;
do rep=1 to 3;
do temp=-44 to 25 by .1;
temp=round(temp,.1);
output;
end;
end;
run;


proc sort data=full;
by rep temp;


data new;
merge w660 full;
by rep temp;
run;


proc sort data=new nodupkey;
by rep temp;
run;


proc print;
run;
proc expand data=new out=new1;
id temp;

```

```

        var trans;
where rep=1;
    run;

    proc expand data=new out=new2;
        id temp;
        var trans;
where rep=2;
    run;
    proc expand data=new out=new3;
        id temp;
        var trans;
where rep=3;
    run;

data new123;
set new1 new2 new3;

proc means nway data=new123;
class temp;
var trans;
output out=b100 mean=;

libname abc 'D:\';
data abc.b100;
set b100;
blend='b100';

proc print;
run;

symbol1 i=j c=blue;
symbol2 i=j c=black;
symbol3 i=j c=yellow;
proc gplot data=new123;
plot trans*temp;
run;

proc gplot;
plot Trans*Temp;
run;

quit;

proc print;
run;

proc print data=w660;
run;

```

The other program was written to merge all the plots for different blends of biodiesel fuel

```

libname abc 'D:\';

data one;
length blend $9;
set abc.d1b0 abc.d1b2 abc.d1b5 abc.d1b20 abc.d2b0 abc.d2b2 abc.d2b5
abc.d2b20 abc.b100;
if Trans>1 then Trans=1;


symbol1 i=j c=blue w=2;
symbol2 i=j c=black w=2;
symbol3 i=j c=magenta w=2;
symbol4 i=j c=gray w=2;
symbol5 i=j c=green w=2;
symbol6 i=j c=purple w=2;
symbol7 i=j c=orange w=2;
symbol8 i=j c=yellow w=2;
symbol9 i=j c=blue w=2;


proc gplot data=one;
plot trans*temp=blend;
run;

```

REFERENCES

- Akasaka, Y and Y. Sakurai. 1994. Effects of oxygenated fuel and cetane improver on exhaust emission from heavy-duty DI diesel engines. SAE Paper No. 942023. Warrendale, PA.: SAE.
- ASTM Standards*. 1999. D6371-99: Standard test method of cold filter plugging point of diesel and heating fuels. West Conshohocken, PA.: ASTM.
- ASTM Standards*. 2002a. D2500-02: Standard test method for cloud point of petroleum products. West Conshohocken, PA.: ASTM.
- ASTM Standards*. 2002b. D5949-02: Standard test method for pour point of petroleum products (Automatic pressure pulsing method). West Conshohocken, PA.: ASTM.
- ASTM Standards*. 2002c. D5771-02: Standard test method of cloud point of petroleum products (Optical detection stepped cooling method). West Conshohocken, PA.: ASTM.
- ASTM Standards*. 2002d. D5772-02: Standard test method of cloud point of petroleum products (Linear cooling rate method). West Conshohocken, PA.: ASTM.
- ASTM Standards*. 2002e. D5773-02: Standard test method of cloud point of petroleum products (Constant cooling rate method). West Conshohocken, PA.: ASTM.
- ASTM Standards*. 2003. D4539-03: Standard test method for filterability of diesel fuels by low- temperature flow test. West Conshohocken, PA.: ASTM.
- ASTM Standards*. 2004. D975-04: Standard specifications for diesel fuel oils. West Conshohocken, PA.: ASTM.
- Bessee, G.B. and J.P. Fey. 1997. Compatibility of elastomers and metals in biodiesel fuel blends. SAE Paper No. 971690. Warrendale, PA.: SAE.
- CDCI. 2005. Bio-diesel – A renewable energy source. Orleans, Canada: Canadian Driver Communications Inc. Available at www.canadiandriver.com. Accessed 5 May 2005.
- Cheng, V.M., A.A. Wessol, P. Baudouin, M.T. BenKinney and N.J. Navick. 1991. Biodegradable and nontoxic hydraulic oils. SAE Paper No. 910964. Warrendale, PA.: SAE.
- Chiu, C., L.G. Schumacher, and G.J. Suppes. 2004. Impact of cold flow improvers on soybean biodiesel blend. *Biomass and Bioenergy*. 27(5): 485-491.
- Choi, C.Y. and R.D. Reitz. 1999. An experimental study on the effects of oxygenated fuel blends and multiple injection strategies on DI diesel engine emissions. *Fuel*. 78: 1303-1317.

Copeland, K, R. Hardy, J. Jeff, C. Selvidge and K. Walztoni. 2006. Blending biodiesel with diesel fuel in cold locations. U.S. Patent Application No. 0037237.

EAL. 2006. Oil product low temperature parameters measurement instrument (Crystal). Tomsk, Russia.: Institute of Petroleum Chemistry. Available at: www.shatox.com/crystal.html. Accessed 14 March 2006.

Hess, M.A., M.J. Haas, T.A. Foglia and W.N. Marmer. 2005. Effect of antioxidant addition on NOx emissions from biodiesel. *Energy and Fuels*. 19: 1749- 1754.

Holfman, V. 2003. Biodiesel Fuel. North Dakota State University Extension Service. AE-1240. Fargo, ND.

Holmberg, K and E. Osterberg. 1989. Process for the transesterification of triglycerides in an aqueous micro emulsion reaction medium in the presence of lipase enzyme. US Patent: 4839287.

Howell, Steve. 1995. Lubricity, the Biodiesel Advantage. Presented at the 1995 ASAE Annual International Meeting. June 18-23, 1995.

ISA. 2004. Biodiesel fueling Illinois. Bloomington, IL.: Illinois soybean association. Available at: www.ilsoy.org. Accessed 23 March 2004.

Javvadi, C. 2005. Design of a non- invasive dielectric sensor to measure the blend ratio of the biodiesel. MS thesis. Columbia, Missouri: University of Missouri, Department of Biological Engineering.

KIC. 2004. Automatic cloud point & pour point system cloud point detection Bohemia, N.Y.: Koehler Instrument Company. Available at: www.koehlerinstrument.com. Accessed 24 March 2004.

Kittiwake. 2006. Cloud point detector Littlehampton, West Sussex: Kittiwake. Available at: www.Kittiwake.com. Accessed 10 February 2006.

Knothe, G.H. 1998. Rapid Monitoring of transesterification and assessing biodiesel fuel quality by near-infrared spectroscopy using a fiber-optic probe. Annual meeting and expo of the American Oil Chemists' Society. Chicago, IL.

Knothe, G.H. 1999. Analysis of biodiesel fuel and monitoring progress of the transesterification reaction by fiber optic near infrared spectroscopy. ASAE Paper No. 996111. St. Joseph, MI.: ASAE.

Knothe, G., A.C. Matheus and T.W. Ryan III. 2003. Cetane numbers of branched and straight- chain fatty esters determined in an ignition quality tester. *Fuel* 82: 971- 975.

- Knothe, G.H., and K.R. Steidley. 2004. Viscosity and Lubricity of Biodiesel Fuel components. Annual meeting and expo of the American Oil Chemists' Society. Cincinnati, OH.
- Kopera, J.J.C. 1992. Method for flexible fuel control. U.S. Patent No. 5119671.
- Krisnangkura, K. 1986. A simple method for estimation of Cetane index for vegetable oil methyl esters. J. American Oil Chemists Society 74(3): 309-315.
- Ladommatos, N. and J. Goacher. 1995. Equations for predicting the Cetane number of diesel fuels from their physical properties. Fuel 74(7): 1083-1093.
- Ma, F. and M.A. Hanna. 1999. Biodiesel production: a review. Bioresource Technology. 70: 1-15.
- Meitzer, A.H., and G.S. Saloka. 1992. Two alternative, dielectric effect, flexible fuel sensors. SAE Paper No. 920699. Warrendale, PA.: SAE.
- NBB. 2004. Biodiesel Production. Jefferson City, MO.: National biodiesel board. Available at www.biodiesel.org. Accessed 7 December 2004.
- NBB. 2005a. Biodiesel Fact Sheet. Jefferson City, MO.: National biodiesel board. Available at www.biodiesel.org. Accessed 7 May 2005.
- NBB. 2005b. Biodiesel Emissions. Jefferson City, MO.: National biodiesel board. Available at www.biodiesel.org. Accessed 10 August 2005.
- NBB. 2005c. Biodiesel on the road to fueling the future. Jefferson City, MO.: National biodiesel board. Available at www.biodiesel.org. Accessed 11 August 2005.
- NI. 2005. Chemsystems Report. White Plains, NY: Nexant Inc. Available at www.nexant.com. Accessed 10 February 2005.
- Niehaus, R. A., C.E. Goering, L.D. Savage, and S.C. Sorenson. 1985. Cracked soy bean oil as a fuel for a diesel engine. ASAE Paper No. 85-1560. St. Joseph, MI.: ASAE.
- PF. 2005. Emissions. UK: planetfuels. Available at www.planetfuels.co.uk. Accessed on 15 February 2005.
- SAS. 1990. SAS User's Guide: Statistics. Ver. 6a.: SAS Institute, Inc. Cary, N.C.
- Schmitz, G. and H.J. Kutz. 1990. Process for operating a fuel- burning engine. U.S. Patent No. 4945863.
- Schmitz, G., R. Bartz, U. Hilger, and M. Siedentop. 1990. Intelligent alcohol fuel sensor. SAE Paper No. 900231. Warrendale, PA.: SAE.

Schuchardta, U., R. Serchelia and R.M. Vargas. 1998. Transesterification of vegetable oils: a review. J. Braz. Chem. Soc. 9(1): 199- 210.

Song, J., K. Cheenkachorn, J. Want, J. Perez, A.L. Boehman, P.J. Young, F.J. Waller. 2002. Effect of oxygenated fuel on combustion and emissions in a light- duty turbo diesel engine. Energy Fuels 2002, 16, 294-301.

Suzuki, H., and K. Ogawa. 1991. Development of an optical fuel composition sensor. SAE Paper No. 910498. Warrendale, PA.: SAE.

Tat, M.E., and J.H. Van Gerpen. 2001. Biodiesel blend detection using a fuel composition sensor. ASAE Paper No. 01-6052. Sacramento, CA.: ASAE.

Vicente, G., M. Martinez and J. Aracil. 2004. Integrated biodiesel production: a comparison of different homogeneous catalysts systems. Bioresource Technology. 92: 297-305.

Wang, P.S. 2003. The production of isopropyl esters and their effects on a diesel engine. MS thesis. Ames, Iowa: Iowa State University, Department of Mechanical Engineering.

Wigg, E.E. and R.S. Lunt. 1974. Methanol as a Gasoline Extender- Fuel economy, emissions and high temperature driveability. SAE Paper No. 741008. Warrendale, PA.: SAE.